1-1-2015

Decision Making in Networked Systems

Mohammad Hadi Afrasiabi
University of Pennsylvania, mha.afrasiabi@gmail.com

Decision Making in Networked Systems

Abstract
Living in a networked world, human agents are increasingly connected as advances in technology facilitates the flow of information between and the availability of services to them. Through this research, we look at interacting agents in networked environments, and explore how their decisions are influenced by other people's decisions. In this context, an individual's decision may be regarding a concrete action, e.g., adoption of a product or service that is offered, or simply shape her opinion about a subject. Accordingly, we investigate two classes of such problems.

The first problem is the dynamics of service adoption in networked environments, where one user's adoption decision, influences the adoption decision of other users by affecting (positively or negatively) the benefits that they derive from the service. We consider this problem in the context of "User-Provided Connectivity", or UPC. The service offers an alternative to traditional infrastructure-based communication services by allowing users to share their "home base" connectivity with other users, thereby increasing their access to connectivity. We investigate when such services are viable, and propose a number of pricing policies of different complexities. The pricing policies exhibit differences in their ability to maximize the total welfare created by the service, and distributing the welfare between different stakeholders.

The second problem is the spread of opinions in a networked environment, where one agent's opinion about an issue, influences and is influenced by that of other agents to whom she is connected. We are particularly interested in the role that people's adherence to specific groups or parties may play in how final opinions are formed. We approach this problem using a model of interactions inspired by the Ising spin-glass model from classical Physics. We consider two related but distinct settings, and show that when party memberships directly influence user interactions, even slightest statistical partisan biases result in partisan final outcomes: where everyone in a party shares the same opinion, opposite to that of the other party. On the other hand, if party membership plays an indirect role in biasing agent interactions, then there is room for intra-party heterogeneity of opinions.

Degree Type
Dissertation

Degree Name
Doctor of Philosophy (PhD)

Graduate Group
Electrical & Systems Engineering

First Advisor
Roch Guerin

Keywords
Adoption, Externality, Ising, Network, Opinion, Partisan

Decision Making in Networked Systems

Mohammad Hadi Afrasiabi

A DISSERTATION

in

Electrical and Systems Engineering

Presented to the Faculties of the University of Pennsylvania

in

Partial Fulfillment of the Requirements for the

Degree of Doctor of Philosophy

2015

Supervisor of Dissertation

.....

Roch Guérin,

Harold B. and Adelaide G. Welge Professor of Comp. Sci, Washington U. in St. Louis

Graduate Group Chairperson

.....

Saswati Sarkar,

Professor of Electrical and Systems Engineering

Dissertation Committee

Roch Guérin, Harold B. and Adelaide G. Welge Professor of Comp. Sci, Washington U. in St. Louis

Kartik Hosanagar, Professor of Internet Commerce, Wharton School of U. of Pennsylvania

Ali Jadbabaie, Alfred Fitler Moore Professor of Network Science, Elec. & Sys. Engineering

Santosh Venkatesh, Associate Professor of Elec. & Sys. Engineering

Decision Making in Networked Systems

ACKNOWLEDGMENTS

I owe my deepest gratitude to my dissertation advisor and my mentor, Dr. Roch Guérin. Roch is a pioneer in the field of networking, a rigorous scientist and a visionary researcher, and has been a dedicated teacher and an inspiring role model for me. I am grateful for having his unreserved help, continuous guidance, and insightful recommendations throughout my PhD studies at Penn.

I would like to sincerely thank Dr. Santosh Venkatesh, my dissertation committee chair, for his generous support and his valuable lessons. I am also thankful to my dissertation committee members, Dr. Kartik Hosanagar and Dr. Ali Jadbabaie, for their time and for kindly offering me their advice.

I thank the National Science Foundation for supporting my research. This dissertation would not have been possible without funding from them.

I warmly thank my parents, Hassan and Banoo, for their selflessness, and for believing in their children, and for always encouraging their children to the pursuit of knowledge. I also thank my siblings, Elham, Somaieh, Maryam and Mohammad Reza.

My last and most special thanks to my fiancé, Golnar, for her love and her support, and for always being by my side even when my time and attention was devoted to the research.

ABSTRACT

Decision Making in Networked Systems

Mohammad Hadi Afrasiabi

Roch Guérin

Living in a networked world, human agents are increasingly connected as advances in technology facilitates the flow of information between and the availability of services to them. Through this research, we look at interacting agents in networked environments, and explore how their decisions are influenced by other people's decisions. In this context, an individual's decision may be regarding a concrete action, *e.g.,* adoption of a product or service that is offered, or simply shape her opinion about a subject. Accordingly, we investigate two classes of such problems. The first problem is the dynamics of service adoption in networked environments, where one user's adoption decision, influences the adoption decision of other users by affecting (positively or negatively) the benefits that they derive from the service. We consider this problem in the context of "User-Provided Connectivity", or UPC. The service offers an alternative to traditional infrastructure-based communication services by allowing users to share their "home base" connectivity with other users, thereby increasing their access to connectivity. We investigate when such services are viable, and propose a number of pricing policies of different complexities. The pricing policies exhibit differences in their ability to maximize the total welfare created by the service, and distributing the welfare between different stakeholders. The second problem is the spread of opinions in a networked environment, where one agent's opinion about an issue, influences and is influenced by that of other agents to whom she is connected. We are particularly interested in the role that people's adherence to specific groups or parties may play in how final opinions are formed. We approach this problem using a model of interactions inspired by the Ising spin-glass model from classical Physics. We consider two related but distinct settings, and show that when party memberships directly influence user interactions, even slightest statistical partisan biases result in partisan final outcomes: where everyone in a party shares the same opinion, opposite to that of the other party. On the other hand, if party membership plays an indirect role in biasing agent interactions, then there is room for intra-party heterogeneity of opinions.

Contents

Chapter 1

Introduction

Individuals[1] living in the networked modern world interact with each other in a variety of ways. They consume and share information, goods and services, whereby influencing each other's decisions and behaviors [33]. These interactions complicate the decision-making patterns in networked settings, and there has been growing interest in understanding and predicting such patterns [28,35,36], which require consideration of how individuals perceive and react to external influences, or "externalities".

The concept of externalities (also called "network effect") has been traditionally used for modeling the adoption of goods and services in networked settings [27]. A product with positive externalities, for example, is one that becomes more appealing as more people use it. In this research, we study[2] various problems in networked settings where individuals face complex positive and negative externalities, and investigate how the tug of war between different types of externalities shapes individuals' decisions and behaviors in those settings. In this context, an individual's decision may be regarding a concrete action, *e.g.,* adoption of a new product or service that is offered, or simply shape her opinion regarding a subject. In both cases, the person's decision includes a component that is contributed by others. Accordingly, we investigate two classes of such problems.

[1] We may use the terms "individual", "person" and "agent" interchangeably to refer to an entity in a networked setting, as may be represented by a "node" in the network's graph.

[2] This dissertation is based on work with Roch Guérin and Santosh Venkatesh, parts of which has appeared in [1–6].

The first problem is the dynamics of service adoption in networked environments, where one user's adoption decision influences the adoption decisions of other users by affecting (positively or negatively) the benefits that they derive from the service. We consider this problem in the context of "User-Provided Connectivity, or UPC, which we introduce in Section 1.1 with full investigation given in Chapter 3.

The second problem is the spread of opinions in networked environments, where one agent's opinion about an issue, influences and is influenced by that of other agents to whom she is connected. We are particularly interested in the role that people's adherence to specific groups or parties may play in how final opinions are formed. We introduce this problem in Section 1.2, with full investigation provided in Chapter 4.

In Chapter 2 we review the related work in this area.

1.1 Adoption of service in user-provided connectivity

Network services often exhibit positive and negative externalities that affect users' adoption decisions. One such service is "user-provided connectivity" or UPC. The service offers an alternative to traditional infrastructure-based communication services by allowing users to share their "home base" connectivity (see [64] for an example) with other users, thereby increasing their access to connectivity.

More users mean more connectivity alternatives, *i.e.,* a positive externality, but also greater odds of having to share one's own connectivity, *i.e.,* a negative externality. The tug of war between positive and negative externalities together with the fact that they often depend not just on how many but also *which* users adopt, make it difficult to predict the service's eventual success. We explore this issue, and investigate not only when and why such services may be viable, but also explore how pricing can be used to effectively and practically realize them.

Towards this goal, we develop a simple model that helps understand how the different factors interact and affect the adoption of a UPC service and the total welfare (sum of users' utility and provider's profit) it creates, and how that welfare can be efficiently distributed

between users and the service provider. To maintain analytical tractability, the model makes a series of simplifying assumptions, many of which may arguably not hold in practice. However, the analysis affords insight that, as we demonstrate, remains valid even under more general settings. Specifically, our main contributions consist of

- Formulating and solving a simple model that captures key features of a UPC type of service;
- Characterizing when and how the service's total welfare, or value, is maximized;
- Identifying practical pricing policies that realize a different trade-off between optimizing welfare and distributing it between stakeholders.
- Numerically validating the robustness of the findings, when relaxing the simplifying assumptions on which the model relies.

1.2 Opinion formation in biased networks

Social interactions commonly take place in a networked setting where an individual's opinion is influenced by the opinions of others. We allow this influence to be positive or negative, biased by partisan affiliations of connected individuals. Such signed influences are akin to the positive and negative externalities described earlier for the adoption of a UPC service. Our work explores the role of partisan influence in the emergence of consensus opinions in social network settings.

We study a network of nodes where each node holds an *opinion* — a binary state that may update over time under the influence of a node's neighbors. Nodes have biased affinities, which logically partition the network into distinct *parties*. Nodes in the same party tend to have a positive influence on each other, but the extent to which this holds varies across nodes and depends on the chosen affinity model.

We consider two variations on an Ising spin-glass network model (from classical physics) that investigate opinion formation in such biased affinity systems. These models differ in how they determine the pairwise influence between nodes.

The first of these in what we term the *random influence model* randomly selects the influence two nodes exert on each other based on their respective party affiliation. The second, a *profile-based model,* relies on a profile, a κ-bit vector of ± 1 entries based on the node's known positions regarding each of κ independent topics. In this model the similarity of the profiles of two nodes determines whether they have a positive or negative influence on each other's opinions.

We investigate the formation of opinions under both models and characterize their fixed points (equilibria). We show that while these systems always converge to a fixed point, they differ in their number and types of fixed points. Under a direct party impact as in the random influence model, opinions nearly always converge to a partisan outcome with parties settling on unanimous, antagonistic positions. In the profile-based model, the shift from a direct to an indirect role in how party affiliation impacts decisions translates into significant differences in the type of outcomes that can arise. In particular, party unanimity is not the norm anymore.

While we initially assume that all nodes are connected (full graph) and also that all nodes are members of one of two parties, with nodes from the same party more likely to exhibit a positive affinity bias, we later relax these assumption. Specifically, we introduce two set of modifications to our models. We first study the effect of a third group of nodes, *e.g.,* independent nodes who have unbiased affinities towards other nodes, irrespective of party affiliations. We then consider the impact of additional structure, in the form of an Erdős-Rényi graph (as opposed to a full graph), that determines which nodes interact with each other.

Chapter 2

Related works

The types of problems described in Chapter 1, that exhibit interconnected agents and mutual interactions, belong to a broader set of questions that naturally emerge in networked settings and have become prevalent in many different areas, *e.g.,* economics, social science, biology, engineering and political science. The growing importance of, and interest in, such questions is behind the emergence of "Network Science" as a new independent field [27, 33, 50, 76].

The breadth of topics that network science spans also means that multi-disciplinary approaches are typically needed when tackling problems [37, 47, 68]. This is well illustrated in our work, which relies on techniques from marketing research and statistical physics to tackle the problems of service adoption and opinion formation in the presence of party biases that it is concerned with. Similarly, researchers from seemingly disparate backgrounds have contributed to the field of network science. In the past decade, a number of books have aggregated the various studies in this field [33, 51, 54, 72, 90]. Such books provide a thorough review of the different techniques for study of network systems, as well as their implications and predictions.

In the next two sections we provide a more specific review of the literature as related to the particular problems that we study, namely, where the "externalities" play a prominent role in the system.

2.1 Adoption of products and services

The service adoption process that we introduce in Chapter 3 involves settings that are studied under the umbrella of systems theory and/or game theory in various fields, from engineering [8, 13, 46, 83] to economics [9]. In the language of the latter, our work considers a forward looking monopolistic service provider who tries to optimally price a service and offers it to a set of heterogeneous myopic users, who in turn play a best-response dynamics game until the system potentially reaches a pure-strategy Nash equilibrium.

Best-response dynamics [41] in game theory refers to scenarios where agents repeatedly improve their choice until a Nash equilibrium is reached. Such a procedure provides a plausible path to realizing a Nash equilibrium of the system, whence the agents are said to "learn the equilibrium" [78]. Learning in game theory is also considered in [40], and is closely related to the subjects of *potential games* [14, 69] and evolutionary game theory [87]. Another related area in game theory consists of the works on the concept of "price of anarchy" [59], which is similar in flavor to our discussion in Section 3.7.3 on sub-optimal welfare realization.

In studying systems with heterogeneous users and in the presence of externalities, it is common [7, 21, 25, 81] to assume some knowledge of the state of the system, *e.g.,* users' characteristics, or "types", for the other users and the provider. For instance, [25] assumes that the monopolist has complete knowledge of the graph structure and therefore is able to measure the individual network characteristics of each user. Similarly, [7] assumes that the seller knows the probability distribution for the users' valuation of the good, and that the knowledge of the state of the system can propagate to users. In our analytical models too, we assume that while the provider does not have knowledge of the individual user types, it knows their probability distribution[1]. We also assume that users know the state of the system, as the level of adoption and the type of current adopters can be inferred by a user by observing the available service coverage and the roaming traffic that goes through one's

[1]Such information can be obtained, for example, using techniques from marketing research as discussed in [45].

home base. As such, our models represent a game with "incomplete information", since while the distribution of users' utility function is known, individual users' utilities are not. Also, users have "perfect information", in that they know the moves previously made by all other players.

An important property of the adoption models that we introduce is that they exhibit both positive and negative externalities. There is a vast literature investigating the effect of externalities, often called *network effects* [34,62,63], but the majority of these works focus on either positive or negative externalities separately. For example, [24] investigates the impact of positive externalities on the product adoption decisions of individuals. The effect of positive externalities on the competition between technologies is considered in [39,55,56] and extended to include converters and switching costs in several other works, *e.g.,* [30,38,53,82]. Conversely, the impact of negative externalities, *e.g.,* from congestion, has been extensively investigated in the context of pricing for both communication networks [43, 57, 66, 75, 85] and transportation systems [16, 23, 58, 73].

The topic of optimal pricing for systems with *both* positive and negative externalities is less studied and seems to have been first addressed in [29] that sought to optimize a combination of provider's profit and consumers' surplus. Different pricing strategies were considered, including flat pricing and pricing strategies that account for the product "amount" consumed by a user, *i.e.,* akin to the usage-based pricing model of Section 3.5. Other works have been primarily conducted in the context of the theory of clubs first formally introduced in [22] (see [10, 77, 80] for more recent discussions). A club has a membership that shares a common good or facility, *e.g.,* a swimming pool, so that increases in membership have a positive effect (externality) by lowering the cost share of the common good, *e.g.,* lower maintenance costs of the shared swimming pool. At the same time, a larger membership also has a negative, congestion-like effect, *e.g.,* a more crowded swimming pool. In general, the co-existence of positive and negative externalities implies an optimal membership size (see also [52] for a recent interesting investigation that contrasts the outcomes of self-forming and managed memberships).

Club-like behaviors also manifest themselves in file-sharing peer-to-peer (p2p) systems. In a file-sharing p2p system, more peers increase the total resources available to store content. However, unless enough peers are willing to share their resources, more peers can also translate into a higher load on those peers willing to serve files to others, and/or a longer time for locating a desired file. This has then triggered the investigation of *incentive* mechanisms to ensure that enough peers share their resources, *e.g.,* BitTorrent "tit-for-tat" mechanism [31] or [32] that also explores a possible application to a wireless access system similar in principle to the one we consider in Chapter 3.

Our model differs from these earlier works in important ways. First and foremost, it introduces a model for individual adoption decisions of a service, which allows for heterogeneity in the users' valuation of the service. In particular, certain users (roaming users) have a strong disincentive to adoption when coverage/penetration is low, while others (sedentary users) are mostly insensitive to this factor. Conversely, this heterogeneity is also present in the negative externality associated with an increase in service adoption. Its magnitude is a function of not just the number of adopters, but their identity as well, *i.e.,* roaming or sedentary users. The presence of heterogeneity in how users value the service and how they affect its value is a key aspect of a UPC–like service; one that influences its value and how to price it to realize this value.

2.2 Formation and spread of opinions

Tools from statistical physics have been adapted for use in economics, models of neural computation, as well as to offer models of social interactions in network settings [15, 20, 71, 74]. In the latter setting, the phenomenon of community structure in social networks and graphs has seen some attention in the literature. Community structure refers to the presence of modular groups in networks where individual members inside a community are highly connected but connections between members of different communities are sparse or non-existent. In particular, members of any one community exert little or no influence on members of other communities.

Works in this area include [44], which uses centrality indices in graphs to detect community structure, [18] which identifies mechanisms to generate networks with community structure, and [60] which studies the formation of opinions in these settings.

These works reflect the tendency of individuals in a society to assemble in smaller groups that are not necessarily connected. They do not, however, capture partisan interactions between parts of a society, where individuals from different groups co-mingle and interact in a manner shaped by their respective party or group, in the process exerting positive and negative influences on each other.

Various models of positive and negative interactions in a spin glass framework have also been considered in the literature [15, 19]. In these settings agents are considered to be statistically exchangeable with no *a priori* biases in the strengths of their random interactions with other agents. These models lead to the characteristic disorder-induced phase transitions of spin glass models but do not in themselves make provision for partisan behaviour in opinion formation.

A variety of other models of opinion formation in sociological settings have been considered in the literature. These include the energy-driven Ising spin glass model, the voter model, the Szanjd model, and the bounded-confidence model [17, 26, 65, 67, 79, 86]. These models all feature agents influencing each other's opinions in a number of different ways. While the posited mechanisms vary, agent interactions in these models are *a priori unbiased* and their influence on each other is only through the prism of their opinions; there is no party or group structure influencing interactions. As we shall see in Chapter 4, fundamentally different behaviours arise when interactions are influenced, however slightly, by an over-arching party structure.

Chapter 3

User-Provided Connectivity

3.1 Introduction

There is no denying that we are a networked society, and many networked goods or services exhibit strong *externalities*, *i.e.,* a change — positive or negative — in the value of one unit of good, as more people use those goods. For example, Metcalfe's law [27, p.71] captures the positive effect on a network value of having more users, while the increased congestion that arises from the added traffic contributes a negative externality. Externalities, and more generally the benefits derived from goods or services, vary across users, *i.e.,* exhibit heterogeneity. This makes predicting the impact of externalities difficult, especially when positive and negative forces interact. A basic question of interest is then to determine (ahead of time) if and how offerings of goods or services that exhibit positive and negative externalities will succeed or fail.

The original motivation for this work was answering this question for a specific service, namely, *user provided connectivity* or UPC. The goal of UPC is to address the rising thirst for ubiquitous data connectivity fueled by the fast growing number of capable and versatile mobile devices. This growth has taxed the communication infrastructure of wireless carriers to the point where it is threatening their continued success [91]. Addressing this issue calls for either upgrading the infrastructure; a costly proposition, or exploring alternatives

for "off-loading" some of the traffic. WiFi off-load solutions (*e.g.,* as embodied in the Hotspot2.0 initiative of the WiFi Alliance and the Next Generation Hotspot (NGH) of the Wireless Broadband Alliance) offer a possible option, of which FON[1] demonstrated a possible realization. FON users purchase an access router (FONERA) that they use for their own local broadband access, but with the agreement that a (small) fraction of their access bandwidth can be made available to other FON users. In exchange, they receive the same privilege[2] when roaming, *i.e.,* can connect through the access points of other FON users.

Under a UPC scheme, connectivity grows "organically" as more users join the network and improve its coverage, and the challenge is to determine if it can reach sufficient critical mass to be viable. Consider for example a FON-like service starting with no users. This makes the service unattractive to users that value ubiquitous connectivity highly, *e.g.,* users that roam frequently, because the limited coverage offers little connectivity beyond that of a user's "home base". On the other hand, sedentary users are mostly insensitive to the initial minimal coverage, and if the price is low enough can derive positive utility from the service; hence join. If enough such (sedentary) users join, coverage may increase past a point where it becomes attractive to roaming users who will start joining. This would then ensure rapid growth of the service, were it not for a negative dimension to that growth.

Specifically, as more roaming users join, they compete for connectivity and may encounter increasingly congested access points. Conversely, sedentary users end-up having to share their home access more frequently. This may be sufficient to convince them to drop the service (unlike roaming users, they do not see much added value from the better coverage). The resulting reduction in coverage would in turn affect roaming users, who could then also start leaving. Hence, after an initial period of growth, the service may experience a decline.

The extent to which such behaviors arise depends on many factors, and in particular

[1] http://www.fon.com. See also AnyFi (www.anyfinetworks.com) or previously KeyWifi, and also more recently Comcast [64] for similarly inspired services.

[2] Alternatively, they can also be offered some form of compensation.

the trade-off between service cost and users' sensitivity to the positive and negative aspects of a growing user-base. Making the service "free" would clearly maximize adoption, but unless other revenue sources are available, *e.g.,* ads, is unlikely to allow it to be viable. Increasing the service price could affect (lower) adoption, but may improve its viability. More generally, service pricing offers a "control knob" that can be used to realize a variety of objectives, *e.g.,* maximizing overall value or welfare, or maximizing provider's profit, etc. This control knob can be complex and involve offering the service at a different price to each user, *i.e.,* discriminatory pricing [11], or very basic, *e.g.,* fixed pricing, and there is typically a trade-off between how well objectives can be met and the complexity of the control (pricing) used to meet them.

In this chapter we develop a simple model that helps understand how these factors interact and affect the adoption of a UPC service and the welfare (sum of users' utility and provider's profit) it creates, and how that welfare can be efficiently distributed between users and the service provider. To maintain analytical tractability, the model makes a series of simplifying assumptions, many of which may arguably not hold in practice. However, the analysis affords insight that, as we demonstrate, remains valid even under more general settings. Specifically, this chapter's main contributions consist of

- Formulating and solving a simple model that captures key features of a UPC type of service;
- Characterizing when and how the service's total welfare, or value, is maximized;
- Identifying practical pricing policies that realize a different trade-off between optimizing welfare and distributing it between stakeholders.
- Numerically validating the robustness of the findings, when relaxing the simplifying assumptions on which the model relies.

The rest of the chapter is structured as follows. Section 3.2 presents the model we rely on to capture the properties of a UPC service. Section 3.3 explores when and how the service value (total welfare) is maximized. Section 3.4 introduces the role of pricing in realizing different goals for the service, with subsequent sections dedicated to specific pricing

policies, *i.e.,* usage-based (Section 3.5), hybrid (Section 3.6), and fixed-price (Section 3.7). Section 3.9 discusses generalizations and robustness of the findings. A summary of the chapter's findings is provided in Section 3.10.

3.2 Model Formulation

This section introduces a model that captures key aspects of adoption of a UPC-like service by users. We first present the general form of the model in Section 3.2.1. We then introduce a series of simplifying assumptions in Section 3.2.2 to obtain a simpler model that is analytically tractable. Verifying that the findings afforded by this simplified model remain valid in more general situations calls for a two-prong approach: (1) An explicit solution is developed that offers a qualitative understanding of and insight into what drives the success (or failure) of UPC systems; (2) The robustness of those findings is then numerically tested under configurations that emulate more general settings, *i.e.,* where the model's simplifying assumptions are relaxed and errors are present in the estimation of its parameters.

3.2.1 General form

Given the expected organic growth of a UPC service, the interplay between the coverage it realizes and its ability to attract more users is of primary interest. The service coverage κ depends on the level x of adoption in the target user population, and determines the odds that users can obtain connectivity through the service while roaming. Users are heterogeneous in their propensity to roam, as captured through a variable $\theta, 0 \leq \theta \leq 1$. A user's exact θ value is private information, but its distribution (over the user population) is known. A low θ indicates a sedentary user while a high θ corresponds to a user that frequently roams. Hence, θ determines a user's sensitivity to service coverage.

As commonly done [24], a user's service adoption decision is based on the utility she derives from the service; she decides to adopt if that utility is positive. A user's utility is denoted as $U(\Theta, \theta)$, where θ is the roaming propensity of the user herself, and Θ identifies

the current set of adopters. The general form of $U(\Theta, \theta)$ is given in Eq. (3.1).

$$U(\Theta, \theta) = F(\theta, \kappa) + G(\theta, m) - p(\Theta, \theta)\,, \tag{3.1}$$

where m is the volume of roaming traffic generated[3] by the current set of adopters Θ.

$F(\theta, \kappa)$ reflects the overall utility of connectivity, either at home or roaming, while $G(\theta, m)$ accounts for the negative impact of roaming traffic. Finally, $p(\Theta, \theta)$ is the price charged to the user θ when the adopters' set is Θ.

Note that the price $p(\Theta, \theta)$ is a control parameter that affects service adoption, *i.e.,* it can be endogenized to achieve specific objectives. In this chapter, we explore the use of pricing to maximize total welfare and/or profit. Other parameters are exogenous and can be estimated, *e.g.,* using techniques from marketing research as discussed in [45], but not controlled.

Building on Eq. (3.1), users adopt the service only if their utility is positive, and are myopic when evaluating the utility they expect to derive from the service, *i.e.,* they do not anticipate the impact of their own decision on other users' adoption decisions. However, adoption levels affect coverage, and as coverage changes, so does an individual user's utility and, therefore, her adoption decision.

The level of adoption x is given by

$$x = |\Theta| \triangleq \int_{\theta \in \Theta} f(\theta)\, d\theta,$$

where $f(\theta)$ is a density function and reflects the distribution of roaming characteristics over the user population.

In the next section, we specialize the different terms in the utility function of Eq. (3.1).

[3]Each user is assumed to generate one unit of traffic, whether at home or roaming.

3.2.2 Assumptions and the simplified model

For analytical tractability, we make several assumptions regarding the form and range of the parameters of Eq. (3.1) (Section 3.9 explores the impact of relaxing these assumptions).

First, a user's propensity to roam, as measured by θ, is taken to be uniformly distributed in $[0, 1]$, *i.e.,*

$$f(\theta) = 1, \qquad 0 \leq \theta \leq 1.$$

This implies that given a set of adopters Θ, the adoption level, x is

$$x = \int_{\theta \in \Theta} d\theta \,. \tag{3.2}$$

Conversely, assuming that every user contributes one unit of traffic, the volume of roaming traffic m generated by current adopters is given by

$$m = \int_{\theta \in \Theta} \theta \, d\theta \,. \tag{3.3}$$

Next, we assume that the distributions of users over the service area and their roaming patterns are uniform. A uniform distribution of users implies that the adoption level x also measures the availability of connectivity to roaming users, hence $\kappa = x$. Similarly, uniform roaming patterns mean that roaming users (and traffic) are evenly distributed across users' home bases, *i.e.,* all see the same connectivity while roaming. Therefore, we can write the function $F(\theta, \kappa)$ as

$$F(\theta, \kappa) = (1 - \theta)\,\gamma + \theta\, r x \,. \tag{3.4}$$

The parameter $\gamma \geq 0$ measures the utility of basic home connectivity, while $r \geq 0$ reflects the utility of roaming connectivity.[4] The latter needs to be weighed by the "odds" that such connectivity is available, which are proportional to the current service coverage $\kappa = x$. Hence, rx is the (true) utility of roaming connectivity, when the level of coverage is $\kappa = x$.

[4]The range of the values of roaming connectivity is taken to be $r \geq \gamma$, *i.e.,* the value of roaming connectivity is at least as high as that of home connectivity.

The additional factors $1-\theta$ and θ in Eq. (3.4) capture the impact of a user's roaming characteristic in how it uses, and therefore values, home and roaming connectivity. Specifically, a user with roaming characteristic θ splits its connectivity time in the proportions θ and $1-\theta$ between roaming and home connectivity, respectively.

Further, the impact of roaming traffic is assumed proportional to its volume m, which based on the assumption of uniform roaming patterns, is equally distributed across adopters' home bases. Specifically, the (negative) utility associated with roaming traffic consuming resources in the home base of users is proportional to $-cm$, $c \geq 0$. Roaming traffic affects equally the users whose home base it uses, and the roaming users seeking connectivity through it. Hence, all users experience the same impact of the form $-\theta cm - (1-\theta)cm = -cm$, so that $G(\theta, m)$ is[5]

$$G(m) = -c\,m\,.$$

Under these assumptions, a user's utility is of the form

$$U(\Theta, \theta) = \gamma - c\,m + \theta\,(r\,x - \gamma) - p(\Theta, \theta)\,. \tag{3.5}$$

In the next section, we characterize the total welfare that can be created by a UPC service as a function of the service parameters (exogenous and endogenous).

3.3 Total Welfare

In this section, we characterize the total *welfare* (value) a UPC service can create for its adopters and provider. Adopters' welfare is through the utility they derive from the service, while the provider's welfare is from what it charges adopters for the service. Using the model introduced in the previous section, we derive analytical conditions under which the total welfare is maximized. As argued earlier, the benefit of such analytical solutions is in providing insight into when and why the service may be valuable (worth deploying).

[5]The range of the coefficient of roaming traffic, c, is taken to be $0 \leq c < r$, *i.e.,* it is lower than the max roaming utility.

The validity of that insight is tested under more general conditions in Section 3.9.

To compute the maximum welfare, we first obtain the optimal set of adopters $\Theta^*(x)$ for any given adoption level x, and then solve for the optimal x.

3.3.1 Optimal Adoption Set for Given Adoption Level

For a given adoption level x, we seek the set of adopters Θ, $|\Theta| = x$, that maximizes welfare.

Provider's welfare (or profit) W_P can be written as

$$W_P(\Theta) = \int_{\theta \in \Theta} (p(\Theta, \theta) - e)\, d\theta\,, \tag{3.6}$$

where $p(\Theta, \theta)$ is the price charged to a user with roaming characteristic θ given a set Θ of existing adopters, and e is the per customer cost of providing the service, *e.g.,* as incurred from billing, customer service, or equipment cost subsidies[6]. Conversely users' welfare is given by

$$W_U(\Theta) = \int_{\theta \in \Theta} U(\Theta, \theta)\, d\theta\,. \tag{3.7}$$

The service welfare, $V(\Theta)$, is the sum of these two quantities.

$$\begin{aligned} V(\Theta) &= W_U(\Theta) + W_P(\Theta) \\ &= \int_{\theta \in \Theta} \Big(U(\Theta, \theta) + p(\Theta, \theta) - e \Big)\, d\theta. \end{aligned} \tag{3.8}$$

For notational purposes, we denote the integrand in Eq. (3.8) by $v(\Theta, \theta)$,

$$v(\Theta, \theta) \triangleq U(\Theta, \theta) + p(\Theta, \theta) - e\,,$$

which can be interpreted as the *individual value* adopter θ contributes to the service. Using

[6]Note that this cost is ultimately born by the users, as it affects the price the provider charges for the service.

Eq. (3.5) we can rewrite Eq. (3.8) as

$$V(\Theta) = \int_{\theta \in \Theta} \Big(\gamma + \theta \left(rx - \gamma \right) - cm - e \Big) \, d\theta. \tag{3.9}$$

Characterizing optimal welfare for a given adoption level x, therefore calls for identifying the set $\Theta^*(x)$ of adopters of cardinality x, $|\Theta^*| = x$, which maximizes Eq. (3.9). This is the subject of the next lemma, which is proved in Appendix A.9 in a more general form.

Lemma 1. *For any adoption level x, maximum welfare is always obtained with a set of adopters $\Theta^*(x)$ that exhibit contiguous roaming characteristics. Specifically, $\Theta^*(x)$ is of the form*

$$\Theta^*(x) = \begin{cases} \Theta_1^*(x) = [0,\, x) & \text{if } x < \frac{\gamma}{r-c}, \\ \Theta_2^*(x) = [1-x,\, 1] & \text{if } x \geq \frac{\gamma}{r-c}. \end{cases} \tag{3.10}$$

3.3.2 Optimal Adoption Level

From Lemma 1, we obtain the optimal welfare $V^*(x) \triangleq V(\Theta^*(x))$ given any adoption level x. Following the partition of Eq. (3.10) into two cases $x \in [0,\, \frac{\gamma}{r-c})$ and $x \in [\frac{\gamma}{r-c},\, 1]$, we consider separately the cases of $V\left(\Theta_1^*(x)\right)$ and $V\left(\Theta_2^*(x)\right)$.

Using Eq. (3.10) in Eq. (3.3) gives for $x \in [0,\, \frac{\gamma}{r-c})$,

$$m(\Theta_1^*(x)) = \int_{\theta=0}^{x} \theta d\theta = \frac{x^2}{2},$$

and therefore by and Eq. (3.9)

$$V(\Theta_1^*(x)) = \frac{r-c}{2} x^3 - \frac{\gamma}{2} x^2 + (\gamma - e)x.$$

Similarly, for $x \in [\frac{\gamma}{r-c},\, 1]$, the roaming traffic corresponding to $\Theta_2^*(x)$ is

$$m(\Theta_2^*(x)) = \int_{\theta=1-x}^{1} \theta d\theta = \frac{1}{2} \left(2x - x^2 \right),$$

and therefore by Eq. (3.9)

$$V(\Theta_2^*(x)) = -\frac{r-c}{2}x^3 + (\frac{\gamma}{2} + r - c)x^2 - ex.$$

Combining the above expressions, the optimal service value $V^*(x) \triangleq V(\Theta^*(x))$ for a given adoption level x is given by

$$V^*(x) = \begin{cases} \frac{r-c}{2}x^3 - \frac{\gamma}{2}x^2 + (\gamma - e)x & \text{if } x < \frac{\gamma}{r-c} \\ -\frac{r-c}{2}x^3 + (\frac{\gamma}{2} + r - c)x^2 - ex & \text{if } x \geq \frac{\gamma}{r-c}, \end{cases}$$

where $\Theta^*(x)$ and x are related by Eq. (3.10).

Given $V^*(x)$, we can then solve for the value x^* that maximizes $V^*(x)$. The computations are mechanical in nature and are given in Appendix A.2, with Fig. 3.1 illustrating x^* as a function of γ and e (for $r - c = 1$).

The solution can be partitioned into two different regimes based on the value of γ. When $\gamma \leq r - c$ (corresponding to $\gamma \leq 1$ in Fig. 3.1), optimal adoption is either $x^* = 1$ or $x^* = 0$, depending on the service cost e. If the service cost is low ($e < \frac{\gamma+r-c}{2}$), then maximum welfare occurs for $x^* = 1$, and it is

$$V^*(x = 1) = \frac{\gamma + r - c}{2} - e. \tag{3.11}$$

Conversely, if the service cost is high ($e \geq \frac{\gamma+r-c}{2}$), then it overshadows any benefit or utility the service produces and it is impossible to create positive welfare. In this case, the "optimal" adoption is $x^* = 0$.

In contrast, when $\gamma > r - c$ (corresponding to $\gamma > 1$ in Fig. 3.1), intermediate values $0 < x^* < 1$ are possible (the gradient-shaded region of Fig. 3.1). This is because as γ increases, sedentary users start to derive more utility and progressively become the dominant value contributors. Therefore a set of (mostly) sedentary adopters can make a large positive welfare contribution. Furthermore, because this value is negatively affected by roaming

traffic, the optimal adoption level discourages frequently roaming users. Note that $r - c$ gives a tentative measure of the "net" importance of roaming (roaming utility factor less roaming traffic factor), and as such the condition $\gamma > r - c$ describes a system where home connectivity has a higher value than the overall ("net") effect of roaming connectivity. Such a system may arguably not be a prime candidate for UPC services.

In summary, the main finding that emerges from the results of this section is that when a UPC service can generate significant positive value, that value is typically maximized at full adoption (or close to full adoption[7]) Section 3.9 numerically tests the validity of this finding when the model's assumptions are relaxed.

While this section explored the relationship between service adoption and total welfare, and identified adoption sets that maximize total welfare, the next section focuses on how to *realize* such outcomes. As we shall see, this greatly depends on the flexibility of the pricing policy used.

3.4 Role of Pricing

The analysis of Section 3.3 characterizes maximum service welfare, but does not offer a constructive method to realize it. As shown in Eq. (3.5), adoption and, therefore, welfare, depend on $p(\Theta, \theta)$. Hence, maximizing welfare calls for identifying a suitable *pricing policy.*

Moreover, the price $p(\Theta, \theta)$ is also the parameter that determines how welfare is divided between users and the provider. For example, if $p(\Theta, \theta) = e$, then the provider is only compensated for its expenses e (its profit is $W_P(\Theta) = 0$) and the entire welfare is realized as user's utility, $W_U(\Theta) = V(\Theta)$. Conversely, if $p(\Theta, \theta) = v(\Theta, \theta) + e$, then $U(\Theta, \theta) = 0$, *i.e.,* users derive zero utility (strictly speaking, prices would be set to ensure an infinitesimal but positive utility) and all of the welfare is realized as provider's profit, $W_P(\Theta) = V(\Theta)$.

Other pricing schemes are possible that distribute welfare between users and the provider.

[7]Specifically in more general cases where coverage "saturates" with adoption, the maximum total welfare may predictably be realized at slightly below full adoption. The reason is reaching full adoption in that case would add more roaming traffic without meaningfully improving coverage. Details are given in Appendix A.2.

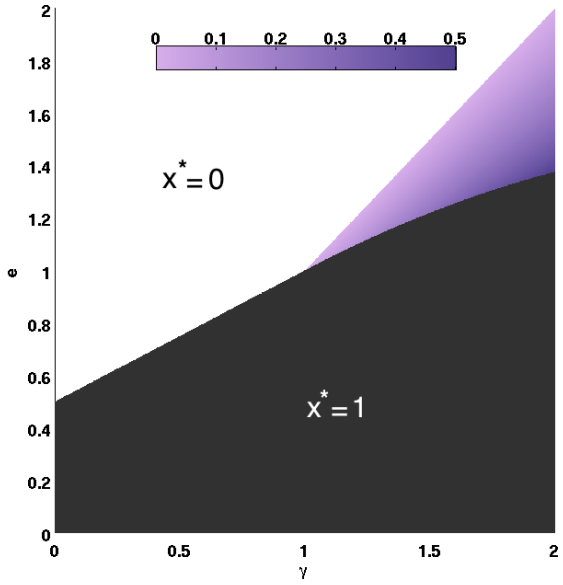

Figure 3.1: Regions of optimal adoption for maximum system value. Parameters are $r = 1.6$ and $c = 0.6$ (and therefore $r - c = 1$). The gradient-shaded area corresponds to $0 < x^* < 1$, whereas the solid black and white areas correspond to $x^* = 1$ and $x^* = 0$, respectively.

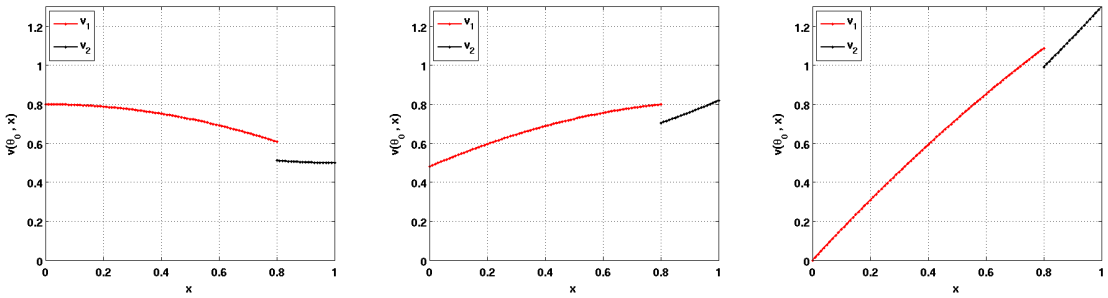

(a) $\theta_0 = 0$ (b) $\theta_0 = 0.4$ (c) $\theta_0 = 1$

Figure 3.2: System value contributed by user θ_0 as a function of x. Parameters are $\gamma = 0.8$, $e = 0$, $c = 0.6$, $b = 0$, $r = 1.6$.

For example, a price of the form

$$\begin{aligned} p(\Theta, \theta) &= v(\Theta, \theta) + e - \delta \\ &= (1 - \theta)\gamma + \theta r x - cm - \delta \,, \end{aligned} \tag{3.12}$$

which is an instance of a *discriminatory* pricing policy, leaves every user with a positive

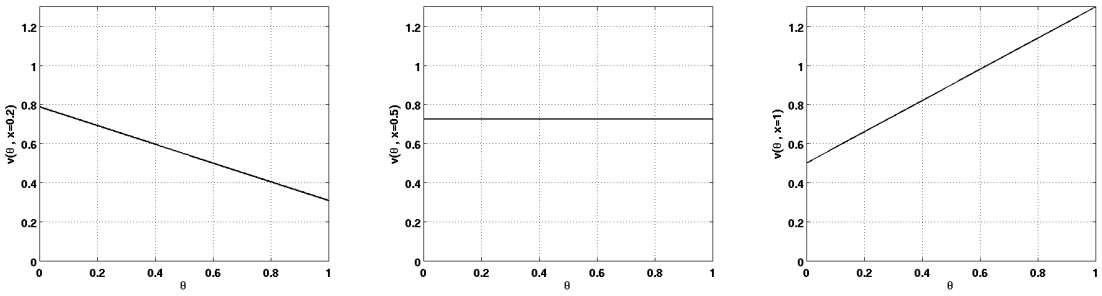

(a) $x = 0.2$ (b) $x = 0.5$ (c) $x = 1$

Figure 3.3: System value contribution across users, at different adoption levels. Parameters are $\gamma = 0.8$, $e = 0$, $c = 0.6$, $b = 0$, $r = 1.6$.

utility $U(\Theta, \theta) = \delta > 0$, hence realizing the optimal adoption level[8] $x = 1$. Therefore, the optimal welfare $V^*(1)$ of Eq. (3.11) is realized and by using $U([0, 1], \theta)$ in Eq. (3.7) it follows that the users' overall welfare is

$$W_U([0, 1]) = \delta\,.$$

This means that without affecting adoption, we can pick any $\delta > 0$ to freely vary $W_U([0, 1])$ in the range $(0, V^*(1)]$, and accordingly by Eq. (3.8),

$$W_P([0, 1]) = V^*(1) - W_U([0, 1]). \tag{3.13}$$

In short, this policy realizes two important goals

- Optimal welfare, and
- Flexible welfare distribution.

Such a discriminatory pricing policy is, however, difficult to implement in practice as it requires knowledge of individual user characteristics (θ) that may not be readily available[9],

[8] When optimal adoption is not at $x = 1$, optimal welfare can still be realized by setting a high price for users who should not adopt.

[9] Even if the provider has full knowledge of individual user characteristics θ, it may not be acceptable to charge users differently.

and also results in a price that varies with the adoption level x. This heterogeneity across both users and adoption levels is illustrated in Figs. 3.2 and 3.3, that plot $v(\Theta, \theta)$ as a function of θ and x.

In the following sections, we introduce pricing policies that offer a different trade-off between realizing maximum welfare, distributing it arbitrarily, and practicality.

3.5 Usage-based Pricing Policy

As mentioned above, a discriminatory pricing policy can both maximize total welfare and distribute it arbitrarily between users and the provider. It is, however, difficult to implement in practice. This section proposes a *usage-based* pricing scheme that mimics the behavior of the discriminatory policy, but makes it feasible in practice. Under a usage-based pricing scheme, users are charged based on how often they connect at home and while roaming. We present next the structure of usage-based pricing, how it is able to capture key aspects of discriminatory pricing, and also the insight that the analysis of the pricing policy affords.

3.5.1 Pricing Structure

In a UPC service, usage has two components, *home usage* denoted by z_h, and *roaming usage* denoted by z_r. A usage-based pricing policy may assign different prices to these two usage types. Assuming that p_h and p_r are unit prices for home and roaming usage, respectively, a user is charged

$$p_z(z_h, z_r) = z_h \cdot p_h + z_r \cdot p_r - a, \tag{3.14}$$

where a corresponds to fixed usage allowance that may be given to each user, *e.g.,* akin to the free minutes commonly included in cellular phone plans.

Eq. (3.14) states what a user pays for the service as a function of her usage. Next, we express this cost in terms of the user and service model of Section 3.2. This calls for characterizing how roaming characteristics θ and the service coverage x affect a user's home and roaming usages.

By definition, θ denotes a user's propensity to roam, *i.e.,* how often she is roaming versus at home. However, because a roaming user successfully connects only where there is coverage, her "typical" roaming usage is only $\overline{z}_r(x, \theta) = \theta x$. Conversely, her typical home usage is simply $\overline{z}_h(\theta) = 1 - \theta$ (home connectivity is always available). Replacing z_h and z_r in Eq. (3.14) by the typical roaming and home usages $\overline{z}_r(x, \theta)$ and $\overline{z}_h(\theta)$ of a user with roaming characteristics θ, we obtain the following expression for what she will typically be charged for using a UPC service with a coverage level of x

$$\overline{p}_z(x, \theta) = p_h(1 - \theta) + p_r\, \theta x - a. \tag{3.15}$$

Eq. (3.15) has three parameters p_h, p_r and a that affect service adoption, *i.e.,* which users derive positive utility. Given our goal of emulating the discriminatory pricing policy of Eq. (3.12) and by comparing it to Eq. (3.15), we choose $p_h = \gamma$ and $p_r = r$, which yields the following usage-based pricing scheme

$$\overline{p}_z(x, \theta) = \gamma(1 - \theta) + r\theta x - a. \tag{3.16}$$

We note that the only difference between Eq. (3.16) and the discriminatory pricing of Eq. (3.12) is in the terms a versus $cm - \delta$, where the former is constant while the latter depends on the level of roaming traffic m. As we shall see next, this difference is minor, and the usage-based pricing policy of Eq. (3.16) is capable of realizing both maximum welfare and flexibility in how welfare is distributed across users and the provider.

3.5.2 Maximal Service Adoption

Using Eq. (3.16) in Eq. (3.5) gives the following expression for the utility derived by user θ from adopting the service

$$U(\Theta, \theta) = a - cm. \tag{3.17}$$

We next use Eq. (3.17) to identify the adoption *equilibria* under usage-based pricing. We say a set of adopters Θ comprises an equilibrium when

$$U(\Theta, \theta) > 0, \quad \text{if} \quad \theta \in \Theta, \qquad \text{and}$$
$$U(\Theta, \theta) \leq 0, \quad \text{if} \quad \theta \notin \Theta.$$

Then,

Proposition 1. *Under the usage-based pricing policy of Eq. (3.16), full adoption, $x = 1$, is the **unique** equilibrium if $a > c/2$, and is not an equilibrium if $a \leq c/2$.*

Proof. Recall that $c \geq 0$, and note that at any adoption level x (corresponding to an adopters' set Θ such that $|\Theta| = x$), the roaming traffic m satisfies $m \leq 1/2$. Hence, $cm \leq c/2$ and Eq. (3.17) yields that $U(\Theta, \theta) \geq a - c/2$. Consequently $U(\Theta, \theta) > 0$ if $a - c/2 > 0$. This is true for all values of θ and Θ, *i.e.,* all users have positive utility at all adoption levels. Therefore no other equilibrium can exist, since that would mean for some $\widehat{\Theta} \neq [0, 1]$, and for $\theta \notin \widehat{\Theta}$ the utility is negative, which is contradictory. This proves sufficiency.

On the other hand, if $a \leq c/2$, then by Eq. (3.17) we have $U(\Theta, \theta) \leq c/2 - cm$. But at full adoption $m = 1/2$ and therefore $U([0, 1], \theta) \leq 0$, which means $[0, 1]$ cannot be an equilibrium. This completes the proof. □

Proposition 1 implies that the usage-based pricing policy maximizes total welfare by realizing full adoption[10], provided the provider sets the usage allowance a higher than the threshold $c/2$. The threshold's value $c/2$ is clearly specific to the assumptions on which the model is predicated. However, as we will see in Section 3.9, such a threshold condition is present under more general conditions. In particular, as long as the usage allowance a is larger than a threshold a_0, full adoption is the unique equilibrium, while if $a \leq a_0$, full adoption is then not an equilibrium.

We explore next the policy's ability to distribute welfare between users and the provider.

[10] Assuming that the parameters are such that total welfare is maximized at $x = 1$.

3.5.3 Welfare Distribution

From Eq. (3.17), the utility of user θ at full adoption is

$$U([0,\,1],\,\theta) = a - \frac{c}{2}.$$

Combining this expression with Eq. (3.7) gives the overall user welfare

$$W_U([0,\,1]) = a - \frac{c}{2}\,,$$

with provider's profit given accordingly by Eq. (3.13).

This means that we can pick any $a > c/2$ without affecting adoption, and therefore freely vary *both* $W_U([0,\,1])$ and $W_P([0,\,1])$ in the full range $[0,\,V^*(1))$.

Although, as mentioned earlier, the usage-based policy does not perfectly emulate the discriminatory policy of Eq. (3.12), it coincides with it at full adoption through the change of variables $\delta \triangleq a - c/2$. Hence, a usage-based pricing policy offers a practical solution to realize optimality and flexibility (in distributing welfare).

Those benefits notwithstanding, implementing usage-based pricing calls for monitoring (logging) usage, which incurs a cost. In addition, some users may prefer the predictability of fixed pricing (independent of usage), even in cases where it may be less advantageous for them [61], *i.e.,* result in a lower utility. This is particularly so in the case of home-connectivity, for which fixed pricing is often the norm. For instance, Time Warner recently announced [84] that its customers would always retain the option of a flat-rate monthly pricing for broadband Internet access, with usage-based plans being optional.

For those reasons, we consider next a *hybrid* pricing policy that combines fixed and usage-based pricing, and evaluate the trade-offs it imposes.

3.6 Hybrid Usage-based Pricing Policy

Consider a pricing policy that combines a fixed price for home connectivity, and a usage-based price for connectivity while roaming.

3.6.1 Pricing Structure

Using notation similar to Section 3.5.1, let z_r denote the roaming usage of a user. The total hybrid usage-based price that a user is charged is then

$$p_y(z_r) = p_h + z_r \cdot p_r, \tag{3.18}$$

where the price of home usage is fixed (independent of usage) at p_h and identical for all users[11], and as before p_r is the unit usage price while roaming.

The only user-dependent term in Eq. (3.18) is, therefore, her roaming usage. Recalling the discussion of Section 3.5.1, the typical roaming usage $\overline{z}_r(x, \theta)$ of a user with roaming profile θ when the service coverage is x is equal to θx. Hence, the typical cost to a user with profile θ for the service is given by

$$\overline{p}_y(x, \theta) = p_h + p_r\, \theta x, \tag{3.19}$$

Next, we investigate if and how p_h and p_r can be set to again emulate the discriminatory policy of Eq. (3.12), or more importantly achieve the same outcomes, namely, maximum welfare and flexibility in allowing distribution of welfare across users and the provider. As per the discussion of Section 3.4, the former calls for selecting p_h and p_r so as to ensure full adoption, *i.e.*, $x = 1$.

[11] Note that the usage allowance a is now included in p_h.

3.6.2 Maximal Service Adoption

Given the price structure of Eq. (3.19), the utility of a user can be obtained from Eq. (3.5) as

$$U(\Theta,\, \theta) = \gamma - cm - p_h + \theta(rx - \gamma - xp_r).$$

By applying the change of variables

$$\delta_h = \gamma - \frac{c}{2} - p_h \quad \text{and} \quad \delta_r = r - \gamma - p_r\,,$$

$U(\Theta,\, \theta)$ can be rewritten as

$$U(\Theta,\, \theta) = \frac{c}{2} - cm + \delta_h + \theta(x(\delta_r + \gamma) - \gamma). \tag{3.20}$$

Note that δ_h corresponds to the net residual utility for home connectivity at full adoption, and conversely δ_r is the corresponding quantity for roaming connectivity.

The next Lemma provides conditions under which full adoption is an equilibrium.

Lemma 2. *Under the hybrid pricing of Eq. (3.19), full adoption, $x = 1$, is an equilibrium if and only if $\delta_h > 0$ and $\delta_r > -\delta_h$.*

Proof. At full adoption we have $\Theta = [0, 1]$, $x = 1$ and $m = 1/2$. Therefore the utility of Eq. (3.20) becomes

$$U([0,\, 1],\, \theta) = \delta_h + \theta\delta_r.$$

For $\Theta = [0, 1]$ to be an equilibrium, all users must have positive utility. This implies

$$\delta_h + \theta\delta_r > 0\,, \quad \forall\theta \in [0, 1].$$

Since this is a linear function of θ, the inequality holds if and only if it is satisfied for both $\theta = 0$ and $\theta = 1$, *i.e.*, $\delta_h > 0$ and $\delta_h + \delta_r > 0$. □

The conditions of Lemma 2 state that full adoption, $x = 1$, is possible only if the fixed

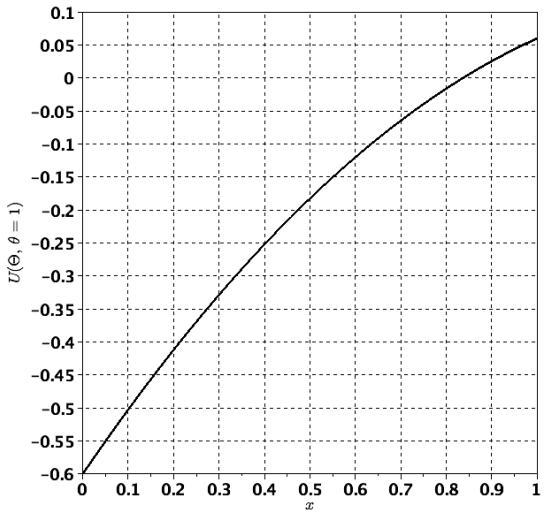

Figure 3.4: Utility of a user with $\theta = 1$ as a function of coverage under hybrid pricing for $\gamma = 1$, $c = 0.7$, $\delta_h = 0.05$ and $\delta_r = 0.01$.

price p_h for home connectivity is not too high, *i.e.,* $\delta_h > 0 \Rightarrow p_h < \gamma - \frac{c}{2}$, and the roaming usage-based price p_r is no higher than the net roaming value at full adoption, $r - \frac{c}{2}$, minus the price p_h already charged for home connectivity, *i.e.,* $\delta_r > -\delta_h \Rightarrow p_r < r - \frac{c}{2} - p_h$.

Unlike the conditions of Proposition 1 that ensured positive utility for all users at *all* levels of coverage, Lemma 2 does not include such guarantees. In particular, and as illustrated in Fig. 3.4 for the $\theta = 1$ user, the utility of a user can vary from negative to positive as coverage increases, with a cross-over value of $x \approx 0.85$ in the case of Fig. 3.4. The $\theta = 1$ user, therefore, adopts only once coverage exceeds 0.85. Hence, her adoption depends on the adoption of enough other users ($x > 0.85$). In general, and as hinted at in Fig. 3.3, users with low θ values have higher utility at low coverage, and are therefore the ones joining the service when it is first offered. As they do, the service becomes more valuable for users with higher θ values, whose utility may then become positive allowing them to adopt. This progression can, however, stall before full adoption is reached, *i.e.,* adoption may stop at a level $x < 1$. This can arise even under the conditions of Lemma 2, as Lemma 2 does not guarantee the uniqueness of the $x = 1$ equilibrium.

As shown in Appendix A.3, when the conditions of Lemma 2 hold, $x = 1$ is the *unique* equilibrium if and only if γ satisfies

$$\gamma < c + 2\delta_h + 2\sqrt{(c/2 + \delta_h)(\delta_r + \delta_h)}. \tag{3.21}$$

This then ensures that adoption increases monotonically until reaching full adoption. The condition of Eq. (3.21) can be combined with Lemma 2 to obtain the equivalent of Proposition 1 for the hybrid pricing policy.

Proposition 2. *Under the hybrid pricing of Eq. (3.19), full adoption, x=1, is the* ***unique*** *equilibrium if and only if*

- *When* $\gamma < c$: $\quad \delta_h > 0$ *and* $\delta_r > -\delta_h$
- *When* $\gamma \geq c$: $\quad \delta_h > 0$ *and* $\delta_r > -\delta_h$ *and*

$$\delta_h > \frac{\gamma^2}{4(\gamma + \delta_r - c/2)} - c/2. \tag{3.22}$$

Proof. As a result of the two conditions $\delta_h > 0$ and $\delta_r > -\delta_h$ and because $c \geq 0$ it follows that $2\delta_h + 2\sqrt{(c/2 + \delta_h)(\delta_r + \delta_h)}$ in Eq. (3.21) is always positive. Therefore Eq. (3.21) always holds if $\gamma < c$, without further constraints on the values of δ_h and δ_r.

On the other hand, when $\gamma \geq c$, δ_h and/or δ_r need to be large enough to ensure that Eq. (3.21) is satisfied. Specifically, algebraic manipulation of Eq. (3.21) in this case yields Eq. (3.22). □

Proposition 2 states that when $x = 1$ is an equilibrium under hybrid pricing, it can coexist with other equilibria when the value of home connectivity utility is high enough, *i.e.*, $\gamma \geq c$ and the condition of Eq. (3.22) is not satisfied. Focusing on cases when $x = 1$ maximizes total welfare, *e.g.*, e is low enough, this means that it is possible for the provider to set prices p_h and p_r (and consequently δ_h and δ_r) for which full adoption is feasible, *i.e.*, the conditions of Lemma 2 are satisfied, without ever being able to reach this target. This

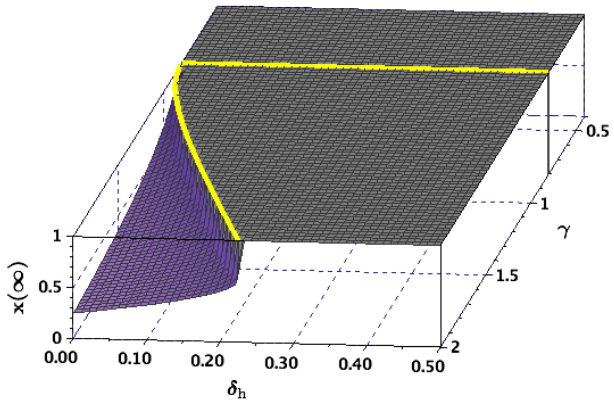

Figure 3.5: Final adoption level for the hybrid pricing policy, and identification of the boundaries demarcating the regions associated with the conditions of Proposition 2. The straight line corresponds to $\gamma = c = 0.8$, and the curved line captures the condition of Eq. (3.22). The system's parameters are $c = 0.8$, $\delta_r = 0$, with γ and δ_h values varying.

occurs when the provider's choice of prices allows the emergence of a *second* equilibrium $\widetilde{x} < 1$, where adoption stops upon reaching it.

As Proposition 2 indicates though, it is possible to avoid such outcomes by properly selecting prices (parameters δ_h and δ_r) to comply with Eq. (3.22). This is illustrated in Fig. 3.5, which plots the system's final adoption as γ and δ_h vary for the case $c = 0.8$ (initial adoption is set to $x = 0$, and for simplicity we assume $\delta_r = 0$ and focus on the impact of varying δ_h). The figure confirms (straight boundary line at $\gamma = c = 0.8$ in the figure) that when $\gamma < c = 0.8$, any value of $\delta_h > 0$ results in full adoption. It also shows that when $\gamma \geq c = 0.8$, the system only converges to full adoption when δ_h further satisfies the condition of Eq. (3.22) (corresponding to δ_h values that lie to the right of the curved boundary line in the figure).

The conditions of Proposition 2 are clearly specific to the assumptions on which the model is predicated. However, we will see in Section 3.9 that the very same behavior arises under more general settings; specifically, a second, sub-optimal equilibrium ($\widetilde{x} < 1$) can arise whenever the value of home connectivity exceeds a certain threshold, and in the process prevent the system from reaching its intended target of full adoption. In addition,

overcoming this issue can again be accomplished by adjusting prices, albeit to different values than those of Proposition 2.

We note that the aspect of adjusting (lowering) prices to ensure full adoption begs the question of what would motivate the provider to do so. We explore this issue next in the broader context of the hybrid pricing policy's ability to distribute welfare between users and the provider. We first explore the pricing policy's ability to support arbitrary welfare distribution at full adoption, including maximizing the provider's profit, and then focus on the extent to which the conditions of Proposition 2 constrain this ability, and what options are available to overcome those limitations.

3.6.3 Welfare Distribution

As before, we focus on scenarios for which total welfare is maximized at full adoption, *i.e.,* combinations that, as illustrated in Fig. 3.1, correspond to a low enough cost e relative to the other system's parameters γ, c, and r. We explore first whether, once at full adoption (and maximum total welfare), the hybrid pricing policy allows an arbitrary distribution of welfare (as the usage-based policy did), from maximum user welfare to maximum provider profit.

Lemma 2 identifies the constraints that pricing must satisfy to ensure that full adoption is an equilibrium, *i.e.,* $\delta_h > 0$ and $\delta_r > -\delta_h$. Combining Eq. (3.20) and Eq. (3.7) gives the following expression for the users' welfare $W_U([0,\,1])$ at full adoption

$$W_U([0,\,1]) = \delta_h + \frac{\delta_r}{2}\,, \tag{3.23}$$

with according to Eq. (3.13) and Eq. (3.11), the provider's profit given by

$$W_P([0,\,1]) = \frac{\gamma + r - c}{2} - e - \left(\delta_h + \frac{\delta_r}{2}\right). \tag{3.24}$$

Realizing maximum user welfare calls for choosing prices such that $W_P([0,\,1]) = 0$, which

according to Eq. (3.24) implies

$$\delta_h + \frac{\delta_r}{2} = \frac{\gamma + r - c}{2} - e.$$

This can be readily accomplished by choosing values of δ_h and δ_r that also satisfy Lemma 2, *e.g.*, $\delta_h = \epsilon > 0$, and $\delta_r = \gamma + r - c - 2e - 2\epsilon > -\epsilon$, where ϵ is arbitrarily small. Conversely, maximizing the provider's profit calls for setting prices that extract (nearly) all the value users realize from the system, *i.e.*, set both δ_h and δ_r equal to arbitrarily small positive values (this again satisfies the conditions of Lemma 2, namely, $\delta_h > 0$ and $\delta_r > -\delta_h$).

Intermediate distributions of welfare are also feasible simply by adjusting the values of δ_h and δ_r. Consider for example a scenario where a regulator wants all users to see the same utility value $\alpha > 0$. From Eq. (3.20) the utility of a user with roaming parameter θ is given by

$$U([0,\,1],\,\theta) = \delta_h + \theta\delta_r = \alpha\,.$$

Eliminating the dependency on θ to ensure that all users see the same utility requires $\delta_r = 0$, which then implies $\delta_h = \alpha > 0$ that again satisfies the conditions of Lemma 2. Hence, we see that *once at full adoption* (and assuming full adoption maximizes welfare), the hybrid pricing policy, like the usage-based policy, is capable of achieving any arbitrary distribution of welfare between users and the provider. However as made explicit in Proposition 2, *reaching* full adoption can, as reflected in Eq. (3.22), impose additional conditions on pricing, which may preclude some welfare distribution configurations. In particular, maximizing the provider's profit, which as just discussed calls for setting both δ_h and δ_r to arbitrarily small positive values, readily conflicts with the conditions of Eq. (3.22).

A possible approach suggested by the discussion of Section 3.6.2, is for the provider to offer an *introductory* pricing that satisfies the conditions of Proposition 2; thereby enabling full adoption to be reached. The motivation for the provider to do so is that once full (or nearly full[12]) adoption has been reached, it can then switch to a pricing scheme that allows

[12]See Appendix A.3 for details on how early the service provider can end the introductory pricing phase.

it to extract a higher profit.

In the next section, we introduce a third family of pricing policies that seeks to eliminate all dependency on monitoring a user's usage; therefore simplifying implementation and possibly facilitating user acceptance.

3.7 Fixed Price Policy

This section considers a pricing policy based on a fixed price that covers both home and roaming connectivity.

As mentioned earlier, the use of a fixed price is not uncommon for home connectivity, but it is arguably less so for wireless roaming access which is the other component of the service we consider. Nevertheless, a number of wireless carriers do offer fixed-price wireless services [89]. Hence it is of interest to investigate the impact such a pricing policy might have on their ability to maximize profit and on the welfare the system realizes.

3.7.1 Pricing Structure

Pricing is independent of usage and based on a single parameter p,

$$p(\Theta, \theta) = p, \forall\, \Theta, \theta. \tag{3.25}$$

We investigate if and how p can be set to realize maximum welfare and flexibility in distributing it across stakeholders. As per the discussion of Section 3.4, the former (typically) calls for selecting p so as to ensure full adoption, *i.e.,* $x = 1$.

3.7.2 Maximum Service Adoption

Given Eq. (3.5) and the price structure of Eq. (3.25), the utility of user θ is

$$U(\Theta, \theta) = \gamma - p - c\,m + \theta\,(r\,x - \gamma)\,. \tag{3.26}$$

Cases	$[0, \gamma/r)$	$[\gamma/r, 1]$
1	—	—
2	•	—
2'	⟳	—
3	—	•
3'	—	⟳
4	•, ○	—
5	—	•, ○
6	•, ○	•
7	•	•, ○
8	•, ○	•, ○

Table 3.1: Equilibria combinations under fixed pricing

The following Lemma then gives the condition under which full adoption is an equilibrium. The proof is in Appendix A.4.

Lemma 3. *Under the fixed price policy of Eq. (3.25), full adoption is an equilibrium if and only if* $p < \gamma - c/2$.

Note that as was the case with Lemma 2, the condition of Lemma 3 does not imply uniqueness of the $x = 1$ equilibrium. In fact, as shown in Appendix A.4, under fixed pricing there may be as many as four equilibria, spanning combinations of stable, unstable, periodic, or chaotic equilibria. Table 3.1 summarizes possible combinations, with (•) denoting stable equilibria, (○) unstable equilibria, (⟳) equilibria associated with an "orbit" that can be either convergent, periodic, or chaotic, and (—) the absence of equilibria.

Ensuring that $x = 1$ is the unique (stable) equilibrium, and therefore that the service always reaches full adoption, calls for additional constraints on p beyond those of Lemma 3. These constraints are formalized in the next Proposition, which mirrors the conditions of Proposition 1 for usage-based pricing. The proof is again in Appendix A.4.

Proposition 3. *Under the fixed price policy of Eq. (3.25), full adoption,* $x = 1$*, is the*

unique *equilibrium if and only if*

$$p < \min\left(\gamma - c/2, \gamma - \frac{\gamma^2}{4r - 2c}\right) .$$

The conditions of Proposition 3 ensure that total welfare is maximized under a fixed price policy. Next, we see if and how these conditions limit the policy's ability to distribute welfare between users and the provider.

3.7.3 Welfare Distribution

From Eq. (3.26), the utility of user θ at full adoption is

$$U([0,\,1],\,\theta) = (1-\theta)\gamma + \theta r - p - c/2\,,$$

which when combined with Eq. (3.7), gives the following expression for user welfare

$$W_U([0,\,1]) = \frac{\gamma + r - c}{2} - p\,,$$

with Eq. (3.13) correspondingly giving the provider's profit as

$$W_P([0,1]) = p - e\,.$$

As before, flexibility in distributing welfare calls for being able to vary $W_U([0,\,1])$ across the full range $(0,\,V^*(1)]$, where $V^*(1) = \frac{\gamma+r-c}{2} - e$. Clearly, this cannot be achieved without violating the conditions of Proposition 3, *e.g.*, $W_U([0,1]) = 0$ calls for $p = \frac{\gamma+r-c}{2} \geq \gamma - c/2$ (recall that $r \geq \gamma$). Therefore the service is not capable of realizing full adoption and maximizing the provider's profit (see Appendix A.4 for a full discussion).

Under hybrid pricing, we suggested the use of introductory prices to first realize full adoption, and then perform the desired welfare allocation. Unfortunately, this is not sufficient under fixed pricing, as certain welfare allocations are incompatible with not just Proposition 3, but also Lemma 3. In particular and as mentioned above, $W_U([0,\,1]) \approx 0$

calls for a price $p \geq \gamma - c/2$ that violates the conditions of both the Lemma and the Proposition. Hence, after an introductory price expires, it forces a drop in adoption below $x = 1$ and prevents welfare maximization.

In other words, the simplicity of the fixed price policy comes at a cost in terms of its ability to simultaneously maximize and distribute welfare. The concern is that this limitation may result in sub-optimal welfare realizations (and lower service coverage), as the provider may be tempted to set prices to maximize profit.

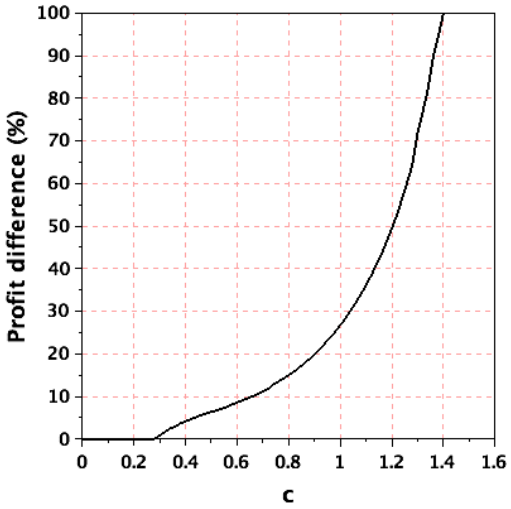

Figure 3.6: Relative profit drop from profit maximization to welfare maximization (fixed-price policy $\gamma = 1, r = 2$ and $e = 0.3$).

Fig. 3.6 helps assess the extent to which this may be a risk. It plots as a function of c and for a combination of parameters $\gamma = 1, r = 2$, and $e = 0.3$, the relative difference in profit between a profit maximizing choice of p and one that yields the best possible profit while also maximizing welfare, *i.e.,* maintaining $x = 1$. The figure indicates that as long as c remains relatively small (compared to γ and r), the incentive to deviate from a welfare maximizing price is small. As a matter of fact, when c is very small maximizing profit and welfare coincide even though welfare cannot be entirely realized as profit (this is an intrinsic limitation of the fixed-price policy). As the negative impact of roaming traffic, c, grows larger, it however becomes increasingly tempting (profitable) for the provider to deviate

from a welfare maximizing strategy and set a price that keeps adoption low. Arguably though, such scenarios where users are highly sensitive to the (negative) impact of roaming traffic are inherently not conducive to the large-scale deployment of a UPC like service.

The analysis of this section and its illustration in Fig. 3.6, are clearly dependent on the specific assumptions of the model. However, as demonstrated in Section 3.9, the findings hold even under more general conditions.

In summary, although the fixed price policy exhibits clear limitations in its ability to jointly maximize welfare and profit, its simplicity still makes it an attractive candidate, at least in scenarios where users are relatively insensitive to the negative aspects of a UPC service (small c values). In addition and as discussed in Appendix A.4, setting the price to maximize profit can be "risky," as the optimal price is such that small errors in parameter estimation can produce a dramatic collapse in adoption and consequently profit[13]. This should make the safer welfare maximization policy more appealing to the service provider.

3.8 Subsidies and pricing by user choice

As we saw, while a UPC service can generate significant value, fully realizing it calls for relatively complex pricing. In this section we show that successful outcomes under any pricing policy often require the ability to subsidize a subset of users, which could in turn render pricing even more complex. We then propose the *Price choice policy,* that seeks to realize another effective compromise between pricing complexity and the policy's ability to maximize system value and extract profit. We illustrate the benefits of the proposed policy by demonstrating when and how it outperforms previously proposed policies.

3.8.1 The Need for Subsidies

We showed in Section 3.3 that under the adoption model of Eq. (3.5), the total system value is generally[14] maximized at full adoption, *i.e.,* when all users adopt the service. An

[13] In other words, the underlying optimization is inherently fragile.

[14] That is, when the per-user service implementation cost, e, is *not* too high.

important goal for a pricing policy is, therefore, achieving full adoption, while also enabling the service provider to recoup most of the service value as profit. As we shall see now, this may require subsidizing a subset of users to achieve full adoption, and therefore maximum service value.

Before we proceed, it will be helpful to rewrite Eq. (3.5) as

$$U(\Theta,\, \theta) = U_i(\Theta,\, \theta) - p(\Theta,\, \theta)\,, \tag{3.27}$$

where

$$U_i(\Theta,\, \theta) = \gamma\,(1-\theta) + \theta\, r\, x - c\, m.$$

is the value or *intrinsic* utility the user derives from the service.

Eq. (3.27) readily shows that full adoption, *i.e.,* $\Theta = [0,1]$, implies[15] $p([0,1],\theta) < U_i([0,1],\theta)$, $\forall\theta \in [0,1]$. An immediate consequence of this observation is that subsidies are needed, *i.e.,* $p([0,1],\theta) < 0$, whenever $U_i([0,1],\, \theta) \leq 0$ for some θ value. The next proposition characterizes when this arises and the users to which it applies.

Proposition 4. *Users requiring subsidies at full adoption have roaming characteristics that satisfy*

$$\theta < \theta^* \triangleq \frac{cm^* - \gamma}{r - \gamma}\,, \tag{3.28}$$

where m^* is the volume of roaming traffic m at full adoption.

Proof. The proof is immediate from Eq. (3.5) with $x = 1$ (full adoption) and $m = m^*$ (note that $r - \gamma > 0$). □

We note that from Eq. (3.28), the set of users requiring subsidies, $\Theta_S = [0, \theta^*]$, is empty only if $\theta^* < 0 \Leftrightarrow c\,m^* < \gamma$. This is intuitive since $c\,m^* < \gamma$ implies that the impact of roaming traffic at full adoption is less than the utility of basic home connectivity. However, when this condition is not satisfied, subsidies are required to offset the impact of roaming

[15] Note that this is a *necessary* condition for full adoption, and may not be *sufficient*. In particular, it does not guarantee that the system *reaches* full adoption, which depends on adoption dynamics.

traffic for users that derive little or no benefits from the service's roaming feature, *i.e.,* users with low θ values.

We also note that the distribution of θ can affect the number of users requiring subsidies, $|\Theta_S|$, in subtle ways. In particular, increasing (decreasing) the roaming propensity of some users, *e.g.,* by creating a mode near $\theta = 1$ ($\theta = 0$), will on one hand decrease (increase) the number of users below θ^*, but on the other hand increase (decrease) the roaming traffic[16] m^* and in the process increase (decrease) θ^*.

3.8.2 Complexities of Service Pricing

We saw earlier that a pricing policy determines the service cost, $p(\Theta, \theta)$, for each user. The pricing policy is a control knob a service provider can use to affect users' adoption decisions and control profit. A sophisticated pricing policy may allow the provider to both maximize overall service value and recoup more of that value as profit (*e.g.,* usage-based pricing policy of Section 3.5). Such a sophisticated policy is, however, likely to be complex, which may translate into a higher cost and in the process affect profit.

To better assess the impact of a pricing policy cost, it is useful to split the service implementation cost e of Eq. (3.9) in two components $e = \widehat{e} + \widetilde{e}$, where $\widehat{e}$ is the *basic* deployment cost of the service, *e.g.,* network equipment and operation, while $\widetilde{e}$ is dedicated to the *billing* costs that depend on the particular pricing policy. Different pricing policies will have different $\widetilde{e}$ values.

We now note that the usage-based pricing policy of Section 3.5 has two major disadvantages. The first is its complexity that contributes to a high billing cost, *i.e.,* $\widetilde{e_u} \gg \widetilde{e_f}$, which could lower overall profit in spite of the policy's ability to extract all service value as profit. The second important disadvantage is that when Eq. (3.28) yields a non-empty set of users requiring subsidies, the usage-based pricing calls for "cashback" payments to those users, *i.e.,* those whose allowance a exceeds their (home and roaming) usage. Having to handle such cases further increases the service's billing complexity and cost, and could

[16] $m^* = \int_{\theta=0}^{1} \theta\, f(\theta)\, d\theta$, where $f(\theta)$, $\theta \in [0, 1]$ denotes the probability density of θ.

also negatively affect users' usage patterns, *i.e.,* by creating an incentive to consume less. Hence, although some service providers have recently announced such a service option [42], it remains highly unusual. The more common version of the usage-based policy is, therefore, one with "no cashbacks," which will however be unable to realize full service adoption when subsidies are needed.

On the other hand, the simple fixed price policy of Section 3.7 often falls short of realizing full adoption, in addition to yielding a much lower profit than feasible (because it does not differentiate between users). however, its predictability of price may lead to higher user satisfaction [61]. Moreover, its billing cost $\widetilde{e}_f$ is low, which contributes to increasing profit.

In the next section we introduce a pricing policy, the *price choice* policy, aimed at the shortcomings of the fixed price and usage-based policies. The policy seeks to, on one hand, improve on the fixed price policy when it comes to realizing profit. On the other hand, it targets a lower billing complexity than the usage-based policy, as well as a subsidy mechanism that avoids direct cashbacks and instead gives low θ users the ability to offset the impact of roaming traffic.

3.8.3 Price choice policy

The price choice policy gives all users the option to choose between two pricing schemes. The two options for pricing under this policy are:

$$\begin{cases} p_1(\Theta, \theta) = p_h, & \text{(option 1)} \\ p_2(\Theta, \theta) = p_h + p_r \cdot \theta x - bm, & \text{(option 2)} \end{cases} \tag{3.29}$$

where, as before, the adoption level x and volume of roaming traffic m are functions of adoption set Θ. Users pick the option that yields the lowest price for them.

In option 1 users do not pay for roaming usage (as with FON), while in option 2 roaming usage (as measured by θx) is charged at a unit price of p_r. In return, option 2 compensates users for the roaming traffic (m) their home access carries, at a rate of b per unit of traffic. This offers a mechanism to subsidize users that see little value in the roaming feature of

the service, and are negatively affected by having to share their home access with other (roaming) users. In addition, the subsidy is directly related to the "service" rendered by those users (the amount of roaming traffic they carry) rather than in the form of a cashback for unused usage.

Both price options boast a fixed flat price for home usage, denoted by p_h, as was the case with the hybrid pricing policy of Section 3.6. In addition to that, the availability of options in the price choice policy may improve users' satisfaction with the service [61].

The price choice policy can also be expected to reduce billing costs $\widetilde{e}_p$ compared to the usage-based policy, as the provider no longer needs to track users' home usage. Roaming usage still needs to be tracked, but only for users who choose pricing option 2.

The lower complexity and deployment cost of the price choice policy, however, means that this policy cannot convert all of the system value to profit (it suffers from the same limitation as the fixed price policy for users that choose pricing option 1). This happens mostly when γ is small, as the provider is then forced to use a small home price p_h to attract users. The next proposition offers a lower bound on the amount of system value the price choice policy is *unable* to convert to profit.

Proposition 5. *Assume γ is strictly less than $r - cm^*$, such that $r - cm^* - \gamma = \kappa > 0$, where, as before, m^* denotes the volume of roaming traffic at full adoption. Then the amount $\widetilde{v}$ of system value that the price choice policy cannot convert to profit is lower-bounded as*

$$\widetilde{v} > \frac{\kappa^2}{2(r-\gamma)},$$

Proof. Consider the service when adoption is zero, *i.e.*, $x = 0$ and $m = 0$. Users' utility under either pricing option is given by $U(\{\}, \theta) = \gamma(1-\theta) - p_h$. In order for anyone to adopt the service, it is then necessary that $p_h < \gamma$. Using this condition in the utility and price functions at full adoption, gives the result after some algebraic manipulation. □

The inevitable profit drop of Proposition 5 notwithstanding, the price choice policy may still outperform (profit-wise) the usage-based pricing policy because of its lower cost. As

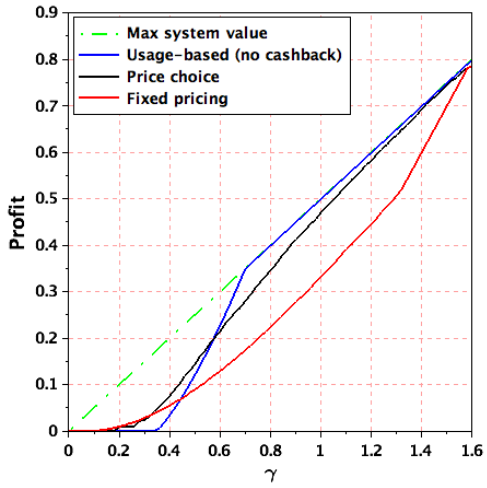

Figure 3.7: Maximum feasible *basic profit* under different pricing policies compared to maximum system value. Basic cost is $\widehat{e} = 0.1$, but billing costs $\widetilde{e}$ are not yet considered.

we shall see, it may also strictly outperform the usage-based policy, irrespective of cost, when the usage-based policy operates in the "no-cashback" mode. Finally, it typically also outperforms the fixed-price policy because of its ability to achieve a higher service value. We illustrate those claims in the next section using a number of service configurations.

3.8.4 Comparing the performance of price choice policy

This section numerically compares the maximum profit under the price choice policy to that under the usage-based and fixed price policies, which provides insight into the regimes where each policy is more profitable than others. In the figures, we take the system parameters to be $r = 1.6$ and $\widehat{e} = 0.1$ (as γ varies), and assuming that θ has a uniform distribution, we obtain $m^* = 0.5$. These are representative values and perturbing them does not change the overall nature of the results. Also in order to highlight the effect of subsidies as described in Proposition 4, we use a relatively large c, taken to be $c = 1.4$.

Fig. 3.7 plots, as a function of γ, the maximum feasible *basic profit* (provider's profit after subtracting the basic costs $\widehat{e}$ but before subtracting the billing costs $\widetilde{e}$) under the three different pricing policies of Section 3.8.2, and compares them to the maximum system value (maximum system value is an upper-bound on the feasible basic profit under any policy).

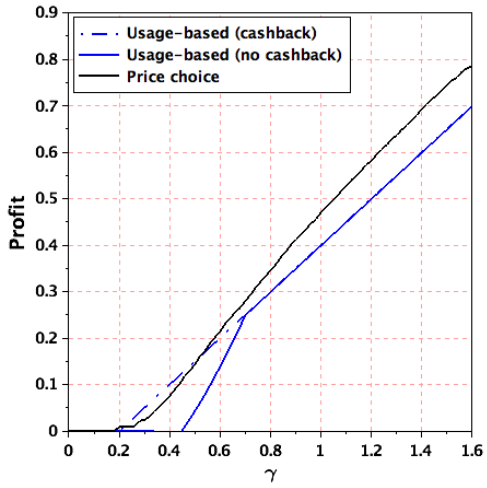

Figure 3.8: Maximum feasible *net profit* under price choice and usage-based policies when $\widehat{e} = 0.1$, and $\widetilde{e}_u - \widetilde{e}_p = 0.1$

We showed in Section 3.5 that the usage-based pricing policy with subsidies (not plotted) is able to achieve a basic profit equal to the system value across all γ values. However, as Fig. 3.7 shows, the usage-based pricing policy without subsidies fails to achieve such a high basic profit when γ is small (more precisely, when $|\Theta_S|$ as described by Eq. (3.28) is non-empty.)

For small values of γ, the fixed price policy yields a basic profit higher than that of the usage-based policy without subsidies. The reason is, in this regime, a fixed-price policy only attracts a limited number of sedentary users who generate minimal roaming traffic, hence reducing the need for subsidies. However, the fixed price policy yields inferior basic profits for a wide range of larger γ values as it cannot differentiate between users to recoup all of the system value.

On the other hand, the price choice policy improves the basic profit in comparison to the usage-based policy without subsidies for small γ values, and also remains competitive for larger γ. This is because as γ increases towards $r = 1.6$, the provider may increase the flat home usage price p_h of the price choice policy without hindering adoption.

The basic profits plotted in Fig. 3.7, however, do not account for the differences in each policy's billing cost. As discussed before, different pricing policies have different billing

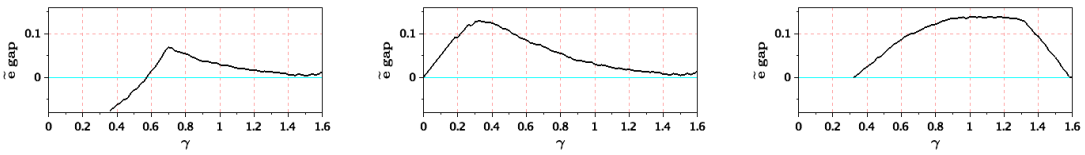

(a) Between usage-based *without* subsidies and price choice policies ($\widetilde{e}_{u2} - \widetilde{e}_p$)

(b) Between usage-based *with* subsidies and price choice policies ($\widetilde{e}_{u1} - \widetilde{e}_p$)

(c) Between price choice and fixed price policies ($\widetilde{e}_p - \widetilde{e}_f$)

Figure 3.9: The threshold $\widetilde{e}$ gap between a high-cost and a low-cost pricing policy, Parameters are $r = 1.6$, $c = 1.4$, and $\widehat{e} = 0.1$.

costs $\widetilde{e}$ and this will impact how the optimal *net profit* under different policies compare to each other. For instance, assume that the billing cost $\widetilde{e}_u$ for the usage-based policy is larger than the billing cost $\widetilde{e}_p$ for the price choice policy, by a margin of 0.1, *i.e.,* $\widetilde{e}_u - \widetilde{e}_p = 0.1$. Then the corresponding plots for their maximum net profit is as shown in Fig. 3.8. We see that with this value of "$\widetilde{e}$ *gap*", the price choice policy always outperforms the usage-based policy without subsidies, and even outperforms the usage-based policy with subsidies for most γ values.

We can quantify the threshold value of $\widetilde{e}$ gap between any two pricing policies. The threshold gives the maximum difference between the billing costs of a high-$\widetilde{e}$ policy and a low-$\widetilde{e}$ policy, such that the high-$\widetilde{e}$ policy still generates more net profit. Fig. 3.9 shows this threshold value for three different pairs of policies. For instance. Fig. 3.9b shows the threshold $\widetilde{e}$ gap between the usage-based policy with subsidies, and the price choice policy, *i.e.,* the threshold for $\widetilde{e}_{u1} - \widetilde{e}_p$. From the figure we see that the threshold gap is larger than 0.1 only for $0.2 < \gamma < 0.5$, and that is also the interval in Fig. 3.8 where the usage-based policy with subsidies outperforms the price choice policy (recall that in Fig. 3.8 we have $\widetilde{e}_{u1} - \widetilde{e}_p = 0.1$).

3.9 Generalizations and Robustness

The user adoption model reflected in the utility function of Eq. (3.5) is obviously highly stylized and predicated on various simplifying assumptions, namely,

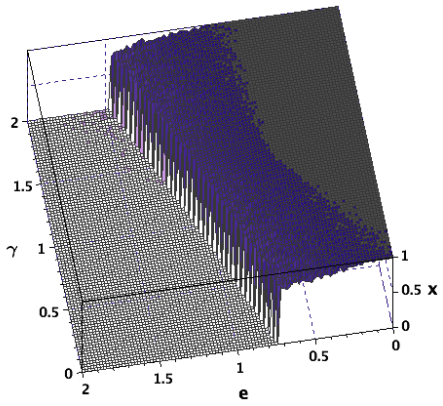

(a) Total welfare: optimal adoption for maximum system value. Compare to Fig. 3.1.

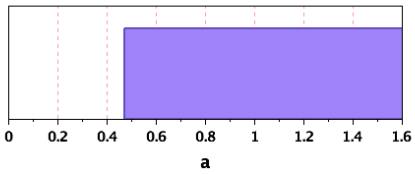

(b) Usage-based pricing policy: values of usage allowance a for which the system goes to full adoption.

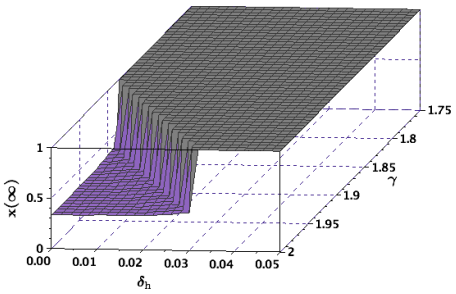

(c) Hybrid pricing policy: final adoption level as a function of the parameters γ and δ_h. Compare to Fig. 3.5.

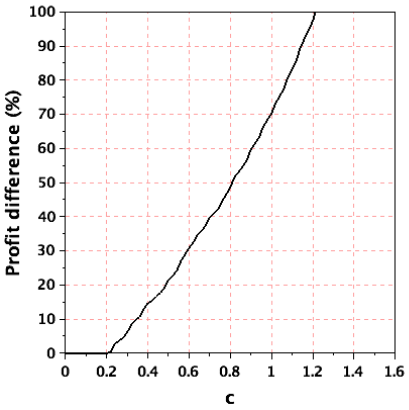

(d) Fixed price policy: relative profit drop from profit maximization to welfare maximization. Compare to Fig. 3.6.

Figure 3.10: Impact of relaxing modeling assumptions on the main findings. [1- Coverage κ is a *concave* function of adoption x that saturates as x increases; 2- Users have a non-linear utility function; 3- Users' roaming characteristics has a non-uniform distribution].

- A user's propensity to roam, θ, is uniformly distributed in $[0, 1]$,
- A user's utility is a specific linear function of coverage κ and volume of roaming traffic m,
- Adoption, x, accurately measures coverage κ,
- All users see the same coverage and contribute the same amount of traffic while roaming.

Similarly, the different pricing policies discussed in this chapter rely on these assumptions, as well as on an implicit knowledge (by the service provider) of the range and values of the different system parameters. This clearly raises valid questions regarding whether our findings hold outside this framework.

This section, and more generally Appendix A.6, seeks to address this issue. It numerically investigates the extent to which relaxations of modeling assumptions and the introduction of estimation errors in the system's parameters affect the results. As expected, modifying the models' assumptions produces quantitative changes in the outcomes. However, as we show next, their main qualitative findings remain valid.

More specifically, the investigation demonstrates the robustness of our findings (summarized in the next section) against a broad range of perturbations. Results are presented here only for representative scenarios, with the full set of results available in Appendix A.6.

The rest of this section is structured as follows. Section 3.9.1 restates the chapter's main findings for completeness. The methodology behind the robustness tests is outlined in Section 3.9.2, while an illustrative example is presented in Section 3.9.3.

3.9.1 Main findings and insight

We briefly recall the main findings that emerged from the results of this chapter's simple model.

- *Maximum total welfare:* Whenever the system is capable of generating value, this value is maximized at full (or close to full) adoption;

- *Usage-based pricing:* Realizing the system's maximum value under a usage-based pricing policy calls for ensuring that users are offered a usage allowance that exceeds a minimum threshold a.
- *Hybrid usage-based pricing:* When the value of home connectivity is high, the hybrid pricing policy may not achieve maximum system value (because of the emergence of a sub-optimal equilibrium) unless prices are sufficiently discounted (high values for parameters δ_h and δ_r). Such discounts prevent the service provider from maximizing profit, unless it resorts to an introductory pricing scheme;
- *Fixed pricing:* Under a fixed price policy, profit and welfare maximization strategies typically differ unless the penalty associated with allowing roaming traffic (the parameter c) is small.

3.9.2 Robustness testing methodology

In testing for robustness, we consider perturbations to the assumptions, parameters and functional expressions of our model. Because those perturbations affect the model's analytical tractability, their impact is evaluated by means of numerical simulations. The simulations also consider the effect of different types of errors in the estimation of system parameters on which the service provider relies when designing pricing strategies. We describe next the dimensions along which we perturb the original model. Additional details can again be found in Appendix A.6.

• **Non-uniform roaming distributions** We consider different probability distributions for a user's propensity to roam, θ. In particular, we consider distributions with both low and high roaming modes (fewer or more users that roam frequently).

• **Modified user utility functions** The original model assumes a specific functional expression for users' utility that grows linearly with coverage (x) and decreases linearly with the volume of roaming traffic (m). We relax the linearity assumption, and also consider two different utility functions inspired by the models of [70].

• **Coverage saturation** The original model assumes that coverage increases linearly with service adoption. We relax this assumption and consider a *saturation* effect for coverage, *i.e.,* coverage is now a concave function of adoption, which captures that adequate coverage may be realized with less than 100% adoption.

• **Users heterogeneity** We consider a scenario where users belong to two "types" with different "profiles." The type of a user affects that user's utility as well as the volume of roaming traffic she generates.

3.9.3 Robustness tests

Because of space limitations, we only report on the outcome of one experiment that combines the first three perturbations of the previous section, namely, a non-uniform roaming distribution with a mode towards high roaming values, a non-linear utility function for users[17], and coverage that increases faster than adoption, *i.e.,* saturates before full adoption. We omit including different types of users in the experiment, as this additional perturbation typically masks the effect of the others. Results reporting on its effect can, however, be found in Appendix A.6, together with results for different utility functions and a range of other scenarios.

Fig. 3.10 displays the results of the evaluation. It consists of four sub-figures, with each sub-figure corresponding to one of the findings summarized in Section 3.9.1, and illustrating the extent to which the corresponding finding has been affected. As we discuss next, the figures illustrate that while quantitative changes can be observed, the overall qualitative outcomes remain similar, thereby demonstrating the robustness of the findings. A similar conclusion held across the broader range of scenarios found in Appendix A.6.

Consider first Fig. 3.10a that mirrors Fig. 3.1, namely, plots the adoption level that maximizes total welfare as a function of the system parameters γ and e. The figure illustrates that, as in the original model, when the system can generate positive value (the system cost

[17]Super-linear in a user's sensitivity to roaming traffic m, and sub-linear in her sensitivity to coverage x, *i.e.,* $U(\Theta, \theta) = \gamma - c\, m^{1.2} + \theta\,(r\, x^{0.8} - \gamma) - p(\Theta, \theta)$.

e is not too high), this is achieved at or near full adoption. The wider "intermediate" area that shows welfare being maximized slightly below full adoption is intuitive in light of the assumption of coverage saturation for the system, *i.e.,* reaching full adoption adds more roaming traffic without meaningfully improving coverage.

Fig. 3.10b in turn displays that under the usage-based pricing policy, the system still exhibits the characteristic "threshold behavior," which had been identified in the original model. Specifically, the pricing policy needs to offer users a certain minimum usage allowance, a, to successfully realize full adoption, and therefore maximum welfare. The exact value of a is clearly different from that predicted by the original model, but the overall behavior is still present.

Fig. 3.10c corresponds to Fig. 3.5. It shows that, as before, when the value of home connectivity γ is large, the hybrid pricing policy exhibits regimes where a sub-optimal equilibrium ($\widetilde{x} < 1$) can arise, thereby preventing the system from reaching full adoption. Overcoming this issue can again be accomplished by appropriately discounting the service prices. The discount values are obviously different, but the mechanism is the same.

Finally, Fig. 3.10d parallels Fig. 3.6. It displays for the fixed price policy, the gap in profit between profit maximizing and welfare maximizing strategies. As before, the gap is small when the parameter c is small, and grows large as c increases.

The above results offer evidence that the findings of this chapter hold under more general settings than those of the specific and relatively simple model used to preserve analytical tractability. As mentioned earlier, further evidence of this robustness can be found in Appendix A.6, which also investigates the impact of various errors in the provider's estimates for the different system parameters.

3.10 Conclusion

The work presented in this chapter was motivated by the emergence of UPC services that feature both positive and negative externalities, and more importantly (negative) externalities that depend not just on the number of adopters, but also on which users have adopted.

The goal was to develop an understanding of the conditions under which such services may succeed and the "welfare" (value) they are able to generate.

As expected given the service's strong positive externality, welfare is typically maximized when adoption is maximum. More interestingly, maximum adoption and welfare can be achieved through relatively simple pricing policies that also afford complete flexibility in deciding how welfare is to be distributed between users and the provider of the service. Of interest is the fact that pricing according to service usage is sufficient to capture differences in how users value the service, and successfully realize both maximum welfare and arbitrary welfare distribution.

The relative simplicity of usage-based pricing notwithstanding, it involves monitoring overhead and may face acceptance challenges on the part of users. This motivated the investigation of alternate policies, which offer a different trade-off between implementation considerations, welfare maximization, and flexibility in welfare distribution.

We demonstrated that when users' valuation of basic home connectivity γ is small relative to the impact of roaming traffic cm, there are a group of users that will need to be given monetary incentives (irrespective of the particular pricing policy), otherwise a UPC system will not reach full adoption.

The chapter's main contributions are in offering new insight into the viability of UPC-like services, as well as simple (pricing) mechanisms to facilitate their successful and effective deployment.

Chapter 4

Opinion Formation in Ising Networks

4.1 Introduction

Ising spin-glass-inspired models of interactions borrowed from statistical physics have been adapted for use in economics, models of neural computation, and in social network settings [15, 20, 71, 74]. In this chapter we describe a variation on this theme with a view to understanding essential features of opinion formation in social networks in a sanitized setting.

Consider a fully connected network of n nodes, where node i holds a binary (for or against) *opinion* $x_i \in \{-1, 1\}$ about an issue under consideration. A node's opinion evolves over time as a function of its own opinion and that of its network neighbors. A neighbor's opinion is weighed based on its *influence*. Neighbors have a symmetric influence on each other which depends on their level of affinity. Affinity is biased positively or negatively based on nodes' *party* affiliations. Nodes from the same party are more likely to exhibit a positive affinity bias. This chapter investigates the extent to which such party-based influence biases affect opinion formation, and in particular which opinions emerge in each party at equilibrium.

The two models considered in this chapter differ in how the inter-nodal influences are specified. In the *random influence model*, neighborhood influences are selected randomly to be positive or negative with a bias based on party affiliation. Two principals from the same party are more likely to have a positive affinity, while the influence on each other of two principals from different parties is more likely to be negative. The second of the models we consider, the *profile-based model*, specifies affinities in a more nuanced fashion. In this model each node comes equipped with a *profile*—a vector of positions on a fixed set of prior issues with nodes in the same party more likely to take similar positions on those issues. Inter-nodal influences in this setting are determined based on profile similarity.

The two models share common properties, and in particular, opinions in both models always converge to stable equilibria. However, they also exhibit significant differences. Of most interest is the fact that with high probability the random influence model gives rise to a partisan outcome with nodes in each party converging to a common opinion opposed to that of nodes in the other party. In contrast, the profile-based model permits a more diverse set of distinct fixed points, with the opinion equilibrium driven by the initial distribution of opinions in each party.

4.2 Embedding a Party Structure in an Ising Network Model of Interaction

In this section we first introduce the basic Ising model, and explain how a party structure can be embedded in that model. Finally we show that in case of a two-party setting, we can use symmetries to simplify the analysis of the model.

4.2.1 Ising Model

The basic Ising model is a stochastic system which specifies a dynamics on the vertices $\{-1, +1\}^n$ of the n-dimensional cube. The system is characterized by a symmetric stochastic matrix $[w_{ij}]$ of interaction weights. At any time the state of the system is represented by

a state vector $\mathbf{x} = (x_1, \ldots, x_n) \in \{-1, +1\}^n$ which represents a collection of spins or, in the current context, opinions in a community of n interconnected principals labelled with indices 1 to n. Updates to the state are performed asynchronously according to some update schedule: at each update epoch (only) one node i is selected and a state update $x_i \mapsto x_i^{\mathrm{u}}$ performed according to the sign of a linear form of the node's current inputs,[1]

$$x_i^{\mathrm{u}} = \operatorname{sgn} S_i = \operatorname{sgn}\left(\sum_{j=1}^{n} w_{ij} x_j\right), \tag{4.1}$$

and all other nodal states are kept unchanged. We refer to $S_i = S_i(\mathbf{x})$ as the *update sum* for node i. In our context x_j is the (current) opinion of node j, w_{ij} denotes the weight of the influence node j has on node i, and x_i^{u} represents the updated opinion of node i. The updates determine a dynamics $\mathbf{x}(0) \mapsto \mathbf{x}(1) \mapsto \mathbf{x}(2) \mapsto \cdots$ in the state space of vertices where, at any update epoch, the new state $\mathbf{x}(l+1)$ differs from the previous state $\mathbf{x}(l)$ in at most one coordinate (if the node update actually resulted in a change in sign). The specific update schedule is not critical for our purposes; it suffices if each state is updated infinitely often with probability one. A simple deterministic update schedule with this property is a round-robin schedule of state updates; a stochastic example is provided by a random update schedule where the node whose state is to be updated is selected randomly and independently at each update epoch. Call any such update schedule *honest*.

We assume throughout that the matrix $[w_{ij}]$ of interaction weights is symmetric, $w_{ij} = w_{ji}$, and w_{ii} is non-negative. In the context of interacting principals in a social network this models a situation where inter-agent influences are bilateral and symmetric, each agent having a positive self-reinforcement. A key classical result in this setting says that *under any honest update schedule the system dynamics converges to a fixed point* (see [15, 49]). A state $\mathbf{x}^*$ is a fixed point (or *equilibrium*) of the system if, and only if, it satisfies[2] the

[1] For definiteness, set $\operatorname{sgn}(0) = -1$.

[2] There is an irritating possibility of the sum being zero in which case the adopted convention of the sign function becomes important. But this has an exponentially small probability and we will ignore this nuisance. Alternatively, assume n is even.

stationary system of update equations

$$x_i^* = \operatorname{sgn}\left(\sum_{j=1}^{n} w_{ij} x_j^*\right) \qquad (1 \le i \le n)$$

i.e., each update sum $S_i(\mathbf{x}) = \sum_j w_{ij} x_j$ has the same sign as x_i. This leads to the following.

Fixed point criterion. *A state* $\mathbf{x}$ *is a fixed point of the system if, and only if,* $x_i S_i(\mathbf{x}) > 0$ *for each* i.

As $S_i(-\mathbf{x}) = -S_i(\mathbf{x})$, it follows that if $\mathbf{x}$ is a fixed point then so is $-\mathbf{x}$, and vice versa. Thus, fixed points appear in pairs. It is now naturally of interest to characterize the number and nature of such equilibria.

4.2.2 Party Structure

In the classical Ising paradigm, the weights $\{ w_{ij}, 1 \le i < j \le n \}$ are independent, standard normal random variables. We consider a variation on this theme where there is an embedded party structure with individuals within a party more likely to have a positive influence on each other, while individuals across party lines tend to have a neutral or negative influence on each other.

The general setting is as follows. The nodes $\{1, \ldots, n\}$ are partitioned into, say, m groups $G_1, \ldots, G_m$ which determine party memberships in a multi-party system. For each group G_k, the intra-group interaction weights $\{ w_{ij}, i < j, (i,j) \in G_k \times G_k \}$ form a system of (positively biased) exchangeable random variables. Likewise, inter-group interaction weights $\{ w_{ij}, (i,j) \in G_k \times G_l \}$ form systems of (negatively biased) exchangeable random variables. The nature of the dynamics is now, of course, determined by the specifics of the interaction distributions.

We restrict our attention in this chapter to a symmetric two-party system leaving extensions for elsewhere. In the setting at hand, $\{G_1, G_2\}$ is a partition of the nodes into memberships in two parties. We suppose further that the intra-party distributions are the same for both parties, that is to say, $\{ w_{ij}, i < j, (i,j) \in G_1 \times G_1$ or $(i,j) \in G_2 \times G_2 \}$ is a

system of (positively biased) exchangeable random variables, and the inter-party distributions are complementary, that is to say, the negatives of the inter-party interaction weights have the same distributions as the intra-party interaction weights. Consequently, if we define

$$\widetilde{w}_{ij} \triangleq \begin{cases} w_{ij} & i < j, (i,j) \in G_1 \times G_1 \text{ or } (i,j) \in G_2 \times G_2 \\ -wij & i < j, (i,j) \in G_1 \times G_2 \text{ or } (i,j) \in G_2 \times G_1, \end{cases}$$

then $\{ \widetilde{w}_{ij}, i < j \}$ is a system of *positively biased* exchangeable random variables. Therefore, the symmetries inherent in the situation permit us to simplify exposition and consider an equivalent single party system (though it should be borne in mind that these algebraic simplifications will not be available when there are more than two parties). Next, we briefly sketch the argument.

4.2.3 Single-Party Isometry

Begin with a two party partition $\{G_1, G_2\}$ and an associated symmetric stochastic system of weights $[w_{ij}]$. Form a new membership partition $\{G_1', G_2'\}$ by moving one member, say, k from G_2 into G_1, $G_1' = G_1 \cup \{k\}$ and $G_2' = G_2 \setminus \{k\}$, associating with the new partition a new symmetric system of weights $[w_{ij}']$ where $w_{ij}' = w_{ij}$ if $i \neq k$ and $j \neq k$, $w_{kk}' = w_{kk}$, and $w_{jk}' = -w_{jk}$ for $j \neq k$, by simply negating the weights of all the interconnections incident on k. We may now establish an isomorphism between dynamics in the $\{G_1, G_2\}$ and $\{G_1', G_2'\}$ systems by putting states $\mathbf{x} = (x_1, \ldots, x_n)$ in the $\{G_1, G_2\}$ system into one-to-one correspondence with states $\mathbf{x}' = (x_1', \ldots, x_n')$ in the $\{G_1', G_2'\}$ system, where $\mathbf{x}'$ is obtained from $\mathbf{x}$ by setting $x_j' = x_j$ if $j \neq k$ and $x_k' = -x_k$. It is now easy to verify that the update sums in the two systems starting with states $\mathbf{x}$ and $\mathbf{x}'$, respectively, satisfy $S_j'(\mathbf{x}') = S_j(\mathbf{x})$ if $j \neq k$ and $S_k'(\mathbf{x}') = -S_k(\mathbf{x})$, and so a dynamics $\mathbf{x}(0) \mapsto \mathbf{x}(1) \mapsto \mathbf{x}(2) \mapsto \cdots$ in the $\{G_1, G_2\}$ system is exactly mirrored by the dynamics $\mathbf{x}'(0) \mapsto \mathbf{x}'(1) \mapsto \mathbf{x}'(2) \mapsto \cdots$ in the $\{G_1', G_2'\}$ system, the symmetry of the distributions ensuring that all probabilities are preserved. By iterating the process we end up with a single party system with weights $\{ \widetilde{w}_{ij}, i < j \}$ forming an exchangeable system of random variables with a positive bias. The new system is

stochastically equivalent to the original two party system, the dynamics in the two systems being isomorphic. The single party formulation provides the greatest transparency in the statement of the results and the proofs and *we assume without comment henceforth that we are dealing with an equivalent single party system of nodes where the weights* $\{\,\widetilde{w}_{ij}, i<j\,\}$ *form a system of exchangeable random variables.* Also for notational purposes, we shall simply use $\{\,w_{ij}, i<j\,\}$ to denote the weights.

4.3 Random Influence Model

The interaction model most closely related to the classical Ising model of Gaussian influences is to consider a system of independent variables with a drift. And the simplest of these arises when we have signed Bernoulli influences. Next we formally introduce the random influence model.

4.3.1 Model Formulation

Suppose $1/2 < p \le 1$ and let $\{\,w_{ij}, i<j\,\}$ be a system of signed Bernoulli trials with success parameter p: $\mathbf{P}\{w_{ij}=1\}=p$ and $\mathbf{P}\{w_{ij}=-1\}=1-p$. [In the equivalent two party system, the intra-party weights are $+1$ with probability p (and -1 with probability $1-p$) for both parties, while the inter-party weights are $+1$ with probability $1-p$ (and -1 with probability p). In other words, two nodes are likely to positively influence each other if they belong to the same party; they are likely to negatively influence each other if they belong to different parties.] The algebra is simplest if there are no self-interactions, $w_{ii}=0$, and we so assume. Extensions of this simple model to varying distributions and self-reinforcement may be handled by tweaking this basic framework and are provided in Section 4.3.5.

4.3.2 Main Results

We begin by a characterization of the dominant fixed points in this setting. In view of the fixed point criterion, we see that, for any given state $\mathbf{x} \in \{-1, +1\}^n$,

$$\mathbf{P}\{\mathbf{x} \text{ is a fixed point}\} = 1 - \mathbf{P}\left(\bigcup_{i=1}^{n} x_i S_i(\mathbf{x}) \leq 0\right).$$

Write $\mathbf{x}^+ = (1, 1, \ldots, 1)$ for the vector all of whose components are $+1$ and in increasing compaction of notation, write $S_i(\mathbf{x}^+) = S_i^+$ for the partial sums corresponding to state $\mathbf{x}^+$. Naturally enough, we expect $\mathbf{x}^+$ and $\mathbf{x}^- = -\mathbf{x}^+$ to be fixed points. And this is indeed the case (in a suitable probabilistic interpretation). Identifying the dependence on n explicitly, write $P^+ = P_n^+$ for the probability that $\mathbf{x}^+$ is a fixed point.

Theorem 1. *Fix any $0 < \delta < 1$ and suppose*

$$p \geq \frac{1}{2} + \sqrt{\frac{\log(n/\delta)}{2(n-1)}}.$$

Then $P_n^+ \geq 1 - \delta$. In particular, if $p > 1/2$ is bounded away from $1/2$, then $P_n^+ \to 1$ as $n \to \infty$.

Proof. If the system is in state $\mathbf{x}^+$ the partial sums are given by

$$x_i^+ S_i^+ = S_i^+ = \sum_{j \neq i} w_{ij} x_j^+ = \sum_{j \neq i} w_{ij}.$$

The sum on the right represents a random walk with a positive drift. As the signed Bernoulli variables w_{ij} have expectation $2p - 1$, everything sets up nicely for an application of Hoeffding's inequality [48, Theorem 2] (see [88, Section XVI.1] for the particular version considered here). We hence obtain

$$\begin{aligned}\mathbf{P}(x_i^+ S_i^+ \leq 0) &= \mathbf{P}\left(\sum_{j \neq i} (w_{ij} - (2p-1)) \leq -(n-1)(2p-1)\right) \\ &\leq \exp\left(-\frac{(n-1)^2 (2p-1)^2}{2(n-1)}\right) = \exp\left(-2(n-1)\left(p - \frac{1}{2}\right)^2\right).\end{aligned}$$

By Boole's inequality, it follows that

$$\mathbf{P}\left(\bigcup_{i=1}^{n}\left(x_i^+ S_i^+ \leq 0\right)\right) \leq \sum_{i=1}^{n}\mathbf{P}\left(x_i^+ S_i^+ \leq 0\right)$$
$$\leq n.\exp\left(-2(n-1)\left(p-\frac{1}{2}\right)^2\right) \leq \delta$$

for the given selection of p. □

Our proof shows that the probability that $\mathbf{x}^+$, hence also $\mathbf{x}^-$, is a fixed point converges very fast indeed, exponentially in n, to one. In the rest of this chapter we refer to these states as *partisan* states. [The corresponding states in the equivalent two party model are states where all nodes in a party have an identical opinion which is opposed to the common opinion of the nodes in the other party.]

We can do a little better, the mechanism of proof permitting a characterization of the *region of attraction* around the fixed points $\mathbf{x}^+$ and $\mathbf{x}^-$. The term region of attraction is a little vague; more precisely, we would like to estimate the probability that a given initial state $\mathbf{x}$ is mapped, eventually, over possibly many asynchronous steps, into, say, the fixed point $\mathbf{x}^+$, and determine for what range of Hamming distances $d(\mathbf{x}, \mathbf{x}^+)$ we obtain a high probability convergence to the fixed point.

The situation with respect to $\mathbf{x}^+$ and $\mathbf{x}^-$ is symmetric. Suppose, for definiteness, that an initial state vector $\mathbf{x}$ is at Hamming distance $0 < m < n/2$ from $\mathbf{x}^+$. Write B_m for the set of all $\binom{n}{m}$ such states $\mathbf{x}$,

$$B_m = \{\, \mathbf{x} : d(x, \mathbf{x}^+) = m \,\}.$$

For any $\mathbf{x}$ in B_m, let $M(\mathbf{x})$ be the set of m nodes that have different opinions under $\mathbf{x}$ and $\mathbf{x}^+$, that is to say,

$$M(\mathbf{x}) = \{\, i : x_i \neq x_i^+ \,\}.$$

In an expressive terminology, we call these nodes *non-conforming*. Now, let $S_i(\mathbf{x})$ be the

update sum of node i under state $\mathbf{x} \in B_m$,

$$S_i(\mathbf{x}) = -\sum_{j \in M(\mathbf{x})} w_{ij} + \sum_{j \notin M(\mathbf{x})} w_{ij}.$$

A preliminary estimate of the probability that all nodes have positive update sum under state $\mathbf{x} \in B_m$ sets the stage.

Lemma 4. *Fix any $m < n/2$ and suppose $\mathbf{x} \in B_m$. Then*

$$\mathbf{P}\left(\bigcap_{i=1}^{n}(S_i(\mathbf{x}) > 0)\right) \geq 1 - n \cdot \exp\left(-\frac{(n-1-2m)^2\ (2p-1)^2}{2(n-1)}\right).$$

Proof. By Boole's inequality, we see that

$$\begin{aligned}\mathbf{P}\left(\bigcap_{i=1}^{n}(S_i(\mathbf{x}) > 0)\right) &= 1 - \mathbf{P}\left(\bigcup_{i=1}^{n} S_i(\mathbf{x}) \leq 0\right) \\ &\geq 1 - \sum_{i=1}^{n} \mathbf{P}\left(S_i(\mathbf{x}) \leq 0\right).\end{aligned} \tag{4.2}$$

The event $\{S_i(\mathbf{x}) \leq 0\}$ occurs if, and only if,

$$-\sum_{j \in M(\mathbf{x})} w_{ij} + \sum_{j \notin M(\mathbf{x})} w_{ij} \leq 0. \tag{4.3}$$

(Bear in mind that $w_{ii} = 0$.) Now first consider a node $i \in M(\mathbf{x})$. Then the left side of Eq. (4.3) is the sum of $n-1$ random variables with mean $(n+1-2m)(2p-1)$. Another application of Hoeffding's inequality shows then that

$$\mathbf{P}\left(S_i(\mathbf{x}) \leq 0\right) \leq \exp\left(-\frac{(n+1-2m)^2\ (2p-1)^2}{2(n-1)}\right)\ [i \in M(\mathbf{x})]. \tag{4.4}$$

Next, consider a node $i \notin M(\mathbf{x})$. Then the left side of Eq. (4.3) is the sum of $n-1$ random variables with mean $(n-1-2m)(2p-1)$. Hoeffding's inequality hence shows that

$$\mathbf{P}\left(S_i(\mathbf{x}) \leq 0\right) \leq \exp\left(-\frac{(n-1-2m)^2\ (2p-1)^2}{2(n-1)}\right)\ [i \notin M(\mathbf{x})]. \tag{4.5}$$

Comparing Eq. (4.4) and Eq. (4.5) we see that

$$\mathbf{P}\left(S_i(\mathbf{x}) \leq 0\right) \leq \exp\left(-\frac{(n-1-2m)^2\ (2p-1)^2}{2(n-1)}\right) \tag{4.6}$$

for all i. Substituting the bound on the right into Eq. (4.2) completes the proof. □

The introduction of a little notation and terminology helps streamline the results. Fix $0 < p < 1$ and on the interval $\alpha \in [0, 1/2]$ define the function

$$f(\alpha) = 2(1-2\alpha)^2(p-1/2)^2 - h(\alpha)$$

where, with logarithms to base e, $h(\cdot)$ is the binary entropy function (in nats) defined by

$$h(\alpha) = -\alpha \log(\alpha) - (1-\alpha)\log(1-\alpha).$$

The function $2(1-2\alpha)^2(p-1/2)^2$ is decreasing in the interval $\alpha \in [0, 1/2]$ while $h(\alpha)$ is increasing in this interval. It follows that $f(\alpha)$ decreases monotonically from a value of $f(0) = 2(p-1/2)^2 > 0$ at $\alpha = 0$ to a value of $f(1/2) = -\log 2 < 0$ at $\alpha = 1/2$. By the intermediate value theorem of calculus, it follows that f has a unique root $\alpha_0 = \alpha_0(p)$ in the interior of the interval $(0, 1/2)$ at which $f(\alpha_0) = 0$. Fig. 4.1 shows the dependence of α_0 on p.

Say that a state $\mathbf{x}$ lies in the *attraction region* of the partisan fixed point $\mathbf{x}^+$ if, starting with $\mathbf{x}$ as the initial state, the state updates converge, eventually, to the fixed point $\mathbf{x}^+$. Write $A^+(\mathbf{x})$ for the event that $\mathbf{x}$ is in the attraction region of $\mathbf{x}^+$.

Theorem 2. *Select any small, positive ϵ. Fix any $1/2 < p < 1$ and any value $0 < \alpha < \alpha_0(p)$. If $\mathbf{x}$ is any state with $d(\mathbf{x}, \mathbf{x}^+) \leq \alpha n$, then $\mathbf{P}(A_x^+) > 1 - \epsilon$ whenever n is sufficiently large.*

Proof. Suppose that the system is at a state $\mathbf{x} \in B_m$ for some $m \leq \alpha n$ and the event $\bigcap_{i=1}^n \{S_i(\mathbf{x}) > 0\}$ occurs. Now consider an arbitrary sequence of (asynchronous) opinion updates according to the update rule specified in Eq. (4.1). Since all of the update sums

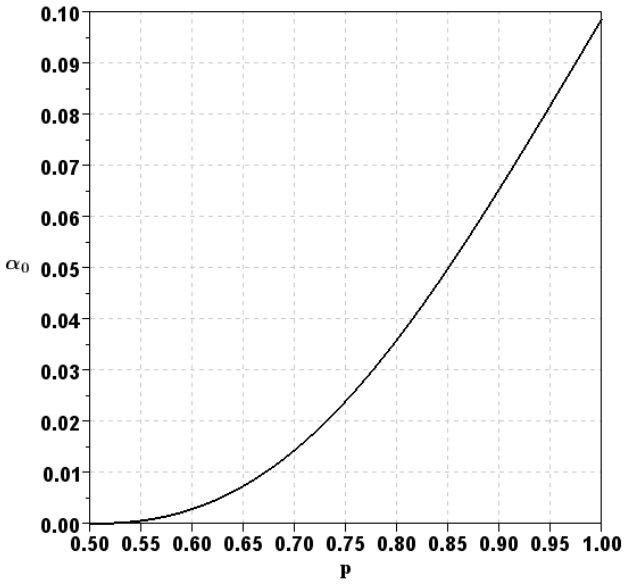

Figure 4.1: Lower-bound on the radius of attraction region for the partisan fixed points as a function of p.

are positive, the first node to change its opinion is a non-conforming node that becomes conforming, the update moving the system to a state $\mathbf{x}' \in B_{m-1}$. At this point we say that *one round* of updates has happened, and the system has *shrunk* one step towards the (closer) partisan fixed point. We denote by $R_{\mathbf{x}}$ the event that the system moves from a particular state $\mathbf{x} \in B_m$ to any state $\mathbf{x}' \in B_{m-1}$ in *one round* of updates. It is now clear that the occurrence of the event $\bigcap_{i=1}^{n}\{S_i(\mathbf{x}) > 0\}$ implies the occurrence of $R_{\mathbf{x}}$ and so, by lemma 4, we obtain

$$\mathbf{P}\left(R_{\mathbf{x}}\right) \;\geq\; \mathbf{P}\left(\bigcap_{i=1}^{n}\{S_i(\mathbf{x}) > 0\}\right) \;\geq\; 1 \,-\, n \,\cdot\, \exp\left(-2n\left(1 - 2\alpha - \frac{1}{n}\right)^2 \left(p - 1/2\right)^2\right),$$

or, what is the same thing,

$$\mathbf{P}\left(R_{\mathbf{x}}^c\right) \leq n \cdot \exp\left(-2n\left(1 - 2\alpha - \frac{1}{n}\right)^2 \left(p - 1/2\right)^2\right).$$

Another deployment of Boole's inequality shows now that

$$\begin{aligned}\mathbf{P}\left(\bigcup_{x\in B_m} R_{\mathbf{x}}^c\right) &\leq \binom{n}{m} n\cdot\exp\left(-2n\left(1-2\alpha-\frac{1}{n}\right)^2(p-1/2)^2\right)\\ &\leq \frac{\exp(h(\alpha)\cdot n)}{\sqrt{n}} n\cdot\exp\left(-2n\left(1-2\alpha-\frac{1}{n}\right)^2(p-1/2)^2\right) \qquad (4.7)\\ &= \sqrt{n}\cdot\exp\left[n\left(h(\alpha)-2\left(1-2\alpha-\frac{1}{n}\right)^2(p-1/2)^2\right)\right].\end{aligned}$$

The expression on the right bounds from above the probability that at least one of the states $\mathbf{x}\in B_m$ fails to demonstrate the shrink property $R_{\mathbf{x}}$. One more application of Boole's inequality now gives

$$\begin{aligned}\mathbf{P}\left(\bigcup_{m\leq\alpha n}\bigcup_{\mathbf{x}\in B_m} R_{\mathbf{x}}^c\right) &\leq \sum_{m\leq\alpha n}\mathbf{P}\left(\bigcup_{\mathbf{x}\in B_m} R_{\mathbf{x}}^c\right)\\ &\leq n\cdot\mathbf{P}\left(\bigcup_{\mathbf{x}\in B_m} R_{\mathbf{x}}^c\right)\leq n\cdot n^{\frac{1}{2}}.\exp(-n\cdot f_n(\alpha)), \qquad (4.8)\end{aligned}$$

where $f_n(\alpha)=2(1-2\alpha-1/n)^2\ (p-1/2)^2-h(\alpha)$.

For every choice of $0<\epsilon\leq 1$, the right side of Eq. (4.8) is strictly less than ϵ if

$$\frac{\frac{3}{2}\log(n)-\log(\epsilon)}{n} < f_n(\alpha).$$

Since the left side of this inequality goes to 0 as n grows large, if $f_n(\alpha)$ is bounded away from zero then there exists $n(\epsilon)$ such that for all $n\geq n(\epsilon)$,

$$\mathbf{P}\left(\bigcup_{m\leq\alpha n}\bigcup_{\mathbf{x}\in B_m} R_{\mathbf{x}}^c\right) < \epsilon.$$

It now remains to be shown that if $\alpha<\alpha_0$ then $f_n(\alpha)>0$ is bounded away from zero for n sufficiently large. Arguing as for $f(\alpha)$, we see that $f_n(\alpha)$ is strictly decreasing in the interval $0\leq\alpha\leq\frac{1}{2}-\frac{1}{2n}$ and goes from $f_n(0)=2(1-1/n)\ (p-1/2)^2>0$ at $\alpha=0$ to $f_n\left(\frac{1}{2}-\frac{1}{2n}\right)<0$ at $\alpha=\frac{1}{2}-\frac{1}{2n}$. By the intermediate value theorem again, it follows that f_n

has exactly one root $\alpha_{0,n}$ in the interior of the interval $\left[0, \frac{1}{2} - \frac{1}{2n}\right]$. But $f_n(\alpha)$ differs from $f(\alpha)$ only in a term of order $1/n$ and, by examination, it is clear that $\alpha_{0,n} = \alpha_0 + O(n^{-1})$. It follows that if $\alpha < \alpha_0$ then $\alpha < \alpha_{0,n}$ for sufficiently large n and this concludes the proof. □

To summarize, the states $\mathbf{x}^+$ and $\mathbf{x}^-$ are fixed points (with high probability) for large n, each having a large (linear in n) region of attraction. The estimates can be improved but the results are intuitive (and limiting) and we won't expend any further effort in this direction.

4.3.3 Numerical Results

The analysis in Section 4.3.2 formally identifies a high-probability region of attraction to a partisan fixed point, and establishes the connection between p and the frequency of convergence. We can numerically verify this, and also that the results of Section 4.3.2 are conservative. For instance, Fig. 4.2 considers sample systems of population $n = 30$, and plots the frequency[3] of convergence to $\mathbf{x}^+$ or $\mathbf{x}^-$ as the strength of party bias varies in $1/2 < p \leq 1$ and as the initial opinion mix increases from 0 (corresponding to all nodes having the same opinion, *e.g.,* $\mathbf{x}^+$), to 0.5 (corresponding to the maximum opinion mix, an even split between $+1$ and -1 opinions). This figure confirms that at any given level of opinion mix, the frequency of convergence to the partisan fixed points grows with the strength of party bias, *i.e.,* the probability of a positive edge-weight between members of the same party, p. In particular, the figure suggests that there exists a threshold interval of p values above which convergence frequency is very high. A trivial case is obtained when $p = 1$; it can be verified (see Section 4.3.4) that at this value a partisan outcome is always achieved and the system converges quickly[4].

The analysis also showed that the probabilistic attraction region grows linearly with n. The growth of this attraction region with n is depicted through further simulations given in Fig. 4.3. The figure shows curves that are similar in nature to the right-most cross section

[3] As measured by simulation over 50,000 different samples in the probability space.
[4] In one "round" of updates.

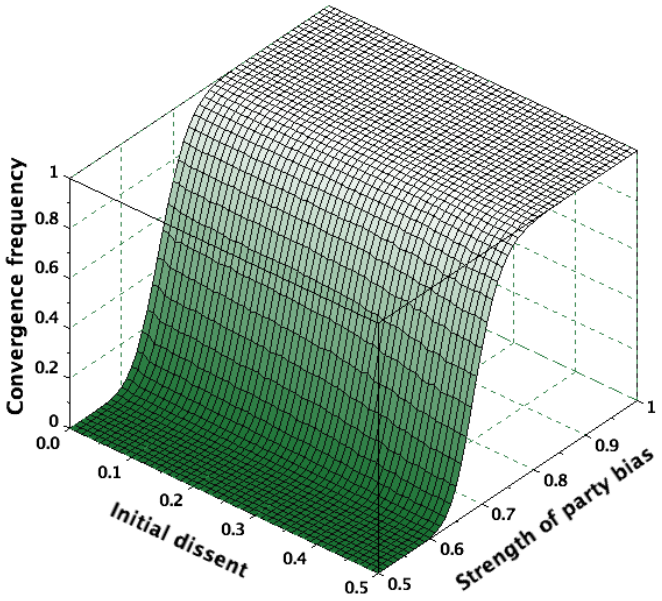

Figure 4.2: For the Random Influence model, the frequency of convergence to a partisan state is plotted as a function of the initial dissent δ and the strength of party bias p in a population of size $n = 30$. The simulation shows results aggregated over 50,000 random network initializations for each value of the abscissae δ and p.

of Fig. 4.2 (corresponding to an initial opinion mix close to 0.5), but for four different population sizes. Specifically, four networks of sizes 30, 100, 400 and 1000 are considered. As before, edge weights are determined by a Bernoulli variable with success probability p. Once a specific p value is chosen, we consider $50,000$ different random realizations of the edge weights each with a random initial state. A random initial state is obtained by randomly assigning $+1$ or -1 opinions to the nodes (with probability $1/2$). The system then starts the update process and eventually converges to a fixed point. At that point we compute the fraction of time that the outcome is one of the partisan fixed points. This fraction is plotted in Fig. 4.3 for different p values. The figure again illustrates the presence of a "threshold effect," where, for moderate population sizes, a partisan outcome rapidly arises when p exceeds $1/2$.

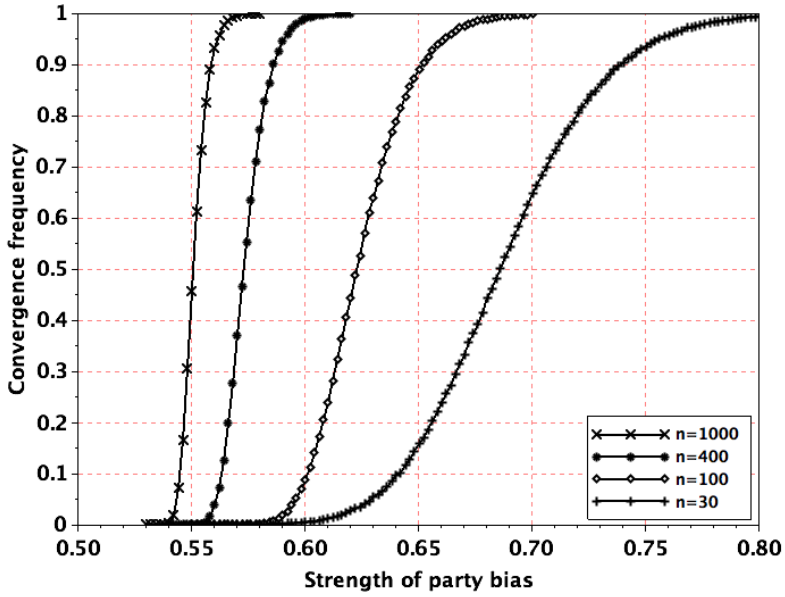

Figure 4.3: Phase transition to partisan fixed points in the Random Influence model: The frequency of convergence to a partisan state is plotted as a function of the strength of party bias p with population size n as a parameter. Each point on the graphs represents the empirical mean of 50,000 random trials with (randomly chosen) initial states at maximum dissent.

To summarize, the two partisan fixed points $\mathbf{x}^+$ and $\mathbf{x}^-$ have large probabilistic regions of attraction that dominate the space of possible states; as n becomes large, this dominance occurs for smaller values of p. Therefore, as n or p increases, we should see more and more nodes of the same opinion in each party, the population of nodes holding the majority opinion growing to potentially span the whole party.

4.3.4 Special Cases

In this section we consider the special case where the probability of a positive edge-weight between members of the same party is $p = 1$. As mentioned earlier, In this case we will show that the partisan outcome is always achieved and the system converges quickly[5]. As before and without loss of generality, taking $|G_1| = n$ and $|G_2| = 0$, we have a graph where

[5]In one "round" of updates.

all the edge-weights between nodes are +1. As a result, the update sum for any node i is

$$S_i = \sum_{j=1}^{n} w_{ij}\, x_j = \sum_{j=1}^{n} x_j, \qquad \forall i.$$

Therefore $\mathrm{sgn}(S_i)$ is that of the majority opinion[6]. Hence, node i does not change its opinion if it is already aligned with that of the majority, and adopts the majority's opinion if it is not. The majority opinion is, therefore, unchanged (possibly strengthened), and the next node's update proceeds in a similar fashion. This continues until all nodes have updated their opinion, at which point they all belong to the majority. The final outcome is a partisan state with every node having the same opinion. This is consistent with our previous findings.

4.3.5 Generalizations

In this section we consider extensions to the Random Influence model and outline their effect, with proofs often relegated to the appendices.

Modified edge-weights w

First, an examination of the proofs of Theorems 1 and 2 reveals that both readily extend to settings where there is self-reinforcement, *i.e.,* $w_{ii} > 0$, and also to settings where the signed Bernoulli variables w_{ij} arise from *different* Bernoulli processes and hence have different probabilities.

Specifically, denote $W_{\min} = \min_i\{w_{ii}\}$, where w_{ii} is the self-weight of node i and can be non-zero, and $p_{\min} = \min_{i,j}\{p_{ij}\}$, where we have assumed that every edge-weight w_{ij} is drawn from a different Bernoulli random variable, each with a probability p_{ij} of being +1. A modified version of Theorem 1 can then be obtained (see Appendix B.1), which states

[6] As before, the case of $S_i = 0$ requires special care.

that for any $0 < \delta < 1$,

$$\mathbf{P}_n^+ \geq 1 - \delta, \qquad \text{if} \qquad p_{\min} \geq \frac{1}{2} - \frac{W_{\min}}{2(n-1)} + \sqrt{\frac{\log(n/\delta)}{2(n-1)}}.$$

Similarly, Theorem 2 can also be shown to hold after modifying the quantity α_0 to now be the unique solution of $f(\alpha, p) = 0$, defined as

$$f(\alpha, p) = 2\left[(1 - 2\alpha - 1/n)\,(p_{\min} - 1/2) - \frac{W_{\max}}{2n} - \alpha\Delta_{\max}\right]^2 + \alpha\log(\alpha) + (1-\alpha)\log(1-\alpha)\,,$$

where $p_{\min}$ is as defined before, $W_{\max} = \max_i\{w_{ii}\}$, and

$$\Delta_{\max} = \max_i \left\{ \max_j\{p_{ij}\} - \min_j\{p_{ij}\} \right\}.$$

Zealots

Another extension to the basic Random Influence model is one that includes *zealot* nodes. Zealots are nodes that put extremely large values on their own opinion and therefore never change it. They, hence, influence the other nodes without getting influenced by them. Let the attraction radius of the partisan fixed points in the absence of zealots be αn, and assume that the total number of zealots in the network is z. Then it can be shown that the attraction region of the partisan fixed points is at least $\alpha n - z$.

Independent Group

We consider the presence of a group of *independents* G_a, in addition to the two parties G_1 and G_2. The independents have non-biased affinities towards every other node in the network, *i.e.,* the interaction weights $\{w_{ij},\, i \in G_a\}$ between a node $i \in G_a$ and any other node j in the network form a system of signed Bernoulli trials with success parameter $\mathbf{P}\{w_{ij} = 1\} = 1/2$. In this case the arguments of section 4.2.3 can still be used to merge the two parties G_1 and G_2 into one party G_b. However, the model may not be further simplified and we are left with one biased party G_b and the group of independents. Let the size of the

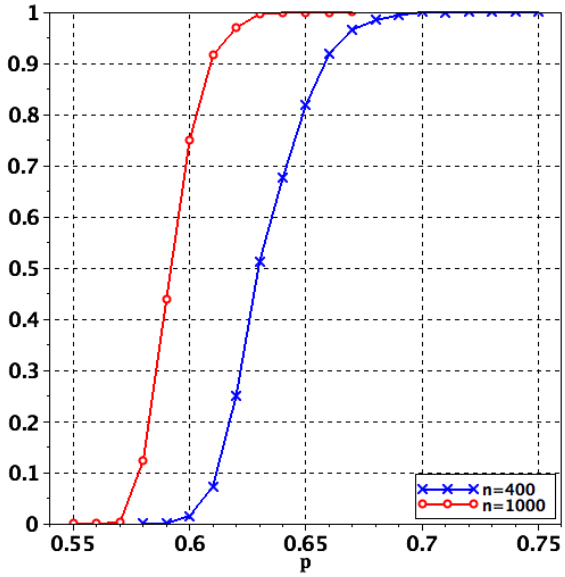

Figure 4.4: The fraction of time that the system converges to a meta-partisan fixed point, from a random, non-biased starting point when 1/2 of the nodes are independents.

biased party be $|G_b| = n_b$ and the size of the group of independents be $|G_a| = n_a = n - n_b$.

In the presence of independents, the partisan states are no longer guaranteed to be fixed points of the system. This is because we cannot identify the opinions of the independent nodes with high probability. Therefore, we create a notation to be able to state the results for the members of the biased party only. Specifically, we define $\mathbf{x}^{\mu+}$ as a *meta-partisan* state, for which $x_i = +1$, $\forall i \in G_b$. Note that under $\mathbf{x}^{\mu+}$ the independent nodes can take any opinion and therefore there are a total of 2^{n_a} such meta-partisan states. For a meta-partisan state, a modified version of Theorem 1 can now be obtained (see Appendix B.2), which states that, starting from any of the meta-partisan states $\mathbf{x}^{\mu+}$, there is a high probability $\widehat{\mathbf{P}^+}$ that the system remains within the set of the meta-partisan states indefinitely.

We can also numerically investigate the convergence frequency to the meta-partisan fixed points in the presence of independents. The results are shown in Fig. 4.3.5 in which a phase transition is evident, similar to that in Fig. 4.3.

Graphs with Erdős-Rényi structure

The analysis of Section 4.3.2 was for a fully-connected graph, where all nodes interact with each other. In this section, we will consider a graph with Erdős-Rényi structure $\mathbb{G}(n, \rho)$, where n is, as before, the number of nodes in the graph (or the number of agents), and an edge between any two nodes exists independently with a probability $\rho > 0$. This system can be thought about as one where $w_{ij} \in \{-1, 0, +1\}$, and it is easy to verify that the single-party isometry argument of Section 4.2.3 still holds. Hence, we can take the edge-weight probabilities to be

$$\begin{aligned} \mathbf{P}\{w_{ij} = +1\} &= \rho \cdot p, \\ \mathbf{P}\{w_{ij} = -1\} &= \rho \cdot (1-p), \qquad \text{and} \\ \mathbf{P}\{w_{ij} = 0\} &= 1 - \rho. \end{aligned}$$

Therefore, if ρ is relatively large (*e.g.,* , a constant arbitrary number, not shrinking with n), then we can use the above probabilities in the derivations of Section 4.3.2 to obtain equivalent results.

However, a more careful analysis allows us to do better, obtaining results even if the $\rho \triangleq \rho_n$ values asymptotically decrease towards 0 as n becomes large. That is what we aim for in the rest of this section. In particular, we will outline the steps to derive a version of Theorems 1 for the Erdős-Rényi graph with asymptotically small $\rho \triangleq \rho_n$. Similar steps can be taken for obtaining a version of Theorem 2.

Let N_i be the neighborhood set of node i, *i.e.,*

$$N_i = \{j \mid w_{ij} \neq 0,\ 1 \leq j \leq n\},$$

and denote the size of this neighborhood set by $|N_i|$. The expected value of $|N_i|$ is ρn. Let A_ϵ denote the event that $|N_i|$ is in the ϵn–vicinity of its expected value, where $\epsilon = \alpha\, \rho$ for

some fixed $0 < \alpha < 1$. Therefore,

$$A_\epsilon : -\epsilon n \leq |N_i| - \rho n \leq \epsilon n.$$

We define a function $f(\alpha)$ on $0 < \alpha < 1$, as $f(\alpha) = c\left((1+\alpha)\,\log(1+\alpha) - \alpha\right)$ where c is a constant $0 < c \leq 1$. It is easy to verify that $f(\alpha) > 0$ on its domain.

We are now set to start with a lemma, which provides a bound on the probability that A_ϵ^c, the complement of A_ϵ, occurs.

Lemma 5. *The probability that $|N_i|$ lies outside the ϵn–vicinity of its expected value satisfies*

$$\mathbf{P}\left(A_\epsilon^c\right) \leq 2\exp\left(-n\rho f(\alpha)\right).$$

Proof. Let $I(w_{ij})$ be an indicator function for existence of the edge w_{ij}, *i.e.,*

$$I(w_{ij}) = \begin{cases} 1, & \text{if } w_{ij} \neq 0 \ (w_{ij} \text{ exists}), \\ 0, & \text{if } w_{ij} = 0 \ (w_{ij} \text{ does not exist}), \end{cases}$$

Therefore the expected value of $I(w_{ij})$ is ρ, and we can use Chernoff's inequality (see [88, Section XVII.1] to get

$$\begin{aligned} \mathbf{P}\left(|N_i| - \rho n > \epsilon n\right) &= \mathbf{P}\left(\sum_{j\neq i} I(w_{ij}) > n\,\rho\,(1+\alpha)\right) \\ &\leq \exp\left(-n\,D\Big(\rho(1+\alpha),\,\rho\Big)\right), \end{aligned} \tag{4.9}$$

where $D(\cdot,\,\cdot)$ is the relative entropy function between two Bernoulli distributions with the given success probabilities, and can be written as

$$\begin{aligned} D\Big(\rho(1+\alpha),\,\rho\Big) &= \rho(1+\alpha)\,\log(1+\alpha) + (1-\rho\,(1+\alpha))\log\left(\frac{1-\rho\,(1+\alpha)}{1-\rho}\right) \\ &= (1+\alpha)\,\log(1+\alpha)\,\rho + (1-(1+\alpha)\,\rho)\log\left(\frac{1-\rho\,(1+\alpha)}{1-\rho}\right). \end{aligned} \tag{4.10}$$

We can write the series expansion for $\log(\cdot)$ to get

$$\log\left(\frac{1-\rho\,(1+\alpha)}{1-\rho}\right) = -\frac{\alpha\,\rho}{1-\rho} - \frac{\alpha^2\,\rho^2}{2\,(1-\rho)^2} - \frac{\alpha^3\,\rho^3}{3\,(1-\rho)^3} - \cdots .$$

Using the expansion in Eq. (4.10) gives

$$\begin{aligned} D\Big(\rho(1+\alpha),\,\rho\Big) &= (1+\alpha)\,\log(1+\alpha)\,\rho - \frac{\alpha\,\rho}{1-\rho} + O\left(\rho^2\right) \\ &= (1+\alpha)\,\log(1+\alpha)\,\rho - \alpha\,\rho + O\left(\rho^2\right) \\ &> c\left((1+\alpha)\,\log(1+\alpha) - \alpha\right)\rho \\ &= \rho\,f(\alpha), \end{aligned}$$

where the constant c is chosen appropriately to account for the higher order terms $O\left(n^2\right)$. Use the above in Eq. (4.9), and similarly compute the probability $\mathbf{P}\left(|N_i| - \rho n < -\epsilon n\right)$ to conclude the proof.

□

We now provide the steps necessary to obtain a result similar to that of Theorem 1. As before, we shall start with the partial sums, $x_i^+ S_i^+$. If the system is in state $\mathbf{x}^+$ the partial sums are given by

$$x_i^+ S_i^+ = S_i^+ = \sum_{j \in N_i} w_{ij} x_j^+ = \sum_{j \in N_i} w_{ij}.$$

The sum on the right represents a random walk with a positive drift, and will depend on the specific value of N_i. Therefore, we condition the rest of the computation on the value

of N_i.

$$\begin{aligned}\mathbf{P}(x_i^+ S_i^+ \leq 0) &= \mathbf{P}\left(\sum_{j\in N_i} w_{ij} \leq 0\right) \\ &= \mathbf{P}\left(\sum_{j\in N_i} w_{ij} \leq 0 \,\middle|\, A_\epsilon\right) \times \mathbf{P}(A_\epsilon) + \mathbf{P}\left(\sum_{j\in N_i} w_{ij} \leq 0 \,\middle|\, A_\epsilon^c\right) \times \mathbf{P}(A_\epsilon^c) \\ &\leq \mathbf{P}\left(\sum_{j\in N_i} w_{ij} \leq 0 \,\middle|\, A_\epsilon\right) \times 1 \;+\; 1 \times \mathbf{P}(A_\epsilon^c)\end{aligned} \tag{4.11}$$

Where A_ϵ^c is the complement of the event A_ϵ, and its probability was computed in Lemma 5. On the other hand, and remembering that $\epsilon < \rho$, an application of Hoeffding's inequality as before gives

$$\begin{aligned}\mathbf{P}\left(\sum_{j\in N_i} w_{ij} \leq 0 \,\middle|\, A_\epsilon\right) &\leq \mathbf{P}\left(\sum_{j\in N_i} w_{ij} \leq 0 \,\middle|\, |N_i| = \rho n - \epsilon n\right) \\ &\leq \exp\left(-2n(\rho-\epsilon)\left(p-\frac{1}{2}\right)^2\right).\end{aligned} \tag{4.12}$$

Using Eq. (4.12) and Lemma 5 in Eq. (4.11) gives

$$\mathbf{P}(x_i^+ S_i^+ \leq 0) \leq \exp\left(-2\,n\,\rho\,(1-\alpha)\left(p-\frac{1}{2}\right)^2\right) + 2\exp\left(-n\,\rho f(\alpha)\right). \tag{4.13}$$

Now we can, as before, use Boole's inequality to get

$$\begin{aligned}\mathbf{P}\left(\bigcup_{i=1}^n \left(x_i^+ S_i^+ \leq 0\right)\right) &\leq \sum_{i=1}^n \mathbf{P}\left(x_i^+ S_i^+ \leq 0\right) \\ &\leq n \cdot \exp\left(-2\,n\,\rho\,(1-\alpha)\left(p-\frac{1}{2}\right)^2\right) + 2n \cdot \exp\left(-n\,\rho f(\alpha)\right).\end{aligned}$$

Now we can pick specific values of $0 < \alpha < 1$ and obtain suitable asymptotic results.

4.4 Profile-Based model

The Random Influence model is attractive in its simplicity and elegance, and as shown in the previous section, results in opinions which conform along party lines. Somewhat more nuanced and varied opinion formations arise in the profile-based model that we describe next.

4.4.1 Model Formulation

In the profile-based model each node i has a *profile* $\pi_i = (\pi_{i1}, \ldots, \pi_{i\kappa}) \in \{-1, +1\}^\kappa$ where each entry in the profile takes a positive $(+1)$ or negative (-1) value based on the node's known position regarding one of κ independent topics. The influence weight w_{ij} between two nodes is specified as the inner product of their profiles, *i.e.,*

$$w_{ij} = \pi_i \cdot \pi_j = \sum_{k=1}^{\kappa} \pi_{ik}\pi_{jk}.$$

We suppose that the profile bits are randomly chosen for each node and independently across nodes. Reusing notation for success probabilities, suppose $1/2 < p < 1$. The sequence of profile bits $\{\, \pi_{ij}, 1 \le j \le \kappa, 1 \le i \le n \,\}$ then constitutes a family of independent, signed Bernoulli variables with success parameter p: $\mathbf{P}\{\pi_{ij} = +1\} = p$, $\mathbf{P}\{\pi_{ij} = -1\} = 1 - p$. By symmetry, the collection of weights $\{\, w_{ij}, 1 \le i < j \le n \,\}$ forms an exchangeable system of random variables in the de Finetti sense, each weight w_{ij} having a positive bias.

Our description is for the equivalent single party formulation of section 4.2.3. In the two party formulation, the profile bits for members of one party are $\pm$Bernoulli(p) while the profile bits for members of the other parts are $\pm$Bernoulli($1-p$). Thus, if i and j are nodes in the same party then w_{ij} is likely to be positive; if they are from different parties then w_{ij} is likely to be negative. The equivalence between the two formulations is as outlined in Section 4.2.3.

$\Pi_0 = (-1, -1 - 1)$
$\Pi_1 = (-1, -1 + 1)$
$\Pi_2 = (-1, +1 - 1)$
$\Pi_3 = (-1, +1 + 1)$
$\Pi_4 = (+1, -1 - 1)$
$\Pi_5 = (+1, -1 + 1)$
$\Pi_6 = (+1, +1 - 1)$
$\Pi_7 = (+1, +1 + 1)$

Table 4.1: Profile vectors for $\kappa = 3$.

4.4.2 Cluster-Based Analysis

For a profile size of κ, there are 2^κ distinct profile *types*, each associated with distinct profile vectors, Π_ν, $0 \leq \nu < 2^\kappa$. It is useful to index the profile vectors according to their entries, such that $\Pi_\nu = 2\mathbf{b}_\nu - \mathbb{1}_{1\times\kappa}$, where $\mathbf{b}_\nu$ is the binary vector[7] representation of decimal ν, and $\mathbb{1}_{1\times\kappa}$ is the $1 \times \kappa$ vector of all 1s. For instance, the all "-1" profile is denoted by Π_0, and the all "1" profile is denoted by $\Pi_{2^\kappa-1}$. For the case of $\kappa = 3$, we have listed all the 2^κ different profile types in table 4.1.

Nodes that have the same profile type can be grouped into what we term a *cluster*. Let *cluster* C_ν be the set of all nodes whose profile is equal to Π_ν. In what follows we show that nodes in the same cluster always converge to the same opinion. Therefore, given a partitioning of nodes into clusters, *cluster opinions* fully describe the state of the system, so that fixed points only need to be characterized at the cluster level, *i.e.,* what opinion prevails in each cluster.

Proposition 6. *At equilibrium, nodes in a cluster all have the same opinion.*

Proof. Let i and j be any two nodes in C_ν. Per the fixed point criterion, at equilibrium, the update sums for i and j satisfy $x_i S_i > 0$ and $x_j S_j > 0$. Noting that $\pi_i = \pi_j = \Pi_\nu$ and

[7] If needed, higher-order zeros are appended on the left to make $\mathbf{b}_\nu$ of the length κ.

using it in the inner product $w_{ik} = \pi_i \cdot \pi_k$, we have

$$\begin{aligned} 0 < x_i S_i &= x_i \sum_{k=1}^{n} w_{ik} x_k \\ &= x_i \sum_{k=1}^{n} (\Pi_\nu \cdot \pi_k)\, x_k \\ &= x_i \sum_{k \neq i,\, j} (\Pi_\nu \cdot \pi_k)\, x_k + \left(x_i^2 + x_i\, x_j\right) (\Pi_\nu \cdot \Pi_\nu) \\ &= x_i \sum_{k \neq i,\, j} (\Pi_\nu \cdot \pi_k)\, x_k + \kappa \left(x_i^2 + x_i x_j\right) \\ &\triangleq x_i S + \kappa(x_i x_j + 1), \end{aligned}$$

where S stands for the sum $\sum_{k \neq i,\, j} (\Pi_\nu \cdot \pi_k)\, x_k$. Likewise,

$$\begin{aligned} 0 < x_j S_j &= x_j \sum_{k \neq j,\, i} (\Pi_\nu \cdot \pi_k)\, x_k + \kappa \left(x_j^2 + x_j x_i\right) \\ &= x_j S + \kappa(x_j x_i + 1). \end{aligned}$$

Now suppose the proposition is not true, *i.e.,* $x_i x_j = -1$. Then we replace $x_i x_j = -1$ and $x_j = -x_i$ in the above equations to get $x_i S > 0$ and $-x_i S > 0$. This is a contradiction and completes the proof. □

Let c_ν denote the size (number of nodes) of cluster C_ν and let $\mathbf{c}$ be the vector of cluster sizes, $\mathbf{c} = (c_0, \ldots, c_{2^\kappa - 1})$. Furthermore, write X_ν for the common opinion of cluster C_ν and let $\mathbf{X}$ be the vector of all cluster opinions $\mathbf{X} = (X_0, \ldots, X_{2^\kappa - 1})$. Then,

Corollary. *Given a vector of cluster sizes, cluster opinions fully describe the system at equilibrium up to a re-labelling of the nodes.*

Proof. Consider any specific vector of realized cluster sizes $\mathbf{c} = (c_0, \ldots, c_{2^\kappa - 1})$. We introduce a *nominal labelling* of nodes, which labels the c_ν nodes in cluster C_ν as $\sum_{\eta=0}^{\nu-1} c_\eta + 1, \sum_{\eta=0}^{\nu-1} c_\eta + 2, \ldots, \sum_{\eta=0}^{\nu-1} c_\eta + c_\nu$. For this nominal labeling, Proposition 6 states that the cluster opinions $\mathbf{X}$ determine the opinions of all nodes and hence the state of the system. We shall refer to this state as the *nominal state* corresponding to $\mathbf{c}$ and $\mathbf{X}$. Note, however,

that for a given combination of cluster sizes $\mathbf{c}$, there are $n!/\prod_{\eta=0}^{2^\kappa-1} c_\eta!$ different permutations of nodes and therefore labels that realize those cluster sizes. Each such permutation corresponds to a different state, which can, however, be mapped to the corresponding nominal state simply by relabelling its nodes.

□

Hence, in the rest of this chapter we only consider the system's *nominal states*, which we simply refer to as *states* for conciseness. As a result, the state of the system can now be fully described solely by the vector of cluster opinions $\mathbf{X} = (X_0, \ldots, X_{2^\kappa-1})$. State $\mathbf{X}$ is stable if all clusters are stable, *i.e.,* their updated opinion equals their current opinion. The updated opinion of cluster C_ν can be obtained considering any of its member nodes. Specifically,

Lemma 6. *A state* $\mathbf{X}$ *is a fixed point if and only if,*

$$X_\nu = \operatorname{sgn}\left(\sum_{\nu'=0}^{2^\kappa-1} (\Pi_\nu \cdot \Pi_{\nu'})\, c_{\nu'} X_{\nu'}\right), \qquad 0 \le \nu \le 2^\kappa - 1.$$

The stability of a state $\mathbf{X}$ is, therefore, determined by the vector of realized cluster sizes $\mathbf{c} = (c_0, \ldots, c_{2^\kappa-1})$.

Using a simple combinatorial counting argument, lemma 6 proffers a crude upper bound of 2^{2^κ}, the maximum number of cluster–level states, for the number of possible fixed points. While the bound is not particularly sharp, it is already informative: *the number of fixed points in the profile-based model is bounded.* As we shall see, the number of fixed points is not trivially small nor are they so large (growing with n) that analysis is fruitless. The number of fixed points falls in the Goldilocks zone of not too many and not too few.

Lemma 7, that follows, shows that the bound 2^{2^κ} can be improved by considering symmetries across clusters.

Recall for the ν^{th} profile vector that $\Pi_\nu = 2\mathbf{b}_\nu - \mathbb{1}_{1\times\kappa}$, where $\mathbf{b}_\nu$ is the binary vector representation of decimal ν, and $\mathbb{1}_{1\times\kappa}$ is the $1 \times \kappa$ vector of all 1s.

Lemma 7. *At equilibrium, clusters* C_ν *and* $C_{2^\kappa-1-\nu}$ *have opposite opinions.*

Proof. For the respective profiles Π_ν and $\Pi_{2^\kappa-1-\nu}$ corresponding to these clusters, we have

$$\begin{aligned}\Pi_\nu + \Pi_{2^\kappa-1-\nu} &= 2\mathbf{b}_\nu - \mathbb{1}_{1\times\kappa} + 2\mathbf{b}_{2^\kappa-1-\nu} - \mathbb{1}_{1\times\kappa} \\ &= 2\left(\mathbf{b}_\nu + \mathbf{b}_{2^\kappa-1-\nu} - \mathbb{1}_{1\times\kappa}\right) \\ &= 2\left(\mathbb{1}_{1\times\kappa} - \mathbb{1}_{1\times\kappa}\right) = 0,\end{aligned}$$

and as a result

$$\Pi_\nu = -\Pi_{2^\kappa-1-\nu}.$$

Furthermore, since the system is at equilibrium, updated and current opinions are identical. Therefore using lemma 6 we have

$$\begin{aligned}X_\nu &= \operatorname{sgn}\left(\sum_{\nu'=0}^{2^\kappa-1}\left(\Pi_\nu \cdot \Pi_{\nu'}\right) c_{\nu'} X_{\nu'}\right) \\ &= -\operatorname{sgn}\left(\sum_{\nu'=0}^{2^\kappa-1}\left(\Pi_{2^\kappa-1-\nu} \cdot \Pi_{\nu'}\right) c_{\nu'} X_{\nu'}\right) \\ &= -X_{2^\kappa-1-\nu}.\end{aligned}$$

This concludes the proof. □

Lemma 7 establishes that any fixed point is of the form $\mathbf{X} = [\mathbf{X}^L, -\mathbf{X}^L]$, where $\mathbf{X}^L$ is a vector of size $2^{\kappa-1}$ consisting of -1 and $+1$ entries only. Then we have the following theorem which is an improvement over the bound 2^{2^κ} that we previously discussed..

Theorem 3. *The number of fixed points is upper-bounded by* $2^{2^{\kappa-1}}$.

For a fixed κ, Theorem 3 gives a constant upper-bound on the number of fixed points which does not depend on the number of nodes n. In the case of $\kappa = 3$ this upper bound is $2^{2^{\kappa-1}} = 16$, and those 16 possible fixed points are listed in table 4.2.

As we shall see later, even the bound given in Theorem 3 is not particularly tight; several of these states may not be feasible fixed points. For instance, a numerical experiment for the case of $\kappa = 3$ shows that the number of realized fixed points is less than $2^{2^{\kappa-1}} = 16$, and changes with p. The result is shown in Fig. 4.5.

state index	X_0	X_1	X_2	X_3	X_4	X_5	X_6	X_7
0	-1	-1	-1	-1	$+1$	$+1$	$+1$	$+1$
1	$+1$	-1	-1	-1	$+1$	$+1$	$+1$	-1
2	-1	$+1$	-1	-1	$+1$	$+1$	-1	$+1$
3	$+1$	$+1$	-1	-1	$+1$	$+1$	-1	-1
4	-1	-1	$+1$	-1	$+1$	-1	$+1$	$+1$
5	$+1$	-1	$+1$	-1	$+1$	-1	$+1$	-1
6	-1	$+1$	$+1$	-1	$+1$	-1	-1	$+1$
7	$+1$	$+1$	$+1$	-1	$+1$	-1	-1	-1
8	-1	-1	-1	$+1$	-1	$+1$	$+1$	$+1$
9	$+1$	-1	-1	$+1$	-1	$+1$	$+1$	-1
10	-1	$+1$	-1	$+1$	-1	$+1$	-1	$+1$
11	$+1$	$+1$	-1	$+1$	-1	$+1$	-1	-1
12	-1	-1	$+1$	$+1$	-1	-1	$+1$	$+1$
13	$+1$	-1	$+1$	$+1$	-1	-1	$+1$	-1
14	-1	$+1$	$+1$	$+1$	-1	-1	-1	$+1$
15	$+1$	$+1$	$+1$	$+1$	-1	-1	-1	-1

Table 4.2: Opinions of different clusters (opinion X_ν corresponds to to cluster C_ν) under all 16 potential fixed points (indexed 0 to 15) for $\kappa = 3$

As per Lemma 6, whether a specific state is a fixed point depends on the particular realization of the cluster sizes $\mathbf{c}$, which are stochastic values. However, in the following we establish that with probability approaching 1, *expected values* of cluster sizes are sufficient to characterize feasible fixed points.

4.4.3 Concentration at the Cluster Level

In this section we first compute the expected sizes of the clusters, then we will show that these expected values can be used to characterize feasible fixed points.

Since the probability distribution of every profile entry is known, the probability μ_ν that a node profile is of a certain type Π_ν can be readily computed. For $\kappa = 3$, for example,[8] $\mu_0 = q^3$ and $\mu_1 = q^2 p$, where $q = 1 - p$. Expected cluster sizes can now be easily computed

[8] Considering the single-party equivalent model.

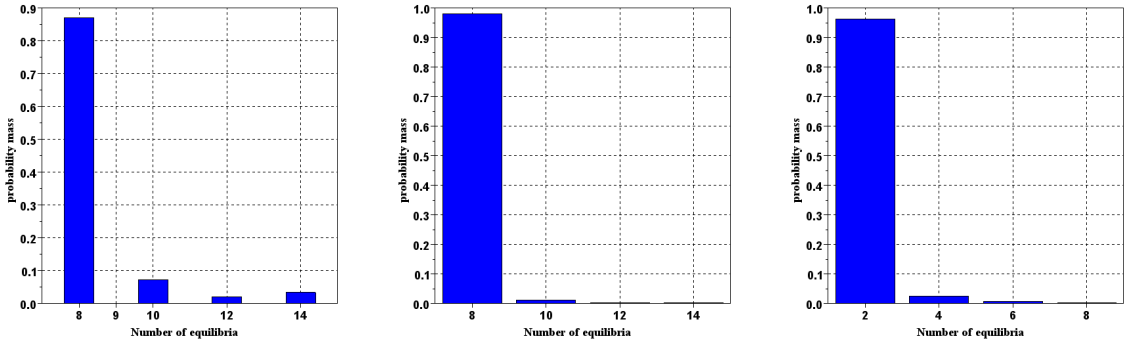

(a) $n = 400$ and $p = 0.8$ (b) $n = 2000$ and $p = 0.8$ (c) $n = 100$ and $p = 0.9$

Figure 4.5: Probability mass function of the number of observed fixed points for $\kappa = 3$.

as follows.

Let $I_j(\Pi)$ be an indicator random variable which takes value $+1$ if $\pi_j = \Pi$, and 0 if $\pi_j \neq \Pi$. It is clear that $\mathbf{E}\left(I_j(\Pi_\nu)\right) = \mu_\nu$. Furthermore, the size c_ν of cluster C_ν can be written in the form

$$c_\nu = |C_\nu| = \sum_{j=1}^{n} I_j(\Pi_\nu). \tag{4.14}$$

By additivity, the expected cluster size is hence given by

$$\mathbf{E}(c_\nu) = \sum_{j=1}^{n} E\left(I_j(\Pi_\nu)\right) = \sum_{j=1}^{n} \mu_\nu = n\mu_\nu.$$

In any realization of the profile vectors, cluster sizes will vary around these expected values, and these variations can conceivably affect the set of possible fixed points. Fig. 4.5 illustrates this by plotting the distribution of the number of fixed points obtained across a set of $10,000$ realizations for $\kappa = 3$ and different combinations of n and p. We see that while, as expected, the upper bound of 16 holds, the number of observed fixed points varies as a function of p. More interesting though is the fact that as n increases for a constant p (Fig. 4.5a and Fig. 4.5b), the number of observed fixed points appears to concentrate on fewer values. We formalize this insight next, starting with a lemma that bounds the probability of cluster size variations around their mean value.

Lemma 8. *The fractional cluster size c_ν/n is concentrated at its mean value μ_ν. Specifically: fix any $\epsilon > 0$. Then*

$$\mathbf{P}\left(\left|\frac{c_\nu}{n} - \mu_\nu\right| \leq \epsilon\right) \geq 1 - 2\exp\left(-2n\epsilon^2\right).$$

Proof. Start from Eq. (4.14) and note that since the profiles π_j and $\pi_{j'}$ of nodes $j \neq j'$ are independent of one another, $I_j(\Pi_\nu)$ and $I_{j'}(\Pi_\nu)$ are also independent for any ν. Therefore Eq. (4.14) expresses c_ν as the sum of n independent random variables, each of which satisfies $I_j(\Pi_\nu) \in \{0, 1\}$. This allows for an application of Hoeffding's inequality (Theorem 1 of [48]), which gives

$$\mathbf{P}\left(\frac{c_\nu}{n} - \mu_\nu \geq \epsilon\right) \leq \exp\left(-2n\epsilon^2\right)$$

and

$$\mathbf{P}\left(\frac{c_\nu}{n} - \mu_\nu \leq -\epsilon\right) \leq \exp\left(-2n\epsilon^2\right).$$

An application of Boole's inequality shows hence that

$$\mathbf{P}\left(\left|\frac{c_\nu}{n} - \mu_\nu\right| \geq \epsilon\right) \leq 2\exp\left(-2n\epsilon^2\right).$$

Taking the complement of both sides finishes the proof. □

Now that we know c_ν/n is close to μ_ν, we will show that for identifying the possible outcomes it typically suffices to only investigate the *expected value* of cluster sizes, $n\mu_\nu$, or the expected fractional size, μ_ν.

To facilitate the statement of the result and its derivation, we define an update sum S_ν for cluster C_ν based on lemma 6. Specifically,

$$S_\nu \triangleq \sum_{\nu'=0}^{2^\kappa - 1} \frac{(\Pi_\nu \cdot \Pi_{\nu'})}{\kappa} \frac{c_{\nu'}}{n} X_{\nu'}. \tag{4.15}$$

We have scaled S_ν by a factor $\kappa \cdot n > 0$ from the expression in lemma 6, which does not change its sign and therefore does not change any of the update decisions. Note that the

expected value of the term $\frac{c_{\nu'}}{n}$ on the right is μ_ν which is a function of p, the probability that a profile entry is positive. Therefore, taking the expected values from both sides of this equation, shows that the expected value $\overline{S}_\nu$ of the update sum is a function of state X as also of p, and it will be useful to take explicit note of this by writing $\overline{S}_\nu = \overline{S}_\nu(X, p)$. It will also be convenient to define

$$\sigma(p) \triangleq \min_{\substack{0 \le \nu \le 2^\kappa - 1 \\ X \in \{-1,+1\}^{2^\kappa}}} \left| \overline{S}_\nu(X, p) \right| .$$

Theorem 4. *For any p such that $\sigma(p) > 0$, the probability Q_n that the set of fixed points of the system under actual cluster sizes c_ν is the same as that under expected cluster sizes $n\mu_\nu$ is bounded from below by*

$$Q_n \ge 1 - 2^{\kappa+1} \exp\left(-n \left(\frac{\sigma(p)}{2^\kappa} \right)^2 \right) .$$

In particular, $Q_n \to 1$ as $n \to \infty$.

Proof. In the proof of Lemma 8 we saw that the probability that any of the c_ν values lies outside $[\mu_\nu - \epsilon, \mu_\nu + \epsilon]$ is bounded by $2\exp\left(-2n\epsilon^2\right)$. By Boole's inequality we see that the probability that at least one of the c_ν values lies outside that interval is bounded by $2^\kappa \times 2\exp\left(-2n\epsilon^2\right)$. Taking complements we obtain

$$\mathbf{P}\left(\bigcap_\nu \left\{ \left| \frac{c_\nu}{n} - \mu_\nu \right| \le \epsilon \right\} \right) \ge 1 - 2^{\kappa+1} \exp\left(-2n\epsilon^2\right) .$$

Now consider Eq. (4.15), and note that replacing $\frac{c_{\nu'}}{n}$ with $\mu_{\nu'}$ can introduce an error of at most ϵ to each term in the sum and at most $\epsilon 2^\kappa$ to the total sum. Therefore

$$\mathbf{P}\left(\bigcap_\nu \left\{ \left| S_\nu - \overline{S_\nu} \right| \le \epsilon 2^\kappa \right\} \right) \ge 1 - 2^{\kappa+1} \exp\left(-2n\epsilon^2\right) . \tag{4.16}$$

If $\sigma(p) \neq 0$, then we can pick $\epsilon < \frac{\sigma(p)}{2^\kappa}$, *e.g.*, $\epsilon = \frac{\sigma(p)}{2^{\kappa+1/2}}$ and Eq. (4.16) becomes

$$\begin{aligned}\mathbf{P}\left(\bigcap_\nu \left\{\left|S_\nu - \overline{S_\nu}\right| \leq \sigma(p)\right\}\right) &\geq \mathbf{P}\left(\bigcap_\nu \left\{\left|S_\nu - \overline{S_\nu}\right| \leq \epsilon 2^\kappa\right\}\right) \\ &\geq 1 - 2^{\kappa+1} \exp\left(-n\left(\frac{\sigma(p)}{2^\kappa}\right)^2\right).\end{aligned}$$

But $\left|S_\nu - \overline{S_\nu}\right| \leq \sigma(p)$ means that S_ν and $\overline{S_\nu}$ have the same sign. Since the sign of the update sums determines the dynamics of the system, this concludes the proof. □

Note that at any point p such that $\sigma(p) = 0$ the condition of Theorem 4 does not hold. However, the zeros of $\sigma(p)$ are determined by the zeros of the constituent polynomials comprising the update sums and so are finite in number by the pigeonhole principle. It follows that $\sigma(p)$ is strictly positive except at a finite set of p values.

Corollary. *Except for a finite set of p values, the set of fixed points in a profile-based network with random cluster sizes is, with probability approaching one as $n \to \infty$, the same as that for a deterministic profile-based network with cluster sizes fixed at their expected values.*

As a result of Theorem 4 and the corollary, we can describe the fixed points of the profile-based model in a compact way. In the following we formulate an explicit matrix equation for these fixed points. As before, let Π_i, $i = 0, ..., 2^\kappa - 1$, be the i^{th} profile type of length κ. Then we can represent the system by a graph of 2^κ nodes, where each node represents a cluster. The influence of cluster j on cluster i is determined by the combined effect of the expected size μ_j of cluster j together with the inner product $(\Pi_j \cdot \Pi_i)$. These effects are lumped into the weighted edge from j to i which we denote by

$$a_{ij} = \mu_j \left(\Pi_j \cdot \Pi_i\right), \; i, j = 0, ..., 2^\kappa - 1.$$

The adjacency matrix $A = [a_{ij}]$ for the graph of clusters can now be written in the form

$$\begin{bmatrix} \kappa p^{\kappa} & p^{(\kappa-1)}q\Pi_1 \cdot \Pi_0 & p^{(\kappa-2)}q^2\Pi_2 \cdot \Pi_0 & \dots \\ p^{\kappa}\Pi_0 \cdot \Pi_1 & \kappa p^{(\kappa-1)}q & & \dots \\ \vdots & \vdots & \ddots & \\ p^{\kappa}\Pi_0 \cdot \Pi_{2^{\kappa}-1} & \dots & & \end{bmatrix}$$

whence the fixed points of the system are the solution to the system of simultaneous equations specified by

$$\operatorname{sgn}(A\mathbf{X}) = \mathbf{X},$$

where $\mathbf{X}$ is the vector of cluster opinions, and the signum operation applied to a vector is to be interpreted component-wise. Note that as per the Corollary of Proposition 6, this equation describes the *nominal* fixed points of the system, not the specific *node* opinions.

We solved the above system of equations for different values of of κ and p, and the result is reported in what follows. Specifically, Table 4.3 is for a profile size of $\kappa = 3$, and determines, for all of the states previously given in Table 4.2, whether or not the state is a fixed point, and if so, for what values of p. We classify the fixed points of Table 4.3 according to the size of the p interval in which the fixed point is feasible, or *persists*. As such, we name the states 1, 2, 4, 11, 13 and 14 the "weakly persistent" fixed points. States 0, 3, 5, 10, 12 and 15 are the "moderately persistent" fixed points, and finally the "strongly persistent" fixed points are states 7 and 8.

A distinguishing aspect of the profile-based model is that *dissent from the majority position is present in all three types of fixed points.* This is made precise in the following

Theorem 5. *For profiles of size $\kappa = 3$, the number of dissenting nodes is of order n for all three types of fixed points. More precisely, if p represents the strength of party bias and $q = 1 - p$, then the fraction of dissenting nodes is, with probability approaching one as $n \to \infty$, equal to $q^3 + 2qp^2 + q^2p$, $q^3 + 2q^2p + qp^2$, and $q^3 + 3q^2p$, for weakly persistent, moderately persistent, and strongly persistent fixed points, respectively.*

state index	$p \in (0.5, 0.78)$	$p \in (0.78, 0.86)$	$p \in (0.86, 1)$
0	feasible	feasible	
1	feasible		
2	feasible		
3	feasible	feasible	
4	feasible		
5	feasible	feasible	
6			
7	feasible	feasible	feasible
8	feasible	feasible	feasible
9			
10	feasible	feasible	
11	feasible		
12	feasible	feasible	
13	feasible		
14	feasible		
15	feasible	feasible	

Table 4.3: Feasibility range for each of the fixed points (for $\kappa = 3$)

The proof requires nothing more than a careful tabulation of the sizes of dissenting clusters for fixed points of each type; we provide the details in the Appendix.

Fig. 4.6 illustrates Theorem 5 by showing the extent of intra-party dissent for each of the three types of fixed points. While intra-party dissent is most pronounced in the ephemeral fixed points it is present even in the strongly persistent fixed points: the departure from unanimity persists, albeit as an irritating minority to a partisan majority, at any level of bias short of certainty.

Fig. 4.7 plots the number of fixed points for three different values of κ. As expected from Theorem 6 for $\kappa = 3$ and $\kappa = 5$, when p gets sufficiently close to 1 only two fixed points remain feasible. In the case of the even number $\kappa = 4$, however, the number of fixed points never drops to 2. This is because, again by Theorem 6, there are some clusters that are not forced to change their opinions, and therefore they maintain some level of diversity.

The behaviors in figures 4.7a and 4.7b show a monotone decrease of number of fixed

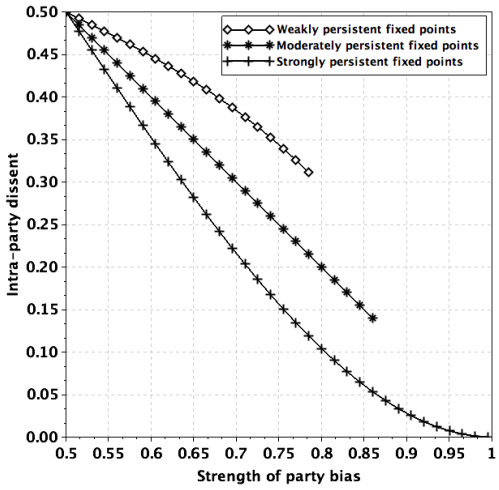

Figure 4.6: *Intra-party dissent at equilibria when interactions are based on biased profiles.* The relative size of the dissenting minority within the parties is plotted as a function of the strength of party bias p for each of the three fixed point classifications in the case of profiles of size $\kappa = 3$. (a) Weakly persistent fixed points. (b) Moderately persistent fixed points. (c) Strongly persistent fixed points.

points as p increases. This could suggest that as p becomes larger, the increasing disparity in cluster sizes results in elimination of fixed points. While this intuition is valid for small κ, it *does* get violated as κ becomes larger and the interactions become more complicated. For instance, Fig. 4.7c gives evidence for a counter example where there is a rise in the number of fixed points at a specific p value. The presence of such instances was analytically and numerically verified.

In the rest of this section we compute the number of fixed points for p values close to 1, and show that for such p values the cluster sizes become so disproportionate that the diversity in opinions gets eliminated. In particular, when p is sufficiently large, the opinions of most clusters at equilibrium will be determined be the opinion of one *dominant* cluster.

Let $C^{(\lambda)}$ denote a cluster whose profile has exactly λ entries that are $+1$ (and, hence, $\kappa - \lambda$ entries that are -1).

Theorem 6. *There exists $p^* < 1$ such that for all p in the interval $p^* \leq p < 1$, and with probability approaching 1 as n grows large, the opinion of any cluster $C^{(\lambda)}$ agrees with that*

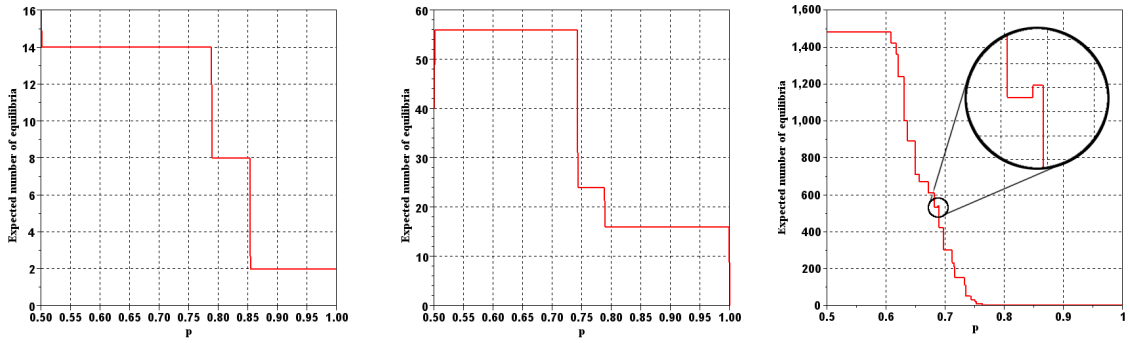

(a) $\kappa = 3$ (b) $\kappa = 4$ (c) $\kappa = 5$

Figure 4.7: The expected number of fixed points in the profile-based model. As seen in (c), this number is not monotone in p.

of $C^{(\kappa)}$ if $\lambda > \kappa/2$ and disagrees with that of $C^{(\kappa)}$ if $\lambda < \kappa/2$. Moreover, the opinions of clusters of type $C^{(\kappa/2)}$ are unaffected[9] *by the ensemble of clusters of other types.*

Proof. The expected size of (the only) $C^{(\kappa)}$ is p^κ which eventually outgrows that of all other clusters combined, as p approaches 1. Since any cluster with $\lambda < \kappa/2$ or $\lambda > \kappa/2$ has a non-zero edge-weight to $C^{(\kappa)}$, this cluster contributes a dominant effect and determines the opinion of $C^{(\lambda)}$, either positively or negatively, based on the sign of their edge-weight. The proof for $C^{(\kappa/2)}$ is in appendix B.3. □

Based on Theorem 6, while the opinion of cluster $C^{(\kappa)}$ determines that of clusters with $\lambda > \kappa/2$ and $\lambda < \kappa/2$ entries taking value $+1$ in their profiles, it does not determine the opinions of clusters with $\lambda = \kappa/2$. The latter are *centric* clusters that have exactly $\kappa/2$ entries of $+1$ in their profiles and are only present when κ is an even number. This is because the centric clusters incur an overall zero influence from the outside world if p is large enough. Consequently, those clusters can decide independently of the rest of the network.

[9] Only for even κ. Also, when the cluster sizes are not exactly the expected values, the outside effect on clusters of type $C^{(\kappa/2)}$ is non-zero but negligible.

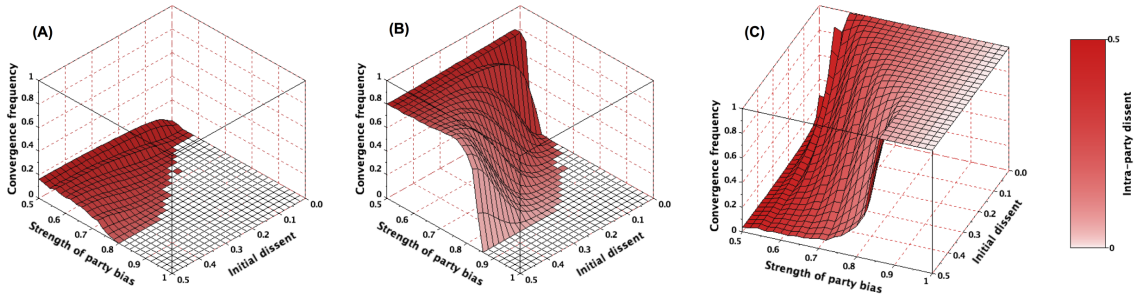

Figure 4.8: Convergence to fixed points of different types for the Profile-based model: The frequency of convergence to each of the three types of fixed points is plotted as a function of the initial dissent δ and the strength of party bias p when $\kappa = 3$. Each point was obtained by aggregating 50,000 random initializations in a population of size $n = 100$. (A) Weakly persistent fixed points. (B) Moderately persistent fixed points. (C) Strongly persistent fixed points.

4.4.4 Numerical Results

In this section we use numerical experiments to observe the convergence frequency to, and attraction region of, each of the three types of fixed points that we earlier identified for $\kappa = 3$.

Fig. 4.8 sheds more light on the convergence rate to the three types of fixed points for $\kappa = 3$. While the strongly persistent fixed points become more dominant as the party bias increases, the ephemeral (weakly and moderately persistent) fixed points have a non-negligible influence when the bias is small. (Figs. 4.6 and 4.8 in tandem clarify the relation between the initial and final levels of dissent.)

Note that Fig. 4.8 may not be very informative about the *attraction regions* of the fixed points. Such a plot is given in Fig. 4.9, where the axes measure the distance from the specified fixed points, rather than measuring the initial dissent.

4.4.5 Special Cases

In this subsection, we analyze the system for some special cases of profile length. In the event that a manual analysis becomes too lengthy to perform, we have used computational tools to facilitate the solution. Proofs are in appendix B.4.

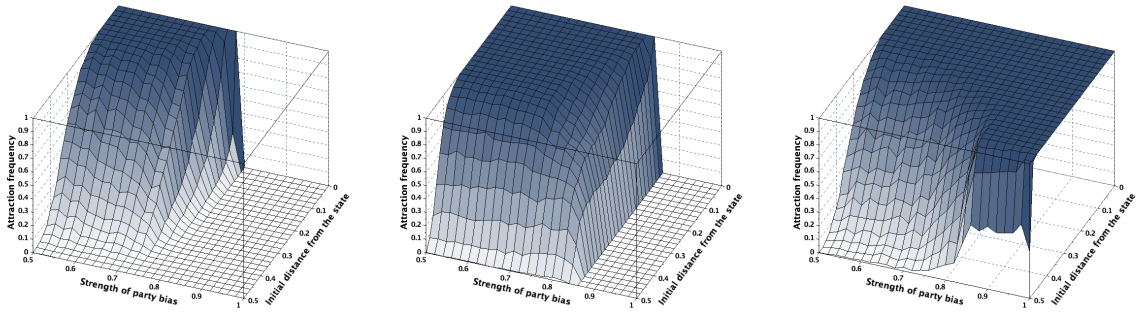

(a) A weakly persistent equilibrium

(b) A moderately persistent equilibrium

(c) A strongly persistent equilibrium

Figure 4.9: Statistical attraction region for the three types of fixed points when $\kappa = 3$. Each point was obtained by aggregating 1,000 random initializations in a population of size $n = 100$.

Proposition 7. *Profile of size* 1. *For any network size* n, *the profile-based model with profile size* $\kappa = 1$ *has exactly two stochastic fixed points. Note that when* $\kappa = 1$, *the profile vector* π_i *is just a scalar.*

The case $\kappa = \infty$ presents another extreme of profile size.

Proposition 8. *Profile of size* ∞. *Suppose* $\kappa = \kappa_n$ *grows sufficiently rapidly with* n *so that*

$$\kappa_n = \frac{2n^2}{(4p^2 - 4p + 1)^2}(\log(n) + \log(n+1)).$$

Then with probability tending to one as $n \to \infty$, *the only fixed points are the pair of partisan fixed points* $\mathbf{x}^+$ *and* $\mathbf{x}^-$.

A very large historical record captured in the profile has the effect of smoothing out all the wrinkles in the dynamics and collapsing the fixed points to two.

Note that while both $\kappa = 1$ and $\kappa = \infty$ result in only two fixed points, the compositions of these fixed points are very different—stochastic in one case, deterministic in the other. As κ grows from 1 to ∞, the nature of the fixed points changes gradually and a range of diverse and interesting possibilities appear for finite κ values. Next we consider a few finite κ values.

$\Pi_a = (+1, +1)$
$\Pi_b = (-1, -1)$
$\Pi_c = (+1, -1)$
$\Pi_d = (-1, +1)$

Table 4.4: Profile types for $\kappa = 2$

Profile of size 2.

If $\kappa = 2$, any profile is one of the four types given in Table 4.4, where we have labeled them with indices a, b, c and d. Nodes with types a and b behave regardless of nodes with types c and d, and vice versa. This is because those profiles have an inner product of zero which results in zero edge-weight. As a result, nodes with types a and b will behave similar to the $\kappa = 1$ case, demonstrating two different outcomes. Similarly, nodes with types c and d will demonstrate two different outcomes. Overall, the results are independent of the value of p; we obtain four different fixed points which are determined *stochastically*, *i.e.,* based on the specific initialization of profile values.

4.4.6 Generalizations

In this section we consider extensions to the Profile-based model and outline their effect, with proofs often relegated to the appendices.

Modified Probability for Profile Entries

Since each profile entry of a node reflects the node's position on one of κ independent topics, a natural extension to this section's model is obtained by assuming different probability distributions for each of the κ profile bits. For example, consider that for any node i the entry k of the profile is a signed Bernoulli variable with success parameter p_k: $\mathbf{P}\{\pi_{ik} = +1\} = p_k$, $\mathbf{P}\{\pi_{ik} = -1\} = 1 - p_k$. Under this modification, it can be shown that the relative sizes of the clusters change, but the results still hold.

Zealots

Inclusion of zealots in the profile-based model is more challenging than it is in the Random Influence model. In particular, assessing the effect of zealots depends not only on how they are distributed across clusters, but it is also rendered more difficult by the fact that their presence invalidates Proposition 6. Hence, unlike the Random Influence model, we are not able to incorporate the zealots in the profile-based model.

Independent Group

An extension to the profile-based model is one in which there is a group of *independent* nodes. For these nodes, each profile bit is chosen randomly with probability 1/2. The presence of such a population changes the cluster sizes and hence by lemma 6 changes the fixed points of the system. Although a very large independent population can considerably change the count of fixed points seen in Fig. 4.7, the general results of this section hold even in the presence of independents.

Graphs with Erdős-Rényi structure

Introducing an Erdős-Rényi graph structure for the profile-based model is challenging, as such a structure conflicts with the native *structure* that exists in the profile-based model, and modifies important aspects of the current model that our analysis relied upon. The reason for the conflict, is that the current profile-based model has a type of structure that is natively implemented. For instance, if the inner product of the profiles between two nodes is zero, then the two nodes do not influence each other. This is somewhat similar to the disconnection effect that an Erdős-Rényi graph brought to the Random Influence model.

The native structure of the profile-based model goes beyond the first order mutual interactions, and as shown in Appendix B.3, there can be relatively large clusters that are wholly (in effect) disconnected from the rest of the graph.

4.5 Conclusion

To summarize, when interactions are directly influenced by party biases then, even for the slightest of biases, $p = 1/2 + \epsilon$, if the population is large enough, the two partisan states dominate the space: *even high levels of initial dissent are quickly extinguished and opinions converge to one of the partisan fixed points.*

The mere fact of party membership, however tenuous, is sufficient to drive a tendency of the party to cohere. There is a marked tendency to unanimity within parties if the influence of party affiliation on interactions is direct. However, dissent is enabled when the influence of party affiliation is indirect. Other sociological factors, of course, will modulate this tendency to cohere but the existence of such a strong driving force based on party membership alone explicates a fundamental mechanism at work in the dynamics of opinion formation in a precise and quantifiable way.

When the interactions are *indirectly* influenced by party biases, there is more variety in the outcomes. The lessons that we draw from the relatively small profile of $\kappa = 3$ carry over to larger values of κ though the complexity of the fixed point structure ineluctably increases as shown in Fig. 4.7. The following features hold in general: (i) Small party biases lead to the most unconstrained systems characterized by a bounded number of possible stable opinion mixes. (ii) As the bias p increases the possible behaviors are generally more constrained and in the limit of large p the behavior is dictated by a few dominant fixed points. (iii) All fixed points contain minority dissenting positions though the dissenting fraction is small if the party bias is large.

Extensions to many parties, varying strengths of party influences, the presence of independents and zealots, self-reinforcement, and localized interactions where considered, which, often follow readily without a significant change in the essential nature of the results.

Appendices

Appendix A

Extras for UPC models

A.1 Discrete Dynamics

In this section we propose a discrete dynamic platform and formally describe how the equilibria of the UPC system are determined over this platform. With Eq. (3.5) in place, it is possible to investigate the dynamics of user adoption over time. We formulate a discrete-time model that evaluates user adoption decisions at successive epochs. For simplicity[1], at epoch $(n+1)$ all users are assumed to know the system state produced by adoption decisions at epoch n. Users with a non-negative utility then proceed to adopt. Specifically, the utility at epoch $(n+1)$, $U_{n+1}(\Theta, \theta)$, of a user with roaming value θ is given by

$$U_{n+1}(\Theta, \theta) = \gamma - c\, m_n + \theta\,(r\, x_n - \gamma) - p(\Theta, \theta)\,, \tag{A.1}$$

where x_n and m_n are the adoption level and volume of roaming traffic produced by adoption decisions at epoch n.

Using Eq. (A.1) and denoting $H(x) \equiv x_{n+1}$ as a function of $x \equiv x_n$, we can characterize the evolution of $H(x)$ and identify adoption equilibria. Equilibria can be *interior* equilibria, *i.e.,* correspond to $x \in (0, 1)$, or *boundary* equilibria, *i.e.,* associated with $x = 0$ or $x = 1$.

[1] Numerical results confirm that a more realistic, diffusion-based adoption model produces similar results.

Interior equilibria satisfy the equation

$$H(x) = x\,. \tag{A.2}$$

Boundary equilibria need not satisfy Eq. (A.2) and instead verify either $x_n = 0 \geq x_{n+1}$ or $x_n = 1 \leq x_{n+1}$.

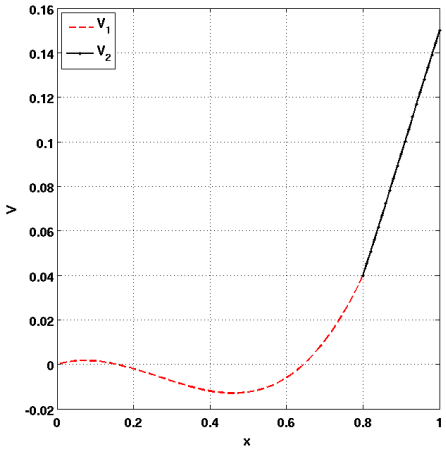

(a) $\gamma = 0.8$, $e = 0.75$, $c = 0.6$, $b = 0$, $r = 1.6$. In this case, the optimal value is achieved at $x = 1$ (Corresponding to the dark solid-colored region in Fig. 3.1).

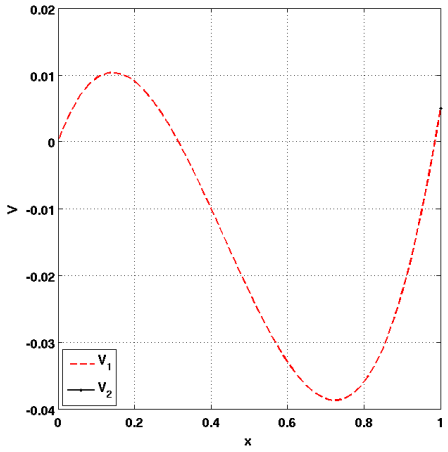

(b) $\gamma = 1.3$, $e = 1.145$, $c = 0.6$, $b = 0$, $r = 1.6$. In this case, the optimal value is achieved at $x \approx 0.14$ (Corresponding to the gradient-colored region in Fig. 3.1).

Figure A.1: System's total value as a function of x for different sets of parameters.

A.2 Derivations for the Optimal Total Welfare

Section 3.3.2 identified the optimal total welfare for a given adoption level x as

$$V^*(x) = \begin{cases} \frac{r-c}{2}x^3 - \frac{\gamma}{2}x^2 + (\gamma - e)x & \text{if } x < \frac{\gamma}{r-c} \\ -\frac{r-c}{2}x^3 + (\frac{\gamma}{2} + r - c)x^2 - ex & \text{if } x \geq \frac{\gamma}{r-c}. \end{cases}$$

Denote the above two expressions by $V_1^*(x)$ and $V_2^*(x)$ for $x < \frac{\gamma}{r-c}$ and $x \geq \frac{\gamma}{r-c}$, respectively (shown in Fig. A.1a as dashed line and solid line, respectively).

Finding the maximum welfare is done in two steps. We first compute the maximum of each function $V_1^*(x)$ and $V_2^*(x)$, and then find the global maximum by comparing the two local maxima.

A.2.1 Maximum of $V_1^*(x)$

For easy reference, we repeat the expression of $V_1^*(x)$ here.

$$V_1^*(x) = \frac{r-c}{2}x^3 - \frac{\gamma}{2}x^2 + (\gamma - e)x\,, \quad x < \frac{\gamma}{r-c}.$$

It is easy to find the roots of this expression as

$$\begin{cases} x = 0 \\ x = \frac{\frac{\gamma}{2} \pm \sqrt{\frac{\gamma^2}{4} - 2(\gamma-e)(r-c)}}{r-c}, \end{cases} \tag{A.3}$$

if they exist (are real numbers). Also its derivative is

$$\frac{\partial V_1^*(x)}{\partial x} = \frac{3}{2}(r-c)x^2 - \gamma x + \gamma - e, \tag{A.4}$$

and the two roots of $\frac{\partial V_1^*(x)}{\partial x}$ are given by

$$\begin{cases} x_{11} = \frac{\gamma - \sqrt{\gamma^2 - 6(\gamma-e)(r-c)}}{3(r-c)} \\ x_{12} = \frac{\gamma + \sqrt{\gamma^2 - 6(\gamma-e)(r-c)}}{3(r-c)}. \end{cases} \tag{A.5}$$

In order to find the maximum total welfare in $x < \frac{\gamma}{r-c}$ regime, we take a step-by-step approach, with each step expressed in a lemma.

Lemma 9. *if $e \geq \gamma$, then $V_1^*(x) \leq 0$ for all values of $x \in [0, \frac{\gamma}{r-c}]$.*

Proof. First assume that $e > \gamma$. From Eq. (A.3) and since $r - c > 0$, the condition $e > \gamma$

guarantees that $V_1^*(x)$ has indeed three roots, $x_1 < 0$, $x_2 = 0$ and $x_3 > \frac{\gamma}{r-c}$. On the other hand, at $x = 0$ the derivative of $V_1^*(x)$ is $g - e < 0$. Therefore $V_1^*(x)$ goes from 0 to negative values for $x > 0$, and may not become non-negative again until its next root at $x_3 > \frac{\gamma}{r-c}$.

Moreover, if $e = \gamma$, then the three roots of Eq. (A.3) are $x_1 = 0$, $x_2 = 0$, and $x_3 = \frac{\gamma}{r-c}$. At $x = 0$ the second derivative of $V_1^*(x)$ is $-\gamma$. Therefore, as before, $V_1^*(x)$ goes from 0 to negative values for $x > 0$, and may not become non-negative again until its next root at $x = \frac{\gamma}{r-c}$. □

This lemma shows that total welfare is *not* positive for $x < \frac{\gamma}{r-c}$ if $e \geq \gamma$. We next look at the case where $e < \gamma$.

Lemma 10. *If $e < \gamma$, then the maximum of $V_1^*(x)$ over values of $x \in [0, \frac{\gamma}{r-c}]$ happens at either $x = x_{11}$ (if it is real) or $x = \gamma/(r-c)$.*

Proof. If $e < \gamma$ it can be easily verified that $x_{11} > 0$ and $x_{12} < \frac{2\gamma}{3(r-c)} < \gamma/(r-c)$ (if they are real). Since $V_1^*(x)$ is an increasing function of x except for $x_{11} < x < x_{12}$, the desired result follows. □

consequently, we deduce that if x_{11} and x_{12} are imaginary, then the maximum of $V_1^*(x)$ over values of $x \in [0, \frac{\gamma}{r-c}]$ happens at $x = \gamma/(r-c)$. More precisely, if e satisfies

$$f_3 : \; e < \gamma - \frac{\gamma^2}{6(r-c)}, \tag{A.6}$$

then the maximum of $V_1^*(x)$ over values of $x \in [0, \frac{\gamma}{r-c}]$ happens at $x = \gamma/(r-c)$.

A.2.2 Maximum of $V_2^*(x)$

For easy reference, we repeat the expression of $V_2^*(x)$ here.

$$V_2^*(x) = -\frac{r-c}{2}x^3 + (\frac{\gamma}{2} + r - c)x^2 - ex\,, \quad x \geq \frac{\gamma}{r-c}.$$

It is easy to find the roots of this expression as

$$\begin{cases} x = 0 \\ x = \frac{\frac{\gamma}{2}+r-c\mp\sqrt{(\gamma/2+r-c)^2-2e(r-c)}}{r-c}, \end{cases} \tag{A.7}$$

if they exist (are real numbers). Also its derivative is

$$\frac{\partial V_2^*(x)}{\partial x} = -\frac{3}{2}(r-c)x^2 + (\gamma+2r-2c)x - e. \tag{A.8}$$

We now have the following lemma.

Lemma 11. *If the roots of* $\frac{\partial V_2^*(x)}{\partial x}$ *are imaginary, then* $V_2^*(x)$ *is always negative on its domain.*

Proof. If the roots are not real then the expression for derivative always has the same sign as of its first coefficient, $-\frac{3}{2}(r-c)$. Since $r-c>0$, then the derivative is always negative, and therefore $V_2^*(x)$ is a decreasing function of x. On the other hand, since $V_2^*(x=0)=0$, therefore $V_2^*(x)<0$, $\forall x \in [\gamma/(r-c),\, 1)$. □

The two roots of $\frac{\partial V_2^*(x)}{\partial x}$ are given by

$$\begin{cases} x_{21} = \frac{\gamma+2r-2c-\sqrt{(\gamma+2r-2c)^2-6e(r-c)}}{3(r-c)} \\ x_{22} = \frac{\gamma+2r-2c+\sqrt{(\gamma+2r-2c)^2-6e(r-c)}}{3(r-c)}. \end{cases} \tag{A.9}$$

By algebraic manipulation we can show that these two roots are imaginary if and only if γ satisfies

$$-2(r-c) - \sqrt{6e(r-c)} < \gamma < -2(r-c) + \sqrt{6e(r-c)}.$$

But the first inequality is always satisfied by positivity of γ. Therefore the roots in Eq. (A.9) are imaginary if and only if γ satisfies

$$\gamma < -2(r-c) + \sqrt{6e(r-c)},$$

or equivalently the roots in Eq. (A.9) are real if and only if γ satisfies

$$f_2: \ \gamma \geq -2(r-c) + \sqrt{6e(r-c)}, \tag{A.10}$$

which, by lemma 11 is required for positivity of $V_2^*(x)$.

Now, lets see what happens when Eq. (A.10) is satisfied and therefore the roots of $\frac{\partial V_2^*(x)}{\partial x}$ are real. Since $r - c > 0$, the derivative is always negative except in between its roots. Then note that as for the smaller root, $x_{21} > 0$. So $\frac{\partial V_2^*(x)}{\partial x} < 0$ at a neighborhood of $x = 0$ and therefore $V_2^*(x)$ is decreasing until a value larger than $x = 0$. After that, $V_2^*(x)$ starts increasing again until $x = x_{22}$ where it again starts to decrease and continues to decrease indefinitely. Considering that $V_2^*(x = 0) = 0$, we deduce that if $V_2^*(x)$ has a positive maximum in $x \in [\gamma/(r-c),\ 1)$ then it happens at $\min\{1,\ x_{22}\}$. On the other hand, and considering that $[\gamma/(r-c),\ 1)$ is only non-empty if $\gamma \leq r - c$, we can perform algebraic manipulations to show that in its valid domain, $x_{22} < 1$ if and only if $e > \gamma + (r-c)/2$.

Therefore, for all values of

$$f_1: \ \gamma \geq e - (r-c)/2, \tag{A.11}$$

the maximum of $V_2^*(x)$ happens at $x = 1$ or $x = 0$, and is the bigger of $\frac{r-c+\gamma}{2} - e$ or 0, respectively.

As mentioned before, we finally compare the maxima of $V_1^*(x)$ and $V_2^*(x)$ for the common parameter ranges. For instance, when Eq. (A.6) is satisfied, it can be shown that Eq. (A.11) is also satisfied, and the bigger of the two maxima happens at $x = 1$. Completing the steps and using numerical comparisons when necessary, results in Fig. 3.1.

A.3 Derivations for Hybrid Usage-Based Policy

Section 3.6 presented the hybrid usage-based pricing policy that combines a fixed price for home connectivity, and a usage-based price for connectivity while roaming.

Also, Lemma 2 provided conditions under which full adoption $x = 1$ is an equilibrium. However, that Lemma did not guarantee the uniqueness of $x = 1$ equilibrium. Indeed, the progression of adoption levels towards $x = 1$ can stall before full adoption is reached. We explore next when this arises (assuming that the conditions of Lemma 2 hold).

A.3.1 Condition for uniqueness of $x = 1$ equilibrium

Consider a scenario where not all users have positive utility when coverage is low, so that only a subset $\Theta \neq [0, 1]$ of users initially adopt. This initial adoption triggers other users to re-evaluate their utility $U(\Theta, \theta)$, which then determines a new set of adopters Θ^{new}, such that $\Theta^{\text{new}} = \{\, \theta \mid U(\Theta, \theta) > 0 \,\}$. Basic algebraic manipulation yields that Θ^{new} comprises either all users (if $x(\delta_r+\gamma)-\gamma \geq 0$), or users that verify $\theta < \frac{c/2-cm+\delta_h}{\gamma-x(\delta_r+\gamma)}$ (if $x(\delta_r+\gamma)-\gamma < 0$), where x and m are determined by the (old) set of adopters Θ. This implies that for any adoption level $x, 0 \leq x \leq 1$, the set Θ of adopters is $[0, x]$. Using Eq. (3.3), this set yields a roaming traffic of the form $m = \frac{x^2}{2}$, which using Eq. (3.20) characterizes the utility of user θ as

$$U(\Theta, \theta) = \frac{c}{2}(1 - x^2) + \delta_h + \theta(x(\delta_r + \gamma) - \gamma).$$

Consequently, the new level of adoption $x^{\text{new}} = |\Theta^{\text{new}}|$ can be expressed as a function of the previous level x. Letting $H(x) \triangleq x^{\text{new}}$ and solving for $U(\Theta, \theta) > 0$ gives[2]

$$H(x) = \begin{cases} \frac{c/2(1-x^2)+\delta_h}{\gamma-x(\delta_r+\gamma)} & \text{if } x(\delta_r + \gamma) - \gamma < 0 \\ 1 & \text{if } x(\delta_r + \gamma) - \gamma \geq 0. \end{cases}$$

Adoption equilibria satisfy $H(x) = x$, and can, therefore, be characterized by solving this equation. It can be shown that

Lemma 12. *when the conditions of Lemma 2 hold, $x = 1$ is the* unique *equilibrium if and*

[2]For notational simplicity, we omit the constraints which ensure that like $x, H(x)$ is lower-bounded by 0 and upper-bounded by 1.

only if γ satisfies

$$\gamma < c + 2\delta_h + 2\sqrt{(c/2 + \delta_h)(\delta_r + \delta_h)}.$$

Proof. It is easy to see that the second expression for $H(x)$ satisfies $H(x) = x$ only at $x = 1$, and therefore if there are any equilibria at $x < 1$, they must satisfy $H(x) = x$ for the first expression of $H(x)$, *i.e.,*

$$H_1(x) \triangleq \frac{c/2(1 - x^2) + \delta_h}{\gamma - x(\delta_r + \gamma)} = x \quad \text{for } x(\delta_r + \gamma) - \gamma < 0.$$

We first show that if γ satisfies the condition of the Lemma, then no such equilibria may exist at $x < 1$.

Basic algebraic manipulation turns the above equation into

$$Q(x) \triangleq (\gamma + \delta_r - c/2)\, x^2 - \gamma x + c/2 + \delta_h = 0,$$

which is a quadratic equation in x and for simplicity we denote it by $Q(x) = 0$. We then compute the discriminant for this equation as

$$\begin{aligned}\Delta_x &= \gamma^2 - 4(c/2 + \delta_h)(\gamma + \delta_r - c/2) \\ &= \gamma^2 - \gamma(2c + 4\delta_h) - 4(c/2 + \delta_h)(\delta_r - c/2),\end{aligned}$$

which, in turn, is a quadratic polynomial in γ. The roots of the discriminant are

$$\begin{aligned}\gamma_1 &= c + 2\delta_h - 2\sqrt{(c/2 + \delta_h)(\delta_r + \delta_h)} \quad \text{and} \\ \gamma_2 &= c + 2\delta_h + 2\sqrt{(c/2 + \delta_h)(\delta_r + \delta_h)}\end{aligned}$$

and the discriminant is negative for γ values in the range (γ_1, γ_2).

Now consider one such γ value in the range (γ_1, γ_2), which is arbitrarily close to γ_2, *i.e.,*

$\gamma = \gamma_2 - \epsilon$ for an arbitrarily small $\epsilon > 0$. Therefore, the coefficient of x^2 in $Q(x)$ becomes

$$\begin{aligned}\gamma + \delta_r - c/2 &= \left(c + 2\delta_h + 2\sqrt{(c/2 + \delta_h)(\delta_r + \delta_h)} - \epsilon\right) + \delta_r - c/2 \\ &= c/2 + (\delta_h + \delta_r) + \delta_h + 2\sqrt{(c/2 + \delta_h)(\delta_r + \delta_h)} - \epsilon,\end{aligned}$$

which is guaranteed to be positive if ϵ is chosen small enough, *e.g.,* $\epsilon = (\delta_h + \delta_r)/2$. (Note that $-\epsilon$ is the only negative term in this expression.) On the other hand, by the previous discussion, Δ_x is negative at $\gamma = \gamma_2 - \epsilon$. Therefore at $\gamma = \gamma_2 - \epsilon$ we have $Q(x) > 0$, $\forall x$ (Of course, by $\forall x$ we mean values of x for which $H(x) = H_1(x)$, *i.e.,* those which satisfy $x(\delta_r + \gamma) - \gamma < 0$).

Furthermore, the only terms in $Q(x)$ that depend on γ are $\gamma(x^2 - x)$. Therefore since $x^2 - x < 0$, $\forall x$, it follows that $Q(x)$, $\forall x$ is a decreasing function of γ. Hence for any $\gamma' \leq (\gamma_2 - \epsilon)$ we also have $Q(x) > 0$, $\forall x$, which means $H_1(x) \neq x$, and it follows that $x < 1$ may not be an equilibrium.

□

Lemma 12 then ensures that adoption increases monotonically until reaching full adoption. The condition of this Lemma was previously referred to in Eq. (3.21).

A.3.2 Depiction of temporary pricing

Fig. A.2 shows the final adoption level for the hybrid pricing policy under the original model. The figure illustrates the presence of a region of (γ, δ_h) values where the system does not go to full adoption, and shows that by increasing the discount factor δ_h we can avoid that region, hence realizing full adoption.

This can be seen from the three sample points indicated by pins in Fig. A.12a. Pin a indicates a point where the system reaches full adoption. Pin b, on the other hand, is at a point where the system converges to a lower equilibrium and full adoption is not possible. However, by increasing the value of δ_h, we move to Pin c where, once again, the system converges to full adoption. The details of system's convergence at each pin is described

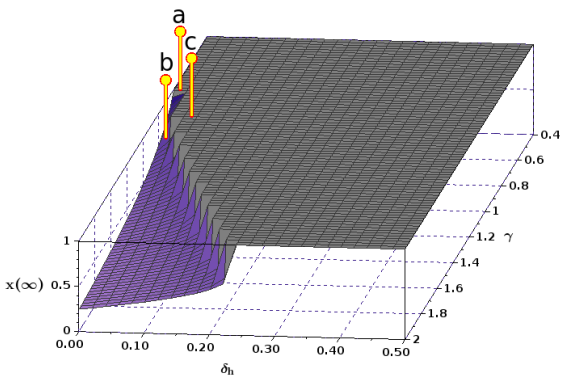

Figure A.2: Final adoption level for the hybrid usage-based pricing policy, as γ and δ_h vary, with pins corresponding to figures Fig. A.3a, Fig. A.3b and Fig. A.3c, respectively. Parameters are $c = 0.8$, $\delta_r = 0$, with different γ and δ_h values.

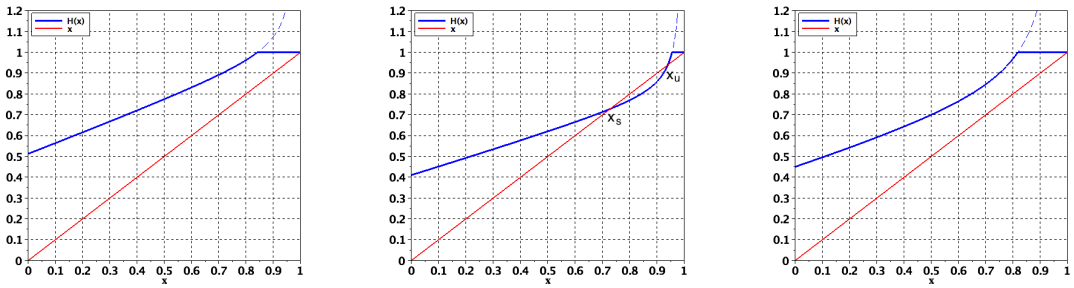

(a) $\gamma = 0.8$, $\delta_h = 0.01$ (b) $\gamma = 1$, $\delta_h = 0.01$ (c) $\gamma = 1$, $\delta_h = 0.05$

Figure A.3: $H(x)$ for the hybrid usage-based pricing policy. Fig. (a) has a single equilibrium at full adoption. Fig. (b) has parameter values which result in sub-optimal equilibria. Fig. (c) has the same parameter γ as Fig. (b), but a higher δ_h, and shows how increasing δ_h eliminates the sub-optimal equilibria. Parameters are $c = 0.8$, $\delta_r = 0$, with different γ and δ_h values.

below.

Fig. A.3 plots the function $H(x)$ under the original model for three values of (γ, δ_h) pair. Figures A.3a, A.3b and A.3c correspond to the three pins in Fig. A.12a, respectively. Fig. A.3a corresponds to a scenario where the multiple-equilibria problem does not exists. Fig. A.3b however, has this problem, and by adjusting its δ_h parameter we are able to eliminate the equilibria at $x < 1$, which results in Fig. A.3c. In the cases of Figs. A.3a and A.3c, the system (starting from zero adoption) will eventually go to full adoption,

while in the case of Fig. A.3b the presence of the stable equilibrium x_s means the final adoption level will be $x(\infty) = x_s \approxeq 0.7$.

A.4 Fixed Price Policy

The simplest pricing policy is one with a single fixed and flat-rate price, *i.e.*, $p(\Theta, \theta) = p$. With this pricing policy, Eq. (A.1) becomes

$$U_{n+1}(\Theta, \theta) = \gamma - p - c\, m_n + \theta\,(r\, x_n - \gamma)\,. \tag{A.12}$$

Since a user's utility is a function of the adoption set Θ, evaluating the system state calls for first characterizing Θ. The next proposition allows us to understand the composition of Θ.

Proposition 9. *For all choices of p, γ and c, the set of adopters is characterized by a range of θ values of the form $[0, \widehat{\theta}\,]$ or $[\widehat{\theta}, 1], 0 \leq \widehat{\theta} \leq 1$.*

Proof. From Eq. (A.12), we have:

$$U_n(\Theta, \theta) = \beta_{n-1} + \theta\alpha_{n-1}\,,$$

where $\beta_{n-1} = \gamma - p - c\, m_{n-1}$ and $\alpha_{n-1} = r\, x_{n-1} - \gamma$. For a user to have a positive utility, and therefore adopt, its θ value must satisfy $\theta\alpha_{n-1} > -\beta_{n-1}$. This translates into different conditions depending on the sign and value of α_{n-1}.

If $\alpha_{n-1} < 0$, *i.e.*, $x_{n-1} < \gamma/r$, θ needs to satisfy $\theta < -\beta_{n-1}/\alpha_{n-1}$. Hence, the set of adopters at epoch n is either empty or corresponds to users with θ values in an interval of the form $[0, \widehat{\theta}_n)$, where $\widehat{\theta}_n = (-\beta_{n-1}/\alpha_{n-1})_{[0,1]}$ and we have used the notation $(x)_{[0,1]}$ to denote the projection of x on the interval $[0, 1]$.

If $\alpha_{n-1} > 0$, *i.e.*, $x_{n-1} > \gamma/r$, θ must now satisfy $\theta > -\beta_{n-1}/\alpha_{n-1}$. In this scenario, the set of adopters at epoch n is again either empty or corresponds to users with θ values in an interval of the form $(\widehat{\theta}_n, 1]$ where $\widehat{\theta}_n = (-\beta_{n-1}/\alpha_{n-1})_{[0,1]}$.

Finally, if $\alpha_{n-1} = 0$, *i.e.*, $x_{n-1} = \gamma/r$, then $U_n(\theta) = \beta_{n-1}, \forall\, \theta \in [0,1]$. The set of adopters in this last case is either the empty set (if $\beta_{n-1} \leq 0$) or the entire interval $[0,1]$ (if $\beta_{n-1} > 0$). □

As a result of proposition 9, we shall capture the adopters' set Θ_n at epoch n through an adoption vector, X_n, that includes the number of adopters, x_n, and specifies their θ values through a simple binary variable. Using Eq. (A.12) and denoting $H(X) \equiv X_{n+1}$ as a function of $X \equiv X_n$, we want to characterize the evolution of $H(X)$ and identify adoption equilibria. We will drop the Θ notation hence forth and simply denote the utility under a flat-rate price at epoch n by $U_n(\theta)$.

From the proof of Proposition 9, we derive expressions for x_n, for the three possible conditions on α_{n-1}.

$$x_n = \begin{cases} \widehat{\theta}_n & \text{if } x_{n-1} < \gamma/r \quad \text{(A.13a)} \\ 1 - \widehat{\theta}_n & \text{if } x_{n-1} > \gamma/r \quad \text{(A.13b)} \\ I_{[\beta_{n-1}]}, & \text{if } x_{n-1} = \gamma/r \quad \text{(A.13c)} \end{cases}$$

As mentioned before, proposition 9 also establishes that the adoption state at epoch n, X_n, can be represented as a two-dimensional vector $X_n = (x_n, y_n)$, where y_n is a binary variable that indicates the "type" of adoption interval of Proposition 9. Specifically,

$$y_n = \begin{cases} 0 & \text{if adopters} \in [0, \widehat{\theta}_n),\ \textit{i.e.},\ x_{n-1} < \gamma/r \\ 1 & \text{if adopters} \in [\widehat{\theta}_n, 1],\ \textit{i.e.},\ x_{n-1} \geq \gamma/r \end{cases} \quad \text{(A.14)}$$

where we arbitrarily took y_n to be 1 for the case where $x_{n-1} = \gamma/r$. We also note that as shown in the proof of Proposition 9, the value of y_n solely depends on x_{n-1}, *i.e.*, $y_n = 0$ when $x_{n-1} < \gamma/r$ and $y_n = 1$ when $x_{n-1} \geq \gamma/r$. In other words, the *identity* of adopters at epoch n depends on the *number* of adopters at epoch $(n-1)$.

The rest of this section is devoted to characterizing equilibria and the dynamics that lead to them. We start with a number of preliminary results on which the derivations rest.

A.4.1 Preliminary Results

Assume that when the service is introduced at $n = 0$ there are no adopters; thus $x_0 = 0$ and $m_0 = 0$. At the next epoch, $n = 1$, the utility $U_1(\theta)$ of a user with roaming value θ is

$$U_1(\theta) = \gamma - p - \theta\,\gamma$$

At epoch 1 adopters consist, therefore, of users with a θ value such that $\theta < (\gamma - p)/\gamma$. Hence, $x_1 = (\gamma - p)/\gamma$ when $\gamma \geq p$, and $x_1 = 0$ otherwise. In other words and as stated in Proposition 10, a positive adoption requires $\gamma > p$, *i.e.,* the price cannot exceed the utility that users derive from home base connectivity. This is likely to hold in practice, *e.g.,* the price of basic Internet connectivity is such that many have adopted the service even in the absence of a roaming option. Throughout the analysis this condition is assumed to hold. Note that under this assumption, $x = 0$ can not be an equilibrium.

Proposition 10. *Starting from an initial state of zero adoption, non-zero adoption is possible only if* $\gamma > p$.

In the next proposition, we formally establish that the vector X_n fully characterizes the adoption process, namely, that m_n can be computed once X_n is known.

Proposition 11. *The vector* $X_n = (x_n, y_n)$*, together with the parameters* γ, p, r *and* c*, are sufficient to compute a user's utility at epoch* $(n + 1)$ *as expressed in Eq. (A.12).*

Proof. From Eq. (A.1), a user's utility at epoch $(n + 1)$ depends on γ, p, r, c, x_n, and m_n. It therefore suffices to show that m_n can be computed based on γ, p, r, c, x_n, and y_n. We consider separately the cases $y_n = 0$ and $y_n = 1$.

If $y_n = 0$, adopters are users with $\theta \in [0, \widehat{\theta}_n)$, so that $\widehat{\theta}_n = x_n$ and m_n is given by:

$$m_n = \int_0^{x_n} \theta\,\mathrm{d}\theta = \frac{1}{2}x_n^2\,, \quad \text{if } y_n = 0 \tag{A.15}$$

Conversely, when $y_n = 1$ adopters are users with $\theta > \widehat{\theta}_n$. Thus $\widehat{\theta}_n = 1 - x_n$ and m_n is given

by

$$m_n = \int_{1-x_n}^{1} \theta \, \mathrm{d}\theta = \frac{1}{2}(-x_n^2 + 2x_n), \quad \text{if } y_n = 1 \tag{A.16}$$

This establishes that, $U_{n+1}(\theta)$ can be computed based on X_n and the parameters γ, p, r and c. Note that this also ensures that X_{n+1} can be computed, and therefore the evolution of the adoption process can be tracked. □

A.4.2 Characterizing Adoption Evolution

We now turn to exploring the evolution of the adoption vector X_n. Our goal is to characterize adoption dynamics and identify eventual equilibria. As mentioned earlier, equilibria are either solutions of

$$H(X) = X, \tag{A.17}$$

or boundary points of the interval $[0, 1]$. The main difficulty in solving Eq. (A.17) stems from the fact that X_n is a two-dimensional vector. In particular, although Eqs. (A.15) and (A.16) show that a user's utility at epoch $(n+1)$ is solely a function of x_n, the choice of which equation to use depends on y_n or in other words on x_{n-1}, *i.e.,* $U_{n+1}(\theta)$ is a function of both x_n and x_{n-1}.

As a result, exploring adoption dynamics calls for accounting for adoption levels in the previous *two* epochs. This is reflected in the approach we describe next. Specifically, we consider separately the cases $y_n = 0$ $(x_{n-1} < \gamma/r)$ and $y_n = 1$ $(x_{n-1} \geq \gamma/r)$, and correspondingly introduce the notation $H_1(x) \equiv H(x, 0)$ and $H_2(x) \equiv H(x, 1)$ to investigate the evolution of adoption in these two scenarios. As we shall see, these two cases will each be divided in two further sub-cases.

Adoption Evolution under $H_1(x)$, *i.e.,* $y_n = 0$

In this scenario, Eq. (A.15) is used to compute $U_{n+1}(\theta)$, which when combined with Eq. (A.1) gives

$$U_{n+1}(\theta) = \gamma - p - \frac{c}{2}x_n^2 + \theta\,(r\,x_n - \gamma)\,. \tag{A.18}$$

Eq. (A.18) allows us to determine the adoption threshold $\widehat{\theta}_{n+1}$ at epoch $(n+1)$, *i.e.,* the θ value such that $U_{n+1}(\widehat{\theta}_{n+1}) = 0$:

$$\widehat{\theta}_{n+1} = \frac{\gamma - p - \frac{c}{2}x_n^2}{\gamma - r\,x_n}\,.$$

To compute the new system state X_{n+1} at epoch $(n+1)$, we distinguish between the cases $y_{n+1} = 0$ and $y_{n+1} = 1$, with Eq. (A.13) correspondingly identifying the expression of x_{n+1}.

When $y_{n+1} = y_n = 0$, both x_n and x_{n-1} are below γ/r. Therefore even when x_{n+1} is above γ/r, the set of adopters at epoch $(n+1)$ is still of the form $[0, \widehat{\theta}_{n+1})$. Since both x_n and x_{n+1} consist of the same type of adopters, we say that adoption stays in the *"home"* region, and for convenience introduce the notation $x_{n+1} \equiv H_{1h}(x)$. Eq. (A.13a) then states that $x_{n+1} = \widehat{\theta}_{n+1}$, so that

$$H_{1h}(x) = \frac{\gamma - p - \frac{c}{2}x^2}{\gamma - r\,x}\,. \tag{A.19}$$

When $y_{n+1} = 1$ and $y_n = 0$, we have $x_n \geq \gamma/r$ while x_{n-1} was below γ/r, and the set of adopters at epoch $(n+1)$ is of the form $(\widehat{\theta}_{n+1}, 1]$. We denote this configuration as x_{n+1} being in the *"away"* region, and correspondingly introduce the notation $x_{n+1} \equiv H_{1a}(x)$. Eq. (A.13b) then states that $x_{n+1} = 1 - \widehat{\theta}_{n+1}$, so that

$$H_{1a}(x) = \frac{\frac{c}{2}x^2 - r\,x + p}{\gamma - r\,x} \tag{A.20}$$

Adoption Evolution under $H_2(x)$, *i.e.,* $y_n = 1$

In this scenario, Eq. (A.16) is used in equation Eq. (A.1), which gives:

$$U_{n+1}(\theta) = \gamma - p - \frac{c}{2}(-x_n^2 + 2x_n) + \theta(r\,x_n - \gamma)\,. \tag{A.21}$$

As before, from Eq. (A.21) we find the adoption threshold $\widehat{\theta}_{n+1}$ for which $U_{n+1}(\widehat{\theta}_{n+1}) = 0$. This gives:

$$\widehat{\theta}_{n+1} = \frac{\gamma - p - \frac{c}{2}(-x_n^2 + 2x_n)}{\gamma - r\,x_n}\,.$$

Following the approach used for $H_1(x)$, we consider separately the cases where $y_{n+1} = 1$ and $y_{n+1} = 0$.

When $y_{n+1} = y_n = 1$, adopters at epoch $(n+1)$ remain characterized by a range $\theta > \widehat{\theta}_{n+1}$, which as before we term the *home* region. Similarly, we let $x_{n+1} \equiv H_{2h}(x)$, which using Eq. (A.13b) gives

$$H_{2h}(x) = \frac{\frac{c}{2}x^2 + (r-c)x - p}{r\,x - \gamma} \tag{A.22}$$

When $y_{n+1} = 0$ and $y_n = 1$, x_n is now below γ/r while x_{n-1} was above γ/r, and the set of adopters at epoch $(n+1)$ is of the form $[0, \widehat{\theta}_{n+1})$. We again denote this configuration as x_{n+1} being in the *away*region, with the corresponding notation $x_{n+1} \equiv H_{2a}(x)$. Eq. (A.13a) gives

$$H_{2a}(x) = \frac{\frac{c}{2}x^2 - cx + \gamma - p}{\gamma - r\,x} \tag{A.23}$$

In summary, the adoption state at epoch $(n+1), X_{n+1}$, has been characterized by considering the four possible combinations of adoption levels in epochs $(n-1)$ and n. In the next sections, these results are leveraged to identify possible equilibria and characterize adoption dynamics.

A.4.3 Characterizing Equilibria

This section leverages the results of Section A.4.2 to identify the type of equilibria to which adoption can converge. Consistent with the discussion of the previous section, we introduce the notation $H_h(x)$ for the function defined as $H_{1h}(x)$ in the interval $[0, \gamma/r)$ and as $H_{2h}(x)$ in the interval $[\gamma/r, 1]$, and $H_a(x)$ for the function defined as $H_{2a}(x)$ in $[0, \gamma/r)$ and as $H_{1a}(x)$ in $[\gamma/r, 1]$.

Since any equilibria must satisfy $y_{n+1} = y_n$, we can rule out half of the combinations of the previous section. Specifically, when $y_n = 0$, only vectors of the form $X_{n+1} = (H_{1h}(x), 0)$ need to be considered. Conversely, when $y_n = 1$, candidate equilibria must be of the form $(H_{2h}(x), 1)$. Equilibria, therefore, correspond to either points $x \in (0, \gamma/r)$ that verify $H_{1h}(x) = x$, points $x \in [\gamma/r, 1)$ that verify $H_{2h}(x) = x$, the point $x = 0$ if $H_{1h}(0) \leq 0$, or

the point $x = 1$ if $H_{2h}(1) \geq 1$.

We therefore explore the relative positions of the functions $H_{1h}(x)$ and $H_{2h}(x)$ with respect to x, and their possible intersections with x. Intersections identify equilibria or fixed points, while the position of $H_{1h}(x)$ and $H_{2h}(x)$ relative to x determines the "nature" of these fixed points, *i.e.,* stable, or unstable, or associated with orbits either periodic or chaotic[3]. The derivations are mechanical and can be found in Appendix A.5. We distinguish between stable fixed points (•) with monotonic trajectories (towards the fixed point inside its attraction region), unstable fixed points (∘) again with monotonic trajectories (away from the fixed point), and fixed points associated with an "orbit" (↻) that can be either convergent, periodic, or chaotic for different (p, l) pairs. Table 3.1 summarizes possible combinations of equilibria in each of the intervals $[0, \gamma/r)$ and $[\gamma/r, 1]$, where — denotes the absence of fixed point in that interval.

Case 1 of Table 3.1 corresponds to a scenario where no fixed point exists. We discuss later when and why this arises, but adoption patterns essentially never stabilize. Cases $2, 2', 3$ and $3'$ are instances where a single fixed point exists in either $[0, \gamma/r)$ or in $[\gamma/r, 1]$. In Cases 2 and 3, the fixed point corresponds to a stable equilibrium, while in Cases $2'$ and $3'$ it can be associated with more complex trajectories that need not converge, *e.g.,* exhibit periodic orbits or chaotic adoption patterns. Cases 4 and 5 correspond to a scenario with both a stable and an unstable equilibrium in either $[0, \gamma/r)$ or in $[\gamma/r, 1]$, with the adoption always converging to the stable fixed point. Cases 6 and 7 exhibit different combinations of equilibria in $[0, \gamma/r)$ or in $[\gamma/r, 1]$, with one having a single stable equilibrium and the other having both a stable and an unstable equilibrium. The important feature of these two latter cases is the presence of two stable equilibria, one in $[0, \gamma/r)$ and the other in $[\gamma/r, 1]$. As a result, final adoption levels can differ based on initial adoption values, *i.e.,* they can vary based on the level of seeding when the service was first offered. A similar situation is present in Case 8, where the two ranges both have a stable and an unstable equilibrium.

In the next section, we characterize the trajectories associated with the different combi-

[3]If either $x = 0$ or $x = 1$ are equilibria, they are stable equilibria.

nations of Table 3.1, while Section A.4.5 articulates implications for a UPC service offering.

A.4.4 Classifying Adoption Dynamics

Table 3.1 readily identifies several possible patterns of adoption. Specifically, adoption dynamics can be of the form:

i) Absence of convergence to an equilibrium. This arises in Cases $1, 2'$, and $3'$. In Case 1, this is *independent* of the initial adoption level, as the absence of a fixed point gives rise to chaotic adoption patterns that never converge. The situation is more subtle in Cases $2'$ and $3'$, for which a fixed point does exist. However, even when a small region of attraction exists around this fixed point, adoption trajectories typically remain outside of it, and orbit around it in either periodic or chaotic manner. Such patterns are common in dynamical systems [12]. The derivations that led to the identification of those trajectories as well as an illustrative example can again be found in Appendix A.5. The conditions under which they arise are discussed in Section A.4.5;

ii) Convergence to a single stable equilibrium in either $[0, \gamma/r)$ or $[\gamma/r, 1]$, *independent* of initial penetration. This arises in Cases $2, 3, 4$, and 5, where a single stable equilibrium exists in the entire adoption range. In those cases, adoption proceeds monotonically towards the equilibrium, either increasing or decreasing depending on the value of the initial adoption level. As it does not affect the final outcome, seeding is of no benefit in these scenarios;

iii) Convergence to one of two stable equilibria in $[0, \gamma/r)$ or $[\gamma/r, 1]$, *dependent* on initial penetration. This arises in Cases $6, 7$, and 8, where a stable equilibrium exists in both $[0, \gamma/r)$ and $[\gamma/r, 1]$. These are instances where seeding may be of value, as it can affect the final adoption level. In particular, a high enough level of seeding can allow the service to realize a much higher final adoption (in $[\gamma/r, 1]$ as opposed to $[0, \gamma/r)$). As in Case ii), trajectories are monotonic towards the final adoption level.

The trajectories of the three types of possible outcomes that have been identified can be easily constructed using a standard cobweb plot[4] based on the functions $H_h(x)$ and $H_a(x)$. For illustration purposes, we consider an example associated with Case 8 from Table 3.1, which involves stable and unstable equilibria in both $[0, \gamma/r)$ and $[\gamma/r, 1]$. The shapes of the corresponding functions $H_h(x)$ (solid line) and $H_a(x)$ (dash-dot line) are shown in Fig. A.4, together with three adoption trajectories associated with different initial adoption levels.

In the first scenario, there are no initial adopters, *i.e.,* $x_0 = 0$, and adoption increases monotonically until it reaches about 10%, the stable equilibrium in $[0, \gamma/r)$. In the second scenario, seeding has been used to create an initial adoption level $x_0 \approx 35\%$. As we can see, this is not enough to prevent adoption from declining back to 10%, the stable equilibrium in $[0, \gamma/r)$. To avoid such an outcome, seeding needs to be further increased, as done in the third scenario where initial adoption is set to around 46%. In this case, the adoption trajectory enters the interval $[\gamma/r, 1]$ and eventually converges to the higher adoption equilibrium in that interval (around 85%). The trajectory also illustrates the use of the function $H_a(x)$ when first entering $[\gamma/r, 1]$ from $[0, \gamma/r)$. We note that although a high level of adoption is ultimately realized, the associated seeding "cost" is high.

In the next section, we characterize how system parameters, in particular the price p, map to different equilibria and trajectories, and identify possible implications for UPC service offerings.

A.4.5 Interpretations

Recall that adoption trajectories and equilibria are determined by the "shape" of the functions $H_h(x)$ and $H_a(x)$ and how they intersect the line x. The shape of those functions depends in turn on the parameters γ, c, r, and p (see Eqs. (A.19) and (A.22)). As a result, it is no surprise that both adoption outcomes and trajectories are determined by values of these parameters and in particular, for any γ and r value, associated with distinct "regions" of the $(p, c)-$plane, *i.e.,* contiguous ranges of p and c values. Fig. A.5 identifies the regions

[4] See http://code.google.com/p/cobweb2008/ for an illustrative applet.

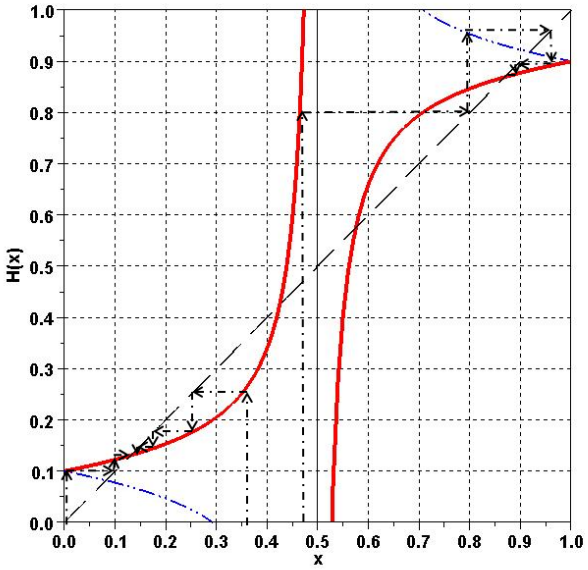

Figure A.4: $H_h(x)$ (solid) and $H_a(x)$ (dash-dot) for Case 8.

of the $(p, c)-$plane that map to the ten combinations of table 3.1, and correspondingly Behaviors i), ii), and iii) used earlier to classify adoption dynamics. The boundaries of those regions are derived from constraints on the parameters, with Table A.1 providing the corresponding functional expressions. Details on the derivations are again in Appendix A.5.

Behavior i)

This maps to regions $1, 2'$ and $3'$ of Fig. A.5, and is associated with configurations that do not yield convergence to an adoption equilibrium.

Region 1 consists of relatively low values of p but rather large values of c. This produces the following dynamics: When there are few or no users in the network, coverage is low and frequently-roaming users find the service unattractive despite the low p. In contrast, sedentary users are unaffected by the limited coverage, so that the low p value entices them to adopt. As they adopt, coverage improves and the service becomes attractive to roaming users. With more users adopting, coverage continues improving. The associated growth in roaming traffic, however, starts to negatively affect sedentary users that derive little

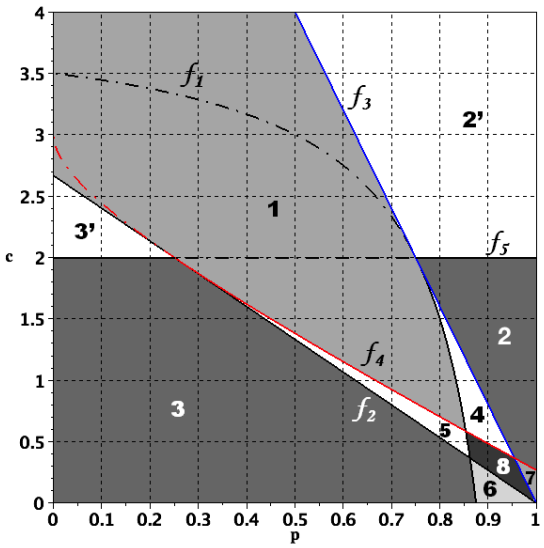

Figure A.5: Regions of the (p, c) plane corresponding to different combinations of equilibria as given by Table 3.1. This is a sample illustration for $\gamma = 1$ and $r = 2$.

benefits from the improved coverage. This leads some of them to disadopt, which reduces coverage so that eventually roaming users start leaving as well. Once roaming traffic has been sufficiently reduced, the service becomes again attractive to sedentary users, and the cycle repeats.

A similar, though more nuanced process is at work in regions $2'$ and $3'$. Region $2'$ also boasts large c values ($c \geq r$), and in the portion of that region where large values of p are allowed, it displays similar adoption patterns as region 1 to which it is adjacent. However, when p is allowed to be large, the negative effect of c never gets a chance to manifest itself. The large p prevents enough sedentary users from adopting, and the service never garners enough coverage to become attractive to frequently-roaming users. In this case, adoption converges to a low value in $[0, \gamma/r)$. As p decreases, the region of attraction of the equilibrium shrinks, and non-converging adoption patterns emerge.

The behavior in region $3'$ is similar, albeit for an equilibrium in $[\gamma/r, 1]$. Specifically, region $3'$ combines small positive p values and very large c values. The small value of p

f_1	$c = 2r - \frac{\gamma^2}{2(\gamma - p)}$
f_2	$c = \frac{2r^2(\gamma - p)}{2r\gamma - \gamma^2}$
f_3	$c = \frac{2r^2(\gamma - p)}{\gamma^2}$
f_4	$c = \gamma + r - p - \sqrt{p^2 + 2p(r - \gamma)}$
f_5	$c = r$

Table A.1: Boundaries for regions of solution in fixed price policy

means that many users want to adopt. The very large c value, however, implies that only frequently roaming adopters derive enough benefits from the large coverage to compensate for the penalty of roaming traffic. As a result, the most sedentary users disadopt. When p is sufficiently small, this disadoption is small enough to not affect coverage to the point where frequently-roaming users start leaving as well. However, as p increases, coverage may decrease enough to trigger an exodus of frequently-roaming user, and create cyclical patterns of adoption and disadoption as in region 1.

Behavior ii)

Regions 2 and 4 of Fig. A.5 have a stable equilibrium in $[0, \gamma/r)$ to which adoption converges. The regions correspond to relatively high p values and relatively high values of c. The high p value is such that few sedentary users adopt and coverage never gets high enough to make the service attractive to frequently-roaming users. Hence, adoption saturates at a low level of penetration. Seeding will not help, as the rather high c value is too much of an impact even for frequently roaming users.

Conversely, in regions 3 and 5 of Fig. A.5 adoption converges to a single stable equilibrium in $[\gamma/r, 1]$. The regions correspond to relatively low values of p and comparatively low c values. The low p value initially attracts sedentary users that are not deterred by the limited coverage, and once enough of them have adopted frequent roamers start joining. Because the impact of increasing roaming traffic is relatively low, few sedentary users leave and adoption stabilizes at a high level.

Behavior iii)

Regions 6, 7 and 8 of Fig. A.5 exhibit a stable equilibrium in both $[0, \gamma/r)$ and $[\gamma/r, 1]$. In these cases, adoption converges to either equilibrium as a function of the initial adoption level (seeding). The three regions share relatively high p values and similarly small c values.

When initial adoption (coverage) is low, frequently-roaming users are not interested in the service and the high p value limits the number of sedentary users who adopt. Hence, adoption saturates at a low level. In contrast, if seeding has produced enough initial coverage to attract frequent roamers, they will start adopting in spite of the high p value. As their number grows and coverage continues improving, some sedentary users will also adopt because of the relatively low impact that they incur from roaming traffic through their home base. As a result, overall adoption eventually stabilizes at a high level.

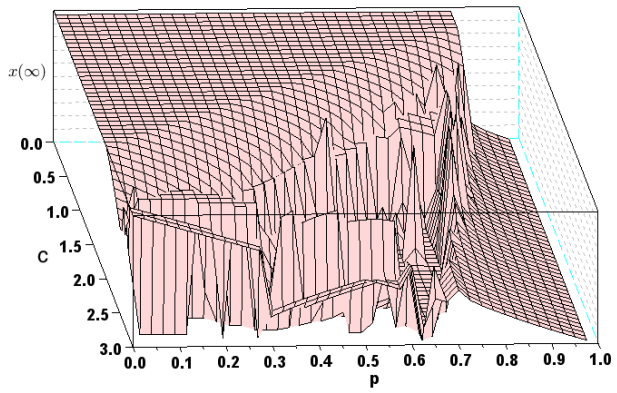

Figure A.6: Adoption Outcomes as a Function of p and c, when $\gamma = 1$ and $r = 2$

The behaviors identified in this section are illustrated in Fig. A.6 that plots the "final" adoption levels for different (p, c) pairs starting from an initial adoption level of $x_0 = 0$. In scenarios where adoption does not converge, *i.e.,* Behavior i), the adoption level reported in the figure was sampled at a particular iteration. The figure clearly identifies the regions of the (p, c) plane that correspond to chaotic or at least non-converging adoption (regions $1, 2'$, and $3'$), low adoption (regions 2 and 4, as well as regions 6, 7, and 8 since $x_0 = 0$ was used), and regions of high adoption (regions 3 and 5).

A.4.6 Optimal Pricing for Provider's Profit

In a flat-price policy, all users pay the same price p. Therefore, the provider's profit (or welfare) $\Pi(p)$ that was introduced in section 3.3.1 as $W_P(\Theta)$ becomes

$$\Pi(p) = (p - e)\, x. \tag{A.24}$$

The UPC provider's goal is to select p so as to maximize its profit at equilibrium[5], *i.e.,* once adoption has stabilized[6]. In other words, the provider seeks to identify p^* such that

$$\Pi(p^*) = \max_p \{\Pi(p)\} \ .$$

Note that in Eq. (A.24) the service adoption level x is itself a function of p and the exogenous parameters of Eq. (A.12). $\Pi(p)$ can, therefore, be expressed as a function with p as its only variable. More precisely, because adoption equilibria have different functional expressions depending on whether adoption is low or high, we also have two distinct expressions for $\Pi(p)$. The first is associated with an equilibrium in the low-adoption region, while the second corresponds to an equilibrium in the high-adoption region.

For the sake of analytical tractability, we keep Π as a function of x (rather than p). This yields two expressions, $\Pi_L^{(1)}(x)$ and $\Pi_H^{(1)}(x)$, for the provider's profit corresponding to equilibria in $[0, 1/2)$ (low adoption), and $[1/2, 1]$ (high adoption). Derivations are mechanical in nature, and the resulting expressions are given in Eqs. (A.25) and (A.26) for completeness.

$$\Pi_L^{(1)}(x) = \frac{4-c}{2}\, x^3 - x^2 + (\gamma - e)\, x \tag{A.25}$$

$$\Pi_H^{(1)}(x) = \frac{c-4}{2}\, x^3 + (3-c)\, x^2 + (\gamma - e - 1)\, x \tag{A.26}$$

Both equations are cubic polynomials in x. Differentiating them yields expressions for the

[5] This forces a price selection that ensures the existence of an equilibrium.

[6] Note that this implicitly assumes a recurring pricing model, as is common with most service offerings.

x values that maximize them, *i.e.,* $\widehat{x}_L$ and $\widehat{x}_H$.

The next step calls for determining which of $\Pi_L^{(1)}(\widehat{x}_L)$ and $\Pi_H^{(1)}(\widehat{x}_H)$ is higher, and consequently decide how to best price the service. The answer can change based on the combination of exogenous parameters, *e.g.,* the service's intrinsic value, γ, the impact of roaming traffic, c, and the value of the service cost e. For instance, it can be shown that the γ value at which high-adoption becomes more profitable than low-adoption increases with c. This is intuitive since a larger c means that sedentary users are more sensitive to roaming traffic. Hence, the service needs to be intrinsically more valuable to allow enough of them to join *and* stay as roaming traffic grows with adoption.

A.5 Derivations of Equilibria under the Fixed Price Policy

The intersections of $H_h(x)$ and x correspond to interior equilibria in adoption levels, *i.e.,* equilibria in $(0,1)$, and the relative positions of $H_h(x)$ and x at $x=0$ and $x=1$ determine whether or not either are boundary equilibria. We consider equilibria in the intervals $[0,\gamma/r)$ and $[\gamma/r,1]$ separately. During the analysis we may use $k \triangleq \gamma - p$ for notational conciseness.

A.5.1 Equilibria in $[0,\gamma/r)$

From Eq. (A.19), $H_{1h}(0) = k/\gamma > 0$, given the earlier assumption that $k>0$. Therefore, the condition $H_{1h}(0) \leq 0$ is never met and $x=0$ is not an equilibrium. Next, we consider interior points, *i.e.,* points in $(0,\gamma/r)$.

From Eq. (A.19), $H_{1h}(x) = x$ yields

$$\left(-\frac{c}{2}+r\right)x^2 - \gamma\, x + k = 0\,. \tag{A.27}$$

We assume $-c/2+r>0$ or $2r>c$, which is a reasonable and hardly restrictive assumption in our model; This means that at full adoption, the most frequently roaming user (with $\theta=1$) will derive more utility from the ability to roam than be impacted by the external roaming traffic. Under the assumption that $2r>c$, Eq. (A.27) has (at most) two roots

given by

$$x = \frac{\gamma \pm \sqrt{\Delta_1}}{2r - c}$$

where $\Delta_1 = \gamma^2 + 2kc - 4kr$. The inequality $H_{1h}(x) < x$ holds (only) between the two roots. We distinguish three cases:

i) $\Delta_1 < 0$ or $c < 2r - \frac{\gamma^2}{2k}$.

In this case, Eq. (A.27) does not have any roots and $H_{1h}(x) > x$ holds $\forall x \in [0, \gamma/r)$. In other words, there are no equilibria in $[0, \gamma/r)$. A sample illustration can be seen in Fig. A.5 where we have chosen $\gamma = 1$ and $r = 2$. This criterion corresponds to the points in the (p, c) plane where $c < f_1$. The functional expressions of the different curves are given in Table A.1.

ii) $\Delta_1 = 0$ or $c = 2r - \frac{\gamma^2}{2k}$

In this case Eq. (A.27) holds at $x = \frac{\gamma}{2r-c} = 2k/\gamma$, so $H_{1h}(x)$ and x touch once in $[0, \gamma/r)$ if $k < \frac{\gamma^2}{2r}$. In this case, there is only one equilibrium $x_1 \in [0, \gamma/r)$ which is easily seen to be stable from the left and unstable from the right. This is because $H_h(x) > x$ when $x < x_1$ (adoption levels increase towards x_1 in each iteration), and $H_h(x) > x$ when $x > x_1$ as well (adoption levels continue increasing once x_1 is exceeded).

iii) $\Delta_1 > 0$ or $c > 2r - \frac{\gamma^2}{2k}$

In this case Eq. (A.27) has two real roots, so that $H_{1h}(x)$ and x intersect twice. These two intersections may or may not indeed be in $[0, \gamma/r)$. Next, we determine conditions for either of these intersections to lie in $[0, \gamma/r)$ and characterize the equilibria they give rise to.

Intersection x_{1s}

Intersection x_{1s} is the smaller of the two roots of Eq. (A.27) and is given by:

$$x_{1s} = \frac{\gamma - \sqrt{\gamma^2 + 2kc - 4kr}}{2r - c}\,. \tag{A.28}$$

For x_{1s} to be an equilibrium, it must be in the interval $[0, \gamma/r)$. The earlier assumptions $k > 0$ and $2r > c$ ensure that $x_{1s} > 0$. For $x_{1s} < \gamma/r$ we need:

$$\frac{-\gamma(r-c)}{r} < \sqrt{\gamma^2 + 2kc - 4kr}$$

This is trivially true if $r - c > 0$. If on the other hand $r - c < 0$, we need

$$\gamma^2\, c^2 - (2r\,\gamma^2 + 2r^2k)c + 4k\,r^3 < 0\,. \tag{A.29}$$

The left side is a quadratic equation in c and the inequality holds between the two (possible) roots, which are given by:

$$\begin{aligned} c &= \frac{(r\gamma^2 + r^2k) \mp \sqrt{(r\gamma^2 - r^2k)^2}}{\gamma^2} \\ &= \frac{(r\gamma^2 + r^2k) \mp |r\gamma^2 - r^2k|}{\gamma^2}. \end{aligned}$$

Based on the sign of $r\gamma^2 - r^2k$ the interval between the two roots of Eq. (A.29) can be specified. We have

$$c \in \begin{cases} \left(\frac{2r^2k}{\gamma^2},\, 2r\right) & \text{if } \gamma^2 \geq rk \\ \left(2r,\, \frac{2r^2k}{\gamma^2}\right) & \text{if } \gamma^2 < rk. \end{cases}$$

But because of our previous assumption that $2r > c$, the second case above cannot happen.

This shows that when $\Delta_1 > 0$, the intersection x_{1s} will be an equilibrium in $[0, \gamma/r)$ if either $c < r$ or $c \in \left(\frac{2r^2k}{\gamma^2},\, 2r\right)$ and $k \in [0, \gamma^2/r]$. These criteria correspond to (p, c) being in Regions $2'$, 2, 4, 6, 7 and 8 of Fig. A.5, again with the functional expressions of the different curves given in Table A.1.

When (p, c) is in any of the Regions 2, 4, 6, 7 or 8, then x_{1s} can be shown to be a stable equilibrium. This is because $x_{1s} > H_h(x) > x$ (adoption increases towards x_{1s} in the next iteration), and $x_{1s} < H_h(x) < x$ (adoption decreases towards x_{1s} in the next iteration). On the other hand if (p, c) is in the Region $2'$, then x_{1s} is an "orbital" equilibrium.

An orbital equilibrium may have a non-empty region of attraction[7], but exhibit cyclical adoption patterns (periodic or chaotic) outside of that neighborhood. Orbital behaviors arise when $H_h(x) > x_{1s} > x$ (adoption increases beyond x_{1s} in the next iteration), and $H_h(x) < x_{1s} < x$ (adoption drops below x_{1s} in the next iteration). This gives rise to cyclical trajectories, which may or may not converge to x_{1s} depending on the slope of $H_{1h}(x)$ at $x = x_{1s}$ and the initial distance between x and x_{1s}. Note also that if $H_{1h}(x) > \gamma/r$ for some $x < x_{1s}$, the next adoption level will be determined using $H_{2a}(x)$ instead of $H_{1h}(x)$, since we have left the interval $[0, \gamma/r)$.

Intersection x_{1u}

Intersection x_{1u} is the larger of the two roots of Eq. (A.27) and is given by

$$x_{1u} = \frac{\gamma + \sqrt{\gamma^2 + 2kc - 4kr}}{2r - c}\,.$$

Again, for x_{1u} to be an equilibrium, it must be in $[0, \gamma/r)$. Since $2r - c > 0$, we have $x_{1u} > x_{1s} > 0$, and therefore we only need to verify when the condition $x_{1u} < \gamma/r$ holds. For this we need:

$$\sqrt{\gamma^2 + 2kc - 4kr} < \frac{\gamma(r - c)}{r}\,.$$

This never holds if $r - c < 0$. When $r - c > 0$, the condition becomes

$$\gamma^2\, c^2 - (2r\,\gamma^2 + 2r^2 k)c + 4k\, r^3 > 0\,.$$

which is the symmetric of Eq. (A.29), and thus it holds for values of c outside the roots of the corresponding quadratic equation.

We also note that equilibrium x_{1u} is unstable. This is because $H_h(x) < x$ when $x < x_{1u}$ (adoption levels keep decreasing once they have dropped below x_{1u}), and $H_h(x) > x$ when $x > x_{1u}$ (adoption levels keep increasing once they have exceeded x_{1u}).

To summarize, in Case **iii)**, *i.e.,* in the case of $c > 2r - \frac{\gamma^2}{2k}$ there can possibly be two

[7] A neighborhood of x_{1s} so that for values of x in that neighborhood, trajectories converge to x_{1s}.

equilibria in $[0, \gamma/r)$. When $c > r$, the root x_{1s} is the only equilibrium in $[0, \gamma/r)$ if the condition $c \in [\frac{2r^2k}{\gamma^2}, 2r]$ is also satisfied (Region $2'$ in Fig. A.5); Otherwise, no equilibrium is present in this interval (The portion of Region 1 in Fig. A.5 for which $c > f_1$). When $c < r$, both x_{1s} and x_{1u} can be equilibria if $c < \frac{2r^2k}{\gamma^2}$ (Regions 4, 8 and 6 in Fig. A.5), and otherwise x_{1s} is the only equilibrium in $[0, \gamma/r)$ (Regions 2 and 7 in Fig. A.5). Again the functional expressions of the different curves are given in Table A.1.

A.5.2 Equilibria in $[\gamma/r, 1]$

For the boundary point $x = 1$ we use Eq. (A.22) and see that:

$$H_{2h}(1) = \frac{-\frac{c}{2} + k + r - \gamma}{r - \gamma} = \frac{-\frac{c}{2} + k}{r - \gamma} + 1\,.$$

Therefore the full adoption level, $x = 1$, will be an equilibrium *if and only if* $-c/2 + k \geq 0$. We will now consider the interior points, *i.e.,* the points in $[\gamma/r, 1)$.

From the equation $H_{2h}(x) = x$ we get:

$$-\left(r - \frac{c}{2}\right) x^2 + (\gamma + r - c)x - p = 0. \tag{A.30}$$

Assuming $r - c/2 > 0$ as before, Eq. (A.30) exhibits (at most) the two roots given by

$$x = \frac{-(\gamma + r - c) \pm \sqrt{\Delta_2}}{-(2r - c)}$$

where

$$\begin{aligned}\Delta_2 &= (\gamma + r - c)^2 - 2p(2r - c) \\ &= c^2 - 2(\gamma - p + r)c + (\gamma + r)^2 - 4pr.\end{aligned}$$

The inequality $H_{2h}(x) > x$ holds[8] only between these two (possible) roots. We again distinguish three cases:

[8] Note that since $x \in [\gamma/r, 1]$, the denominator of $H_{2h}(x)$ is positive.

i) $\Delta_2 < 0$

This is equivalent to

$$c \in \left(-p+\gamma+r-\sqrt{Q}\,,\, -p+\gamma+r+\sqrt{Q}\right)$$

where

$$Q = p^2 + 2p(r-\gamma).$$

In this case, Eq. (A.30) does not have any roots and $H_{2h}(x) < x$ holds $\forall x \in (\gamma/r, 1]$. In other words, there are no equilibria in $(\gamma/r, 1]$.

ii) $\Delta_2 = 0$

This is equivalent to

$$c = -p+\gamma+r \mp \sqrt{p^2+2p(r-\gamma)}$$

and in this case Eq. (A.30) holds at $x = \frac{\gamma+r-c}{2r-c}$. Therefore the two curves $H_{2h}(x)$ and x touch once in $(\gamma/r, 1]$ if $c < r$. In this case, there is only one equilibrium $x_2 \in (\gamma/r, 1]$ which is easily seen to be stable from the right and unstable from the left. This is because $H_h(x) < x$ when $x > x_2$ (adoption levels decreases towards x_1 in each iteration), but $H_h(x) < x$ when $x < x_2$ as well (adoption levels keep decreasing if x goes below x_1).

iii) $\Delta_2 > 0$

This is equivalent to

$$c \notin \left[-p+\gamma+r-\sqrt{Q}\,,\, -p+\gamma+r+\sqrt{Q}\right]$$

where as before

$$Q = p^2 + 2p(r-\gamma).$$

In this case Eq. (A.30) has two real roots, and as a result it is possible for $H_{2h}(x)$ and x to intersect twice in $[0, \gamma/r]$. Next, we characterize the equilibria that these two possible intersections, x_{2u} and x_{2s}, can give rise to.

Intersection x_{2u}

Intersection x_{2u} is the smaller of the two roots of Eq. (A.30) and is given by:

$$x_{2u} = \frac{\gamma + r - c - \sqrt{(\gamma + r - c)^2 - 2p(2r - c)}}{2r - c}.$$

In order for x_{2u} to be an equilibrium, it must be in the interval $(\gamma/r, 1]$. It can be easily verified (under the assumptions already made for parameters c, γ and r) that $x_{2u} \leq 1$ always holds if the root exists. For x_{2u} to be greater than γ/r we need:

$$\sqrt{(\gamma + r - c)^2 - 2p(2r - c)} < (r - \gamma)\frac{r - c}{r}$$

For this equation to hold, it is necessary that $r - c > 0$. If this is the case we then need

$$(2r\gamma - \gamma^2)c^2 + (-6\gamma r^2 + 2\gamma^2 r + 2pr^2)c + 4r^3(\gamma - p) < 0 \tag{A.31}$$

which holds between the roots of the corresponding quadratic equation, which are given by:

$$\begin{aligned} c &= \frac{(3\gamma r^2 - \gamma^2 r - pr^2) \mp (\gamma r^2 - \gamma^2 r + pr^2)}{2r\gamma - \gamma^2}. \\ &= 2r \quad \text{and} \quad \frac{2r^2(p - \gamma)}{2r\gamma - \gamma^2} \end{aligned} \tag{A.32}$$

This implies that x_{2u} is an equilibrium in $(\gamma/r, 1]$ if both $\frac{2r^2(\gamma - p)}{2r\gamma - \gamma^2} < c < r$ and $c < -p + \gamma + r - \sqrt{p^2 + 2p(r - \gamma)}$, where we have taken into consideration the fact that when $c < r$ the inequality $c > -p + \gamma + r + \sqrt{p^2 + 2p(r - \gamma)}$ cannot hold. These criteria correspond to Regions 5, 8 and 7 in Fig. A.5 with the functional expressions of the different curves given in Table A.1.

When these conditions are satisfied, x_{2u} can be shown to be an unstable equilibrium. This is because $H_h(x) < x$ when $x < x_{2u}$ (adoption levels keep decreasing once they have dropped below x_{2u}), and $H_h(x) > x$ when $x > x_{2u}$ (adoption levels keep increasing once

they have exceeded x_{2u}).

Intersection x_{2s}

Intersection x_{2s} is the larger of the two roots of Eq. (A.30) and is given by

$$x_{2s} = \frac{\gamma + r - c + \sqrt{(\gamma + r - c)^2 - 2p(2r - c)}}{2r - c}\,. \tag{A.33}$$

Again, for x_{2s} to be an equilibrium, it must be greater than γ/r. Note that $x_{2s} < 1$ is not necessary, since a x_{2s} value that is larger than 1 will be projected down to the boundary point $x = 1$. For $x_{2s} > \gamma/r$ we need:

$$-(r - \gamma)\frac{r - c}{r} < \sqrt{(\gamma + r - c)^2 - 2p(2r - c)}\,.$$

This always holds if $r - c > 0$. When $c > r$, the condition becomes

$$(2r\gamma - \gamma^2)c^2 + (-6\gamma r^2 + 2\gamma^2 r + 2pr^2)c + 4r^3(\gamma - p) > 0$$

which is the symmetric of the inequality in Eq. (A.31), and thus it holds for values of c outside the roots of the corresponding quadratic equation. This condition reduces to $c < \frac{2r^2(\gamma - p)}{2r\gamma - \gamma^2}$ (Region $3'$ in Fig. A.5).

Thus x_{2s} results in an equilibrium if (p, c) is in any of the Regions 3, $3'$, 5, 6, 7 and 8 of Fig. A.5.

When (p, c) is in any of the Regions 3, 5, 6, 7 and 8, then x_{2s} can be shown to be a stable equilibrium. This is because $x_{2s} > H_h(x) > x$ (adoption increases towards x_{2s} in the next iteration), and $x_{2s} < H_h(x) < x$ (adoption decreases towards x_{2s} in the next iteration). On the other hand if (p, c) is in the Region $3'$, then x_{2s} is an "orbital" equilibrium. An orbital equilibrium may have a non-empty region of attraction[9], but exhibit cyclical adoption patterns (periodic or chaotic) outside of that neighborhood. Orbital behaviors arise when $H_h(x) > x_{2s} > x$ (adoption increases beyond x_{2s} in the next iteration), and

[9] A neighborhood of x_{2s} so that for values of x in that neighborhood, trajectories converge to x_{2s}.

$H_h(x) < x_{2s} < x$ (adoption drops below x_{2s} in the next iteration). This gives rise to cyclical trajectories, which may or may not converge to x_{2s} depending on the slope of $H_{2h}(x)$ at $x = x_{2s}$ and the initial distance between x and x_{2s}.

To summarize, as for the equilibria in $[\gamma/r, 1]$, when $c < \frac{2r^2(\gamma-p)}{2r\gamma-\gamma^2}$, the root x_{2s} is the only equilibrium in $(\gamma/r, 1]$ (Regions 3′, 3 and 6 in Fig. A.5). When $c > \frac{2r^2(\gamma-p)}{2r\gamma-\gamma^2}$, both x_{2s} and x_{2u} equilibria will exist if the condition $c < \min(r, -p+\gamma+r-\sqrt{p^2+2p(r-\gamma)})$ is also satisfied (Regions 5, 7 and 8 in Fig. A.5). Otherwise, no equilibrium is present in $(\gamma/r, 1]$ (Regions 1, 2′, 2 and 4 in Fig. A.5)

A.6 Model perturbations for robustness testing

Our original models make specific assumptions with regards to the magnitude and range of various parameters, functional expressions of the user utilities, and the extent to which information is considered to be known to the service provider. In order to gauge how much these assumptions affect the models' results and more importantly findings, as well as determine how robust the findings are to variations in those assumptions, we consider a series of perturbations to the original models that relax/modify one or more of those specific assumptions.

In this section, we describe perturbations that directly affect the parameters and functional expressions of the models. All scenarios are investigated by means of numerical simulations, and the results are presented in Appendix A.7 (See Appendix A.9 for one example of analytical generalization). Appendix A.7 also evaluates the impact of another type of perturbations, namely, that of errors in estimates of the model's parameters on the part of the service provider. Overall, the results demonstrate that our main findings are relatively robust to a wide range of perturbations.

A.6.1 User propensity to roam θ

Our original models assume that users' propensity to roam, θ, follows a uniform distribution, *i.e.,* it is uniformly distributed in [0, 1]:

$$f(\theta) = 1, \qquad 0 \leq \theta \leq 1.$$

We introduce a perturbation to that assumption by considering different probability distributions for the roaming variable θ. There are obviously many possible distributions to choose from; we consider two representative examples, one with a higher density of sedentary users, and the other with a higher density of roaming users. These two choices cover the effect of both overestimating and underestimating roaming patterns. We present next the details of these two distributions.

The distributions are truncated and modified versions of an exponential distribution, and their density functions are plotted in Fig. A.7. The low-mode distribution with a mode at $x = 0$ has a density function

$$f_{\text{Low-Mode}}(x; \lambda) = \frac{\lambda}{1 - e^{-\lambda}} e^{-\lambda x}, \qquad 0 \leq x \leq 1,\ \lambda > 0,$$

where the parameter λ is taken to be $\lambda = 1.5$. Conversely the high-mode distribution with a mode at $x = 1$ has a density function

$$f_{\text{High-Mode}}(x; \lambda) = \frac{\lambda}{e^{\lambda} - 1} e^{\lambda x}, \qquad 0 \leq x \leq 1,\ \lambda > 0,$$

where the parameter λ is again taken to be 1.5.

As mentioned earlier, Appendix A.7 presents the results on how these perturbations affect the findings of Chapter 3.

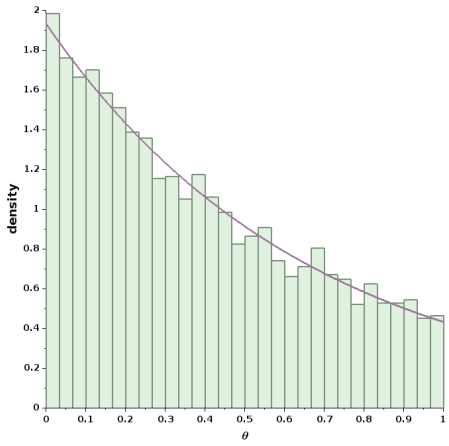

(a) Low-mode: Truncated exponential distribution with parameter $\lambda = 1.5$. (high concentration of sedentary users.)

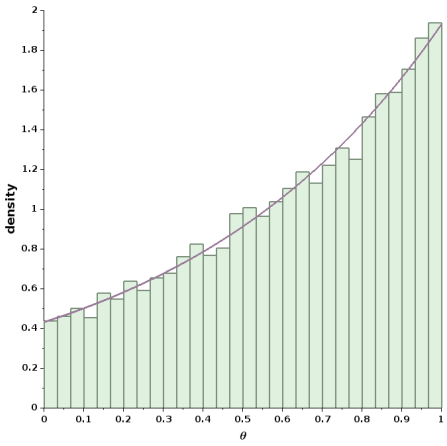

(b) High-mode: Inverted truncated exponential distribution with parameter $\lambda = 1.5$. (high concentration of roaming users.)

Figure A.7: Density functions and sample realizations for for non-uniform θ distributions.

A.6.2 Modified user utility functions

The original model assumes a specific functional expression for users' utility that grows linearly with coverage κ (as measured[10] by x) and decreases linearly with the volume of roaming traffic m.

We first relax the linear dependency assumption, and then consider two different utility functions inspired by the *Web Browsing Model* and the *File Transfer Model* of [70]. As before, Appendix A.7 presents the results of this investigation.

The original utility function is stated in Eq. (3.5), which we restate below for convenience.

$$U(\Theta,\, \theta) = \gamma - c\, m + \theta\, (r\, x - \gamma) - p(\Theta,\, \theta)$$

[10] As mentioned before, in Section A.6.4 we do numerically consider scenarios where coverage κ is not equal to x and instead saturates as x grows).

Non-linear utility function

In order to relax the linear dependency assumption, we consider the following "perturbed" utility function:

$$U(\Theta,\, \theta) = \gamma - c\, m^{1.2} + \theta\, (r\, x^{0.8} - \gamma) - p(\Theta,\, \theta)\,.$$

The non-linear terms $m^{1.2}$ and $x^{0.8}$ are arguably only one of many possible types of non-linearities, but they offer a reasonable evaluation of the effect of non-linearities.

Next we introduce two different utility functions inspired by the models of [70].

Upper-bounded roaming

The *Web Browsing Model* from [70] considers a utility that increases with the connection duration, as long as the connection duration is not longer than an upper-bound τ (which is the duration that a user intends to browse the web).

In the context of [70] the connection duration is the main contributor to a user's utility, while in our model the roaming frequency θ determines the rate at which a user accesses the higher-valued roaming connectivity. Therefore the connection duration of [70] readily maps to roaming frequency in our model.

Hence, in order to emulate the Web Browsing Model from [70], we modify our original utility function to upper-bound the roaming frequency of the users. In a manner similar to Eq. (1) of [70] which includes a term $\min(T,\, \tau)$, we replace the roaming factor θ with $\min(\theta,\, \tau)$.

The new utility function is then given by

$$\begin{aligned} &U(\Theta,\, \theta) = \\ &\quad \gamma - c\, m + \min(\theta,\, \tau) \cdot (r\, x - \gamma) - p[\Theta,\, \min(\theta,\, \tau)], \end{aligned} \tag{A.34}$$

where $0 < \tau < 1$. In the numerical tests of Section A.7 we take $\tau = 0.8$.

Minimum useful coverage

The *File Transfer Model* from [70] considers a utility function with a threshold behavior, *i.e.,* it yields zero value when the connection duration is too short to download a file. Therefore the connection duration has to be longer than a certain threshold to yield a positive utility.

As mentioned before, in our context, users' utility is directly related to the ability to connect while roaming. Therefore, to emulate the File Transfer Model from [70], we modify our utility function to implement a threshold behavior based on roaming connectivity. Namely, a user experiences zero roaming utility, unless the odds of roaming connectivity are above a certain threshold, or equivalently, the system's coverage κ is above a threshold κ_{th}.

The new utility function is then

$$U(\Theta,\, \theta) = \gamma - c\, m + \theta\, (r\, \widehat{\kappa} - \gamma) - p(\Theta,\, \theta) \tag{A.35}$$

where $\widehat{\kappa}$ is the *perceived level* of coverage and is given by

$$\widehat{\kappa} = \begin{cases} 0 & \text{if } x < \kappa_{\text{th}}, \\ x & \text{if } x \geq \kappa_{\text{th}}. \end{cases}$$

The threshold κ_{th} satisfies $0 < \kappa_{\text{th}} < 1$. In the numerical tests of Section A.7 we use $\kappa_{\text{th}} = 0.2$.

A.6.3 Heterogeneous population

In the original models, users are assumed to all have the same utility function, and share a common profile in how much traffic they generate, including while roaming. We relax those assumptions by considering a scenario where users belong to two types with different "profiles." The type of a user, T_1 or T_2, affects that user's utility and the volume of roaming traffic she generates as a function of her roaming parameter θ.

Users are randomly assigned a given type, so that the user population is divided into

two groups of identical size. The utility functions of users of type T_1 and type T_2 are then given by:

$$U(\Theta,\,\theta) = \begin{cases} \gamma - c\,m + \theta\,(r\,x - \gamma) - p(\Theta,\,\theta) & \text{for } T_1 \text{ users} \\ 1.1\,\gamma - c\,m + \theta\,(0.9\,r\,x - 1.1\,\gamma) - p(\Theta,\,\theta) & \text{for } T_2 \text{ users.} \end{cases}$$

In other words, users of type T_2 exhibit a difference of 10% with type T_1 users in how much more (less) they value home (roaming) connectivity (they have a larger γ and smaller r). Moreover, a user's type also affects the volume of traffic she generates while roaming, as follows

$$\text{Contribution to roaming traffic} = \begin{cases} \theta & \text{for } T_1 \text{ users} \\ \theta^{0.7} & \text{for } T_2 \text{ users,} \end{cases}$$

In other words, given two users of types T_1 and T_2 with the same roaming parameter θ, the user of type T_2 generates more roaming traffic while roaming (since $\theta^{0.7} > \theta$ for $\theta \in [0,\,1]$). As mentioned earlier, this can account for differences induced by the type of equipment each type of users uses (*e.g.,* tablet vs. smartphone). The overall roaming traffic m is then given by

$$m = \int_{T_1} \theta f(\theta)\,d\theta + \int_{T_2} \theta^{0.7} f(\theta)\,d\theta\,.$$

Results are again presented in Appendix A.7.

A.6.4 Coverage saturation

The original models assume that coverage κ increases linearly with the level x of service adoption. In particular, we assume that $\kappa = x$. In this section, we relax this assumption and consider a *saturation* effect for coverage. This means that while coverage initially expands in proportion to the adoption level x, its growth slows down ("levels off") as x grows large. In order to capture this effect, we assume a relation between coverage and adoption of the

form $\kappa = \sin(\frac{\pi}{2}x)$ (see Fig. A.8). Results illustrating how this difference in the evolution of coverage affects the conclusions of Chapter 3 are again in Appendix A.7.

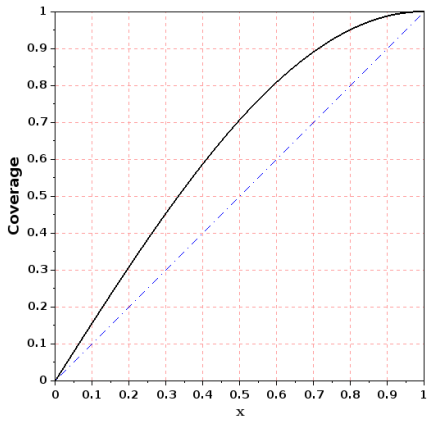

Figure A.8: Coverage saturates as adoption x grows large.

A.7 Numerical simulations

Appendix A.6 introduced a series of perturbations to our original models. In this Appendix, we report on the results of numerical simulations used to investigate the impact of those perturbations. The results demonstrate that the findings of Chapter 3 are robust with regards to those perturbations and errors in the modelling assumptions.

Recall that the main findings of Chapter 3 belong to two broad categories. The first is concerned with the system's ability to create value, *i.e.,* the total system *welfare*. They establish that when the system is capable of creating positive value, the maximum of that value is often realized at full adoption. The second category of findings is concerned with *realizing* that potential: how to use pricing schemes to realize the optimal adoption level and the corresponding total welfare, as well as distribute the total welfare between the users and the provider.

In testing the robustness of that second group of findings, *i.e.,* those regarding pricing schemes, it is important to specify how much knowledge the provider has about potential

discrepancies between the model it is using to determine (optimal) prices, and the actual model and its parameters. This is because that knowledge will affect the provider's ability to set prices that realize its goals. Therefore, throughout this section, when presenting results related to pricing policies, we also specify the extent to which the provider is aware of the perturbations.

For purposes of clarity, we consider each one of the perturbations of Appendix A.6 in isolation, *i.e.,* we perturb one aspect of the model while keeping others intact, and report on its impact on the findings of Chapter 3. We discuss first how different perturbations affect our main conclusions regarding total system welfare.

A.7.1 Optimal total welfare

The main finding of Chapter 3 when it comes to total system welfare was that total welfare (value) is usually maximized when the adoption level is either $x = 1$ or $x = 0$. In other words, whenever the system is capable of generating positive value, this positive value is realized at full adoption $x = 1$.

The result was obtained under the simplifying assumptions of the system's model, but in this section we demonstrate that even under more general conditions, *i.e.,* when various aspects of the original model are perturbed,[11] this finding remains valid.

A.7.1.(a) Original model

A plot of the optimal adoption level x for maximizing system value was given in Chapter 3 for the original model, and is repeated for convenience in Fig. A.9a. The figure indeed shows that for most values of parameters γ and e, the optimal adoption level is either $x = 1$ or $x = 0$. An optimal adoption level of $x = 0$ means that the system cannot create positive value.

A.7.1.(b, c) Modified roaming distribution

We changed the distribution of the roaming parameter θ as per the description of Sec-

[11] Note that because total welfare is only concerned with the system's overall value and not how to realize it, the extent to which the service provider is aware of any discrepancies between the model and the actual system has no impact.

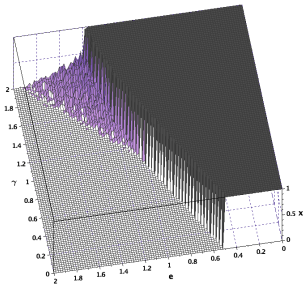

(a) Original model

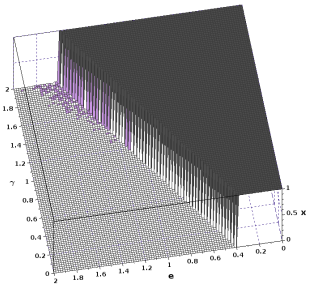

(b) Low-mode θ distribution with parameter $\lambda = 1.5$.

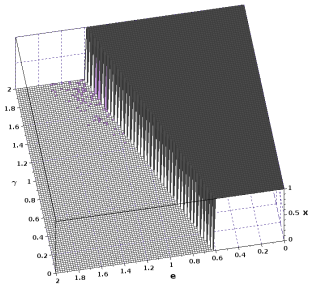

(c) High-mode θ distribution with parameter $\lambda = 1.5$.

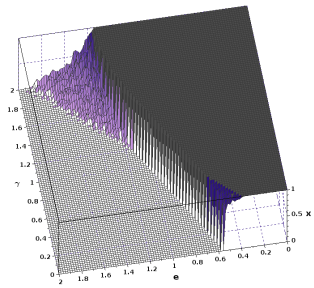

(d) Non-linear utility function

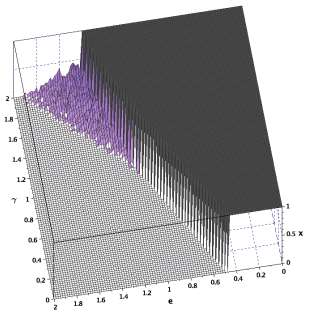

(e) Upper-bounded roaming ($\tau = 0.8$)

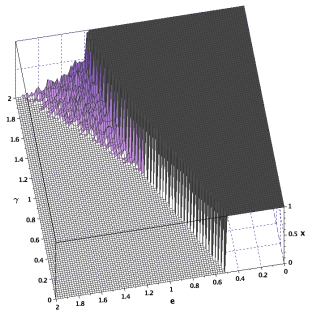

(f) Minimum useful coverage ($\kappa_{\text{th}} = 0.2$)

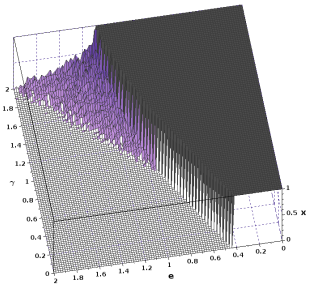

(g) Heterogeneous population

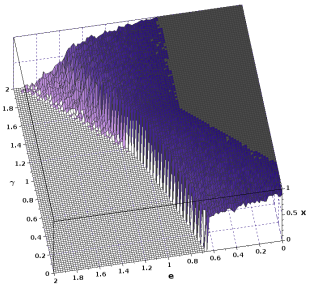

(h) Coverage saturation with adoption

Figure A.9: Values of optimal adoption x for maximum total welfare under different perturbations. Parameters are $r = 1.6$ and $c = 0.6$ (and therefore $r - c = 1$).

tion A.6.1. Under this perturbation, Figs. A.9b and A.9c demonstrate that the maximum total welfare is again mostly achieved at either $x = 1$ or $x = 0$.

Other remarks

Figs. A.9b and A.9c identify the region in the $\gamma - e$ plane where a positive total welfare is possible. The regions in the two figures are slightly different: For large values of home connectivity utility γ, the system with more sedentary users (Fig. A.9b) can tolerate a larger deployment cost e while still yielding a positive value. For instance when $\gamma = 2$, the system with more sedentary users (Fig. A.9b) allows $e \lessapprox 1.6$, whereas the system with a large roaming population (Fig. A.9c) allows only $e \lessapprox 1.4$. This is intuitive as a higher population of sedentary users means more people will enjoy the high home connectivity utility.

On the other hand, for small values of γ the roles are reversed. The system with more roaming users (Fig. A.9c) can tolerate a larger deployment cost e while still yielding a positive value. For instance when $\gamma = 0$, the system with more sedentary users (Fig. A.9b) allows $e \lessapprox 0.4$; however, the system with a large roaming population (Fig. A.9c) is understandably less affected by the small home connectivity utility γ, and allows $e \lessapprox 0.6$.

A.7.1.(d) Non-linear utility functions

We now consider the effect of non-linearities in users' utility functions using the utility function introduced in Section A.6.2. The resulting optimal adoption level for maximizing total welfare is given in Fig. A.9d. It shows that the maximum total welfare continues to be achieved mostly at either $x = 1$ or $x = 0$.

A.7.1.(e) Utility function with upper-bounded roaming

We used the new utility function given in Section A.6.2 with an upper-bound value of $\tau = 0.8$. Under this new utility function, Fig. A.9e displays the optimal adoption level x. Although the figure exhibits small differences with Fig. A.9a, it shows that the maximum total welfare continues to be achieved mostly at either $x = 1$ or $x = 0$.

A.7.1.(c) Utility function with minimum useful coverage

We use the new utility function of Section A.6.2 with a threshold value of $\kappa_{\text{th}} = 0.2$. Under

this new utility function, Fig. A.9f demonstrates that the maximum total welfare is again mostly achieved at either $x = 1$ or $x = 0$, in a manner very similar to Fig. A.9a.

Fig. A.9f is almost identical to Fig. A.9a, because the values of optimal adoption x in Fig. A.9a mostly correspond to a coverage level that is already above the coverage threshold κ_{th}, and therefore are not affected by imposing the criterion of minimum useful coverage in Fig. A.9f. Therefore the regions of Fig. A.9a where the optimal adoption is at $x = 0$ or $x > \kappa_{\text{th}}$ are exactly replicated in Fig. A.9f. This constitutes most of the points in the figure.

(g) Heterogeneous population

In this section, we consider the effect of a heterogeneous user population, as per the two-type user population of Section A.6.3. Recall that a user's type affects both her utility function and the roaming traffic she generates. Fig. A.9g reports the adoption levels associated with maximum welfare for such a configuration. It again shows that the maximum total welfare is usually achieved at either $x = 1$ or $x = 0$.

A.7.1.(h) Coverage saturation with adoption

The last perturbation we consider involves a scenario where coverage saturates as the system approaches full adoption $x = 1$ (as described in section A.6.4). The results are shown in Fig. A.9h.

Fig. A.9h highlights some minor differences with our original findings of Fig. A.9a. Specifically, while maximum total welfare is still often achieved at either $x = 1$ or $x = 0$, an intermediate region has emerged for which the optimal adoption level, while still high and close to 1, is nevertheless slightly lower. The difference is small and quite intuitive, as we explain next.

Recall the two effects of increasing adoption. On one hand, an increase in adoption improves total welfare, both because it improves coverage, which favorably affects the utility of all users, and because the new users themselves contribute to the total welfare. On the other hand, more users means more roaming traffic, which adversely affects all users' utility and, therefore, welfare. The combined contributions of these opposing effects determines whether higher adoption increases or decreases total welfare. When coverage saturates earlier, new

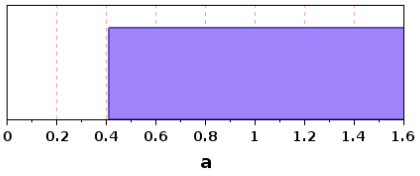

(a) Original model

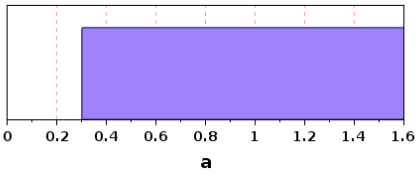

(b) Low-mode θ distribution with parameter $\lambda = 1.5$.

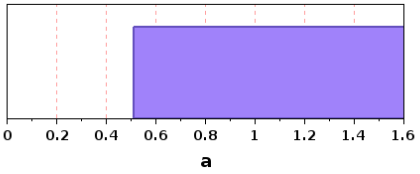

(c) High-mode θ distribution with parameter $\lambda = 1.5$.

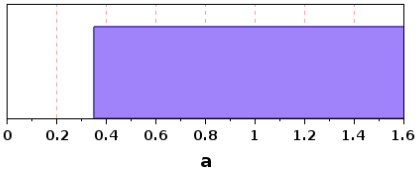

(d) Non-linear utility function

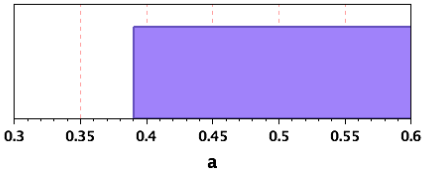

(e) Upper-bounded roaming ($\tau = 0.8$)

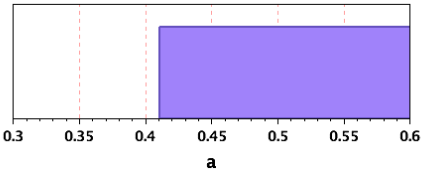

(f) Minimum useful coverage ($\kappa_{\text{th}} = 0.2$)

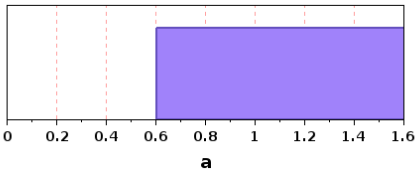

(g) Heterogeneous population

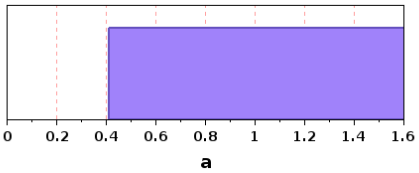

(h) Coverage saturation with adoption

Figure A.10: Usage-based pricing policy: values of usage allowance a for which full adoption $x = 1$ is the (unique) equilibrium of the system, under different perturbations. Parameters are $c = 0.8$, $\gamma = 1$, $r = 1.6$.

users still contribute to the system welfare, but their impact on improving coverage is now diminished while the negative contribution of their roaming traffic is unchanged. Hence, it is to be expected that under a model where coverage saturates before full adoption, maximum welfare may be realized slightly below full adoption as seen in the "blue" region of Fig. A.9h.

A.7.2 Usage-based pricing

Under the original model, we concluded that for the usage-based pricing policy, full adoption $x = 1$ is the unique equilibrium of the system if and only if the usage allowance a is larger than a threshold value.

In this section we demonstrate that even under more general conditions, *i.e.,* when various aspects of the original model are perturbed[12], this finding remains valid.

Throughout the simulations of this section, we fix the parameters $c = 0.8$, $\gamma = 1$, $r = 1.6$ and find the final adoption level that the system converges to, as the value a of usage allowance varies. By observing the final adoption level we can determine whether $x = 1$ is the unique equilibrium of the system. The details of the simulations are as follows: At each value of a, we start the system from zero adoption. After each iteration in the simulation, users evaluate their utility and those with a positive utility adopt. The simulation stops once consecutive iterations yield the same set of adopters. At this point the final adoption level is recorded.

A.7.2.(a) Original model

Under the original model of Chapter 3, full adoption $x = 1$ is the unique equilibrium if and only if the value of usage allowance satisfies $a > c/2$ (Proposition 2). This is illustrated in Fig. A.10a which shows the values of a for which full adoption $x = 1$ is the unique equilibrium (recall that $c/2 = 0.4$). The figure shows that there exists a threshold value a_0 such that for $a > a_0$, full adoption $x = 1$ is the unique equilibrium of the system, and for $a < a_0$, full adoption is not an equilibrium.

A.7.2.(b, c) Modified roaming distribution

[12] Unlike section A.7.1 that only dealt with maximizing the system value, this section and all subsequent ones are concerned with pricing the service. Prices are set by the provider, and as a result the information available to the provider about the system's characteristics is important. In the remainder, we therefore mention not only perturbations to the original model, but also the provider's knowledge of those perturbations.

Provider's knowledge of the perturbations:

The provider does *not* have any knowledge about the modified θ distribution and assumes the θ distribution is still uniform.

The roaming distribution is modified as per the description of Section A.6.1. We see from Figs. A.10b and A.10c that under the two new roaming distributions of Section A.6.1 (low and high mode), the outcome is similar to that of the original model, *i.e.,* there exists a threshold value such that for values of a above it $x = 1$ is the unique equilibrium, and for values of a below it, $x = 1$ is not an equilibrium.

A.7.2.(d) Non-linear utility function

Provider's knowledge of the perturbations:

The provider does *not* have any knowledge about the non-linearity of the utility function and assumes the original function is valid.

We now consider the effect of non-linearities in the utility function, as discussed in Section A.6.2. The outcome is shown, again as a function of the usage allowance a, in Fig. A.10d, which exhibits a similar pattern as Fig. A.10a, *i.e.,* there exists a threshold value such that for values of a above it $x = 1$ is the unique equilibrium of the system and for values of a below it, $x = 1$ is not an equilibrium.

A.7.2.(e) Utility function with upper-bounded roaming

Provider's knowledge of the perturbations:

The provider does *not* have any knowledge about the modified utility function and assumes the original function is valid.

We use the new utility function of Section A.6.2 with an upper-bound value of $\tau = 0.8$. We see from Fig. A.10e that under this new utility function, the outcome is similar to that of the original model, *i.e.,* there exists a threshold value, albeit a different one, such that for values of a above it $x = 1$ is the unique equilibrium, and for values of a below it, $x = 1$ is not an equilibrium.

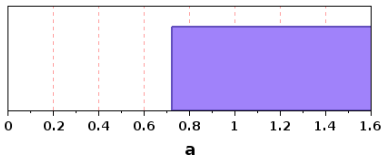

Figure A.11: Results for more drastic changes in the minimum useful coverage ($\kappa_{\text{th}} = 0.6$). Values of usage allowance a in the usage-based pricing policy for which full adoption $x = 1$ is the (unique) equilibrium of the system. Parameters are $c = 0.8$, $\gamma = 1$, $r = 1.6$.

A.7.2.(f) Utility function with minimum useful coverage

Provider's knowledge of the perturbations:

The provider does *not* have any knowledge about the modified utility function and assumes the original function is valid.

As before, we use the new utility function of Section A.6.2 with a coverage threshold of $\kappa_{\text{th}} = 0.2$. We see from Fig. A.10f that under this new utility function, the outcome is very similar to that of the original model, *i.e.,* there exists a threshold in the values of usage allowance a, such that for values of a above it $x = 1$ is the unique equilibrium, and for values of a below it, $x = 1$ is not an equilibrium.

In fact, the allowance threshold value in Fig. A.10f is identical to that of the original model in Fig. A.10a. This is because, as shown in Appendix A.8, the outcome of the usage-based pricing is very robust to this change in the utility function. Nevertheless, differences in the outcome would naturally arise under more drastic changes, *i.e.,* by considering significantly larger values for the coverage threshold.

For instance, as the value for the coverage threshold κ_{th} is changed to $\kappa_{\text{th}} = 0.6$ (roaming users do not consider the system valuable until coverage exceeds 60%), differences appear in the adoption outcomes. This is shown in Fig. A.11. Nevertheless, the figure also shows that even under this more drastic change, the overall behavior remains consistent with that of the original model.

A.7.2.(g) Heterogeneous population

Provider's knowledge of the perturbations:

The provider does *not* have any knowledge about users of type 2 and assumes that everyone is a type 1 user.

This scenario assumes that the users' population is heterogeneous and split into two sub-populations of different type, as described in Section A.6.3. Fig. A.10g reports the results, which are again consistent with those of the original model, *i.e.,* there exists a threshold value such that for values of a above it $x = 1$ is the unique equilibrium of the system and for values of a below it, $x = 1$ is not an equilibrium.

A.7.2.(h) Coverage saturation with adoption

Provider's knowledge of the perturbations:

The provider is not assumed to have any knowledge of the coverage saturation (of course, in practice the provider may be able to estimate coverage, but the simulations do not assume such knowledge).

As with the case of optimal welfare, the last perturbation we consider involves a scenario where coverage saturates as the system approaches full adoption $x = 1$ (as described in section A.6.4). The results are shown in Fig. A.10h, and again yield a similar outcome as in the original model, *i.e.,* there exists a threshold value such that for values of a above it $x = 1$ is the unique equilibrium of the system and for values of a below it, $x = 1$ is not an equilibrium.

We also note that unlike what happened with optimal welfare where optimal adoption could end-up slightly lower than full adoption, the threshold value is unchanged when compared to that of the original model. This is because the usage based pricing (by its nature) does not require knowledge of the actual service coverage by the provider, and is, therefore, insensitive to errors in the coverage level.

A.7.3 Hybrid pricing tests with partial provider's knowledge

Under the original model, we concluded that for the hybrid pricing policy, there are values of home connectivity utility γ for which the system has an equilibrium at $x < 1$, which would prevent the system from reaching full adoption, hence resulting in a sub-optimal total welfare. The hybrid pricing policy, however, offers a way to eliminate the lower equilibria and allow the system to reach full adoption. This is possible by adjusting the value of the discount parameters δ_h or δ_r (for simplicity, we focus on adjusting δ_h).

In this section, we demonstrate that even under more general conditions, *i.e.,* when various aspects of the original model are perturbed, the system also exhibits regimes where a sub-optimal equilibrium ($x < 1$) can arise, thereby preventing the system from reaching full adoption. In addition, overcoming this issue can again be accomplished by adjusting the value of δ_h, albeit typically with a different discount value.

Throughout the simulations of this section, we fix the parameters $c = 0.8$, $\delta_r = 0$ and find the final adoption level, denoted by $x(\infty)$, as we vary γ and δ_h values. The details of the simulations are as follows: At each point (γ, δ_h), we start the system from zero adoption. After each iteration in the simulation, users evaluate their utility and those with a positive utility adopt. The simulation stops once consecutive iterations yield the same set of adopters. At this point the final adoption level is recorded.

Moreover, throughout the simulations, the price parameters of the hybrid policy are computed as:

$$p_h = \gamma - c\,\alpha - \delta_h, \quad \text{and}$$
$$p_r = r - \gamma - \delta_r,$$

where α is the estimate for overall intensity of roaming traffic m at full adoption (for the original model we had $\alpha = 1/2$, which gives $p_h = \gamma - c/2 - \delta_h$). The simulations of this section assume that the provider can accurately estimate the value of α. (We will further eliminate this assumption in section A.7.4 where we assume that the provider has no knowledge of α.)

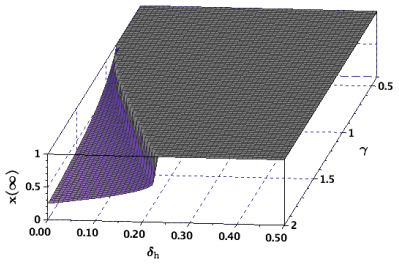

(a) Original model.

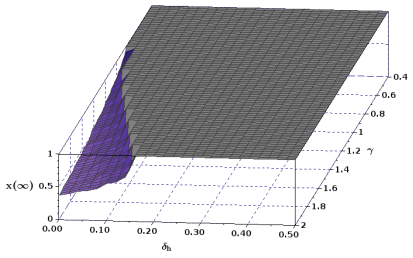

(b) Low-mode θ distribution with parameter $\lambda = 1.5$.

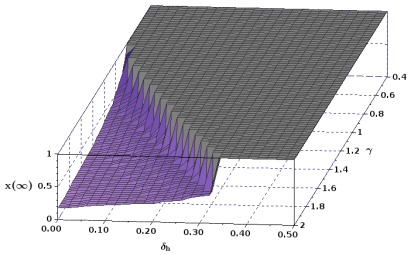

(c) High-mode θ distribution with parameter $\lambda = 1.5$.

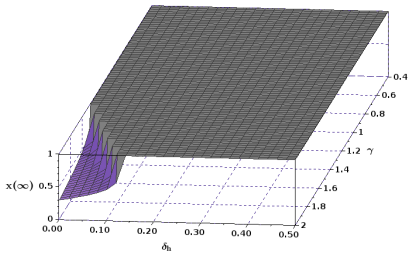

(d) Non-linear utility function

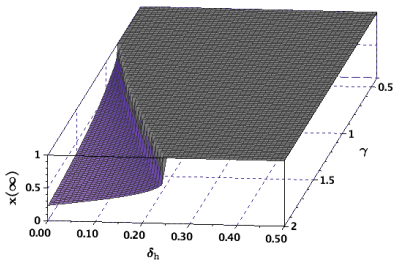

(e) Upper-bounded roaming ($\tau = 0.8$)

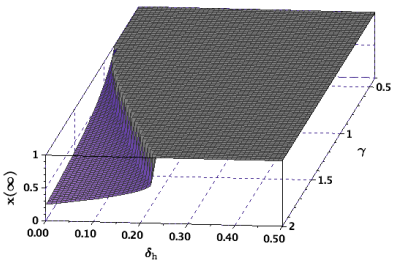

(f) Minimum useful coverage ($\kappa_{\text{th}} = 0.2$)

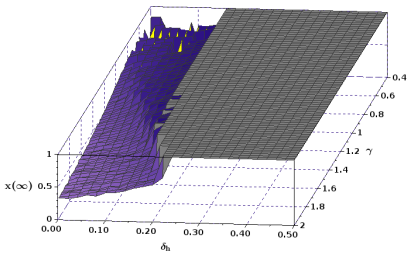

(g) Heterogeneous population

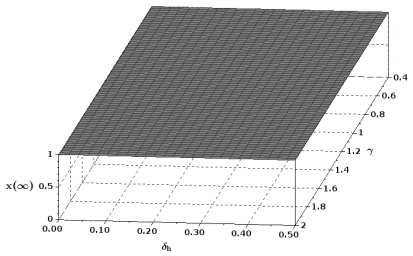

(h) Coverage saturation with adoption

Figure A.12: Final adoption level for the hybrid pricing policy under different perturbations. Parameters are $c = 0.8$, $\delta_r = 0$, with γ and δ_h values varying.

A.7.3.(a) Original model

Fig. A.12a shows the final adoption level for the hybrid pricing policy under the original model. The figure illustrates the presence of a region of (γ, δ_h) values where the system does not go to full adoption, and shows that by increasing the discount factor δ_h we can avoid that region, hence realizing full adoption.

A.7.3.(b, c) Modified roaming distribution

Provider's knowledge of the perturbations:

The simulations assume that the provider can accurately estimate α (the intensity of roaming traffic m at full adoption). We relax this in section A.7.4. Other than that, the provider does *not* have any knowledge about the modified θ distribution.

The roaming distribution is modified as per the description of Section A.6.1. We see from Figs. A.12b and A.12c that adoption outcomes are similar to those of the original model, *i.e.,* the system exhibits regimes where the final adoption is at a sub-optimal level $x < 1$, and that full adoption can be realized by adjusting the value of δ_h.

As expected, the level of discount δ_h required to realize full adoption is different in Fig. A.12b and Fig. A.12c, as the exact amount depends on the exact specifications of the system. However, the overall behavior is similar.

A.7.3.(d) Non-linear utility function

Provider's knowledge of the perturbations:

The provider does *not* have any knowledge about the non-linearity of the utility function and assumes the original function is valid.

We now consider the effect of non-linearities in the utility function as introduced in section A.6.2. The final adoption level is given in Fig. A.12d, which again yields a similar outcome, *i.e.,* the system exhibits regimes where the final adoption is at a sub-optimal level $x < 1$, but full adoption can be realized by adjusting the value of the discount δ_h.

A.7.3.(e) Utility function with upper-bounded roaming

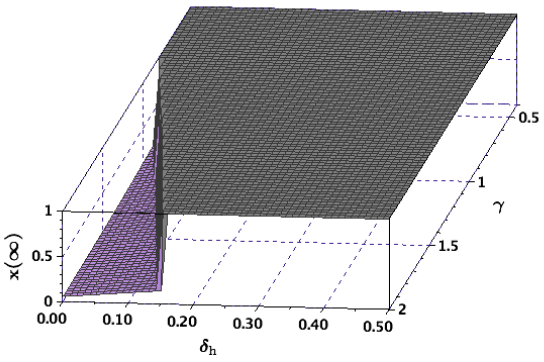

Figure A.13: Result for more drastic changes in the utility function with upper-bounded roaming ($\tau = 0.15$). Compare to Fig. A.12e.

Provider's knowledge of the perturbations:

The simulations assume that the provider can accurately estimate α (the intensity of roaming traffic m at full adoption). We relax this in section A.7.4. Other than that, the provider does *not* have any knowledge about the new utility function.

We use the new utility function of Section A.6.2 with an upper-bound value of $\tau = 0.8$. We see from Fig. A.12e that adoption outcomes under this new utility function are very similar to those of the original model, *i.e.,* the system exhibits regimes where the final adoption is at a sub-optimal level $x < 1$, and that full adoption can be realized by adjusting the value of δ_h.

Note that, as mentioned above, the exact values of discount δ_h required to realize full adoption in Fig. A.12e, are very close to that of the original model (Fig. A.12a). However, greater differences would obviously arise under more drastic changes, *i.e.,* by considering a significantly smaller upper-bound value τ.

For instance, as the value for the upper-bound τ of Section A.6.2 is changed to $\tau = 0.15$ (no user roams more than 15% of the time), greater differences arise. This is shown in Fig. A.13. Nevertheless, the figure also shows that even under this more drastic change, the overall behavior remains consistent with that of the original model.

A.7.3.(f) Utility function with minimum useful coverage

Provider's knowledge of the perturbations:

The provider does *not* have any knowledge about the new utility function.

We use the new utility function of Section A.6.2 with a threshold value of $\kappa_{\text{th}} = 0.2$. We see from Fig. A.12f that adoption outcomes under this new utility function are very similar to those of the original model, *i.e.,* the system exhibits regimes where the final adoption is at a sub-optimal level $x < 1$, and that full adoption can be realized by adjusting the value of δ_h.

Note that, as mentioned above, the exact values of discount δ_h required to realize full adoption in Fig. A.12f, are very close to that of the original model (Fig. A.12a). However, as seen earlier, greater differences would obviously arise under more drastic changes, *i.e.,* by considering a significantly larger threshold value κ_{th}.

For instance, as the value for the threshold κ_{th} of Section A.6.2 is changed to $\kappa_{\text{th}} = 0.4$ (roaming users do not consider the system valuable until coverage exceeds 40%), greater differences arise. This is shown in Fig. A.14. Nevertheless, the figure also shows that even under this more drastic change, the overall behavior remains consistent[13] with that of the original model.

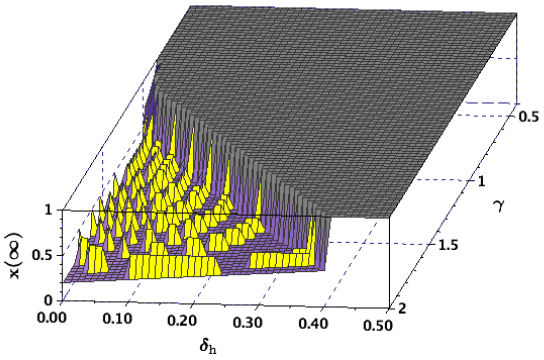

Figure A.14: Result for more drastic changes in the utility function with minimum useful coverage $\kappa_{\text{th}} = 0.4$. Compare to Fig. A.12f.

[13] The yellow stripes in Fig. A.14 correspond to points where the system does not converge to an equilibrium. However, we still have the previous behavior, *i.e.,* as δ_h increases, full adoption becomes the unique equilibrium of the system.

A.7.3.(g) Heterogeneous population

Provider's knowledge of the perturbations:

The provider does *not* have any knowledge about the users of type T_2 and assumes that everyone is a user of type T_1. But the simulations assume that the provider can accurately estimate α (the intensity of roaming traffic m at full adoption). We relax this in section A.7.4.

In this section, we consider the effect of a heterogeneous user population, as per the two-type user population of Section A.6.3. The results are shown in Fig. A.12g. We see that again the system exhibits regimes where the final adoption is at a sub-optimal level $x < 1$, but that we can still realize full adoption by adjusting the value of the discount δ_h.

There are, however, unavoidable differences between Fig. A.12g and Fig. A.12a. Notably, we now need a positive discount ($\delta_h \gtrapprox 0.18$) to reach full adoption at *all* γ values. This is because the provider is totally unaware of the existence of the type $T2$ users, which introduces relatively big errors in the pricing policy. As a result and because we need to compensate for those large errors, reaching full adoption now requires a bigger discount factor δ_h than before. In general, the larger the errors in the assumptions used to set prices, the bigger the discount "margin" required to compensate for them. Nevertheless, the *structure* of the system remains unchanged.

A.7.3.(h) Coverage saturation with adoption

Provider's knowledge of the perturbations:

The provider is not assumed to have any knowledge of the coverage saturation (of course, in practice they can measure the coverage if they want to, but our simulations do not assume that knowledge).

As before, we consider a scenario where coverage saturates as the system approaches full adoption $x = 1$ (see Section A.6.4). The results for this scenario are shown in Fig. A.12h that displays a somewhat different structure from the other figures, namely, the system appears to always reach full adoption even with a discount of $\delta_h = 0$. This is, however, not

surprising given that at any adoption level the coverage is higher than in the original model (the saturating coverage function has a concave shape). As a result of this higher coverage, more users find the service useful, and hence adopt, eventually resulting in full adoption.

Nonetheless, the analysis of Chapter 3 can help us understand this result as well. For instance, consider the case of zero discounts, *i.e.,* $\delta_h = \delta_r = 0$. The utility function for each user becomes

$$U(\Theta, \theta) = c\,(\alpha - m) + \theta\,\gamma(\kappa - 1).$$

As before, α is the estimate for the roaming traffic m at full adoption, so that $\alpha - m$ is non-negative. Similarly, because coverage κ is less than or equal to 1, it follows that $(\kappa - 1)$ is negative (or 0). Because coverage saturates earlier, the term $\theta\,\gamma(\kappa - 1)$ is greater than in the original model, hence enticing more roaming users to adopt, therefore facilitating reaching full adoption[14].

A.7.4 Hybrid pricing tests with zero provider's knowledge

Provider's knowledge of the perturbations:

The provider does *not* have any knowledge about any of the perturbations in this section.

This section presents simulations similar to those of the previous section, with the difference that we assume that the provider has *no knowledge* of the system's parameters. Specifically, we *relax* the assumption that the provider can accurately estimate the actual level of roaming traffic m generated at full adoption. The results are given in Fig. A.15 that parallels Fig. A.12.

Note that Figures. A.15d, A.15f and A.15h are identical to their counterparts in Fig. A.12. The reason is that the perturbations associated with the scenarios of those three figures do not alter the value of m at full adoption. Hence, the provider still estimates the correct value for m. The same does not hold for the other scenarios and Figures (b), (c), (e) and

[14]Obviously, a scenario where coverage proceeds more slowly as adoption increases, *i.e.,* a convex rather than concave coverage function, would have the opposite effect.

(g) differ from their counterparts in Fig. A.12. However, in spite of those differences, they exhibit similar overall behaviors, *i.e.,* they display regimes where a sub-optimal equilibrium $x < 1$ arises, but full adoption can still be realized by adjusting the value of the discount δ_h.

The differences between Fig. A.15 and Fig. A.12 are not surprising, as the perturbations now result in more severe errors in the pricing policy, due to the complete lack of insight by the provider about the system. These larger errors work in favor of full adoption in (b) and (e), and against it in (c) and (g). As expected, differences in errors result in different necessary discount values, even if the overall pattern and structure are preserved.

A.7.5 Fixed price policy

Provider's knowledge of the perturbations:

The provider does *not* have any knowledge about any of the perturbations in this section.

Under the original model and the fixed price policy, a profit maximizing strategy would often differ from a welfare maximizing one. In Chapter 3 we quantified this gap by comparing the overall profit under both types of strategies. The gap was small when the parameter c was small, but grew large as c increased.

In this section, we demonstrate that even under more general conditions, *i.e.,* when various aspects of the original model are perturbed, this finding remains valid.

Throughout the simulations of this section, we fix the parameters $\gamma = 1$, $r = 2$ and $e = 0.3$ and consider a range of c values. The details of the simulations are as follows: At each point, we iterate over different values of p to find the price p^* that maximizes the provider's profit with no constraint, as well as the price $\widehat{p}$ that maximizes provider's profit with the constraint that the total welfare is also maximized. We denote the corresponding values of maximum profit by W_P^* and $\widehat{W}_P$, respectively. We then compute the relative profit

drop from profit maximization to welfare maximization as

$$\text{Profit difference} = \frac{W_P^* - \widehat{W}_P}{W_P^*} \times 100\%.$$

Fig. A.16 compares the resulting profit drops for both the original model and the seven different perturbations introduced in Appendix A.6. The figure illustrates that the overall behavior is similar across all scenarios, *i.e.,* there is no profit difference for small values of c, but the gap increases rapidly as c increases beyond some moderate threshold value.

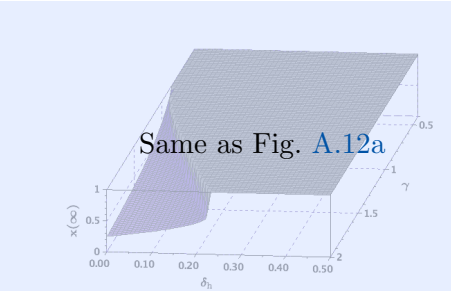

(a) Original model

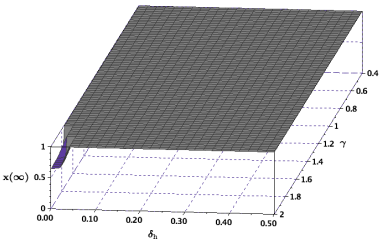

(b) Low-mode θ distribution with parameter $\lambda = 1.5$.

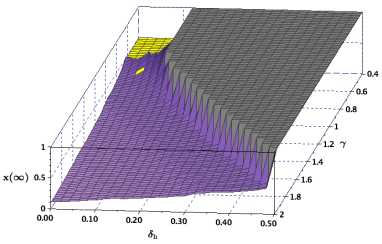

(c) High-mode θ distribution with parameter $\lambda = 1.5$.

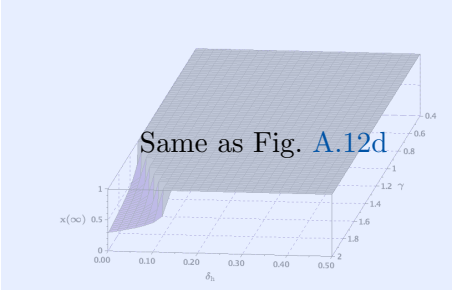

(d) Non-linear utility function

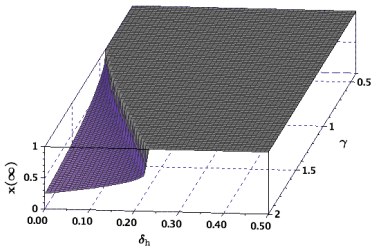

(e) Upper-bounded roaming ($\tau = 0.8$)

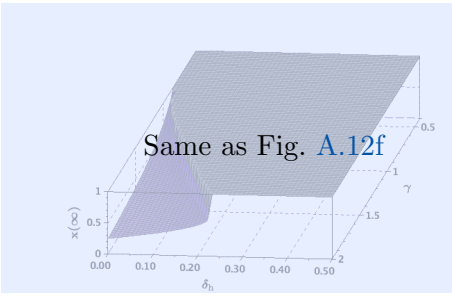

(f) Minimum useful coverage ($\kappa_{\text{th}} = 0.2$)

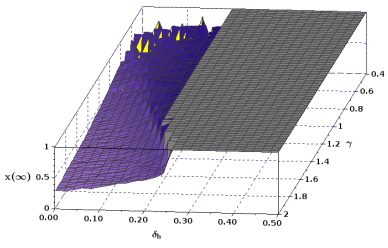

(g) Heterogeneous population

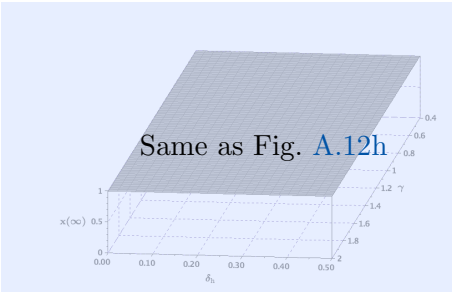

(h) Coverage saturation with adoption

Figure A.15: Final adoption level for the hybrid pricing policy (the provider does *not* know m at full adoption) under different perturbations. Parameters are $c = 0.8$, $\delta_r = 0$, with γ and δ_h values varying.

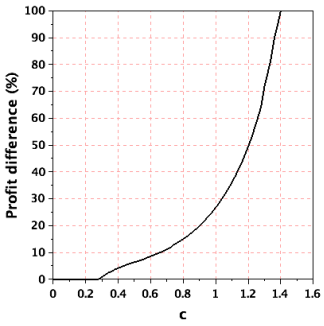

(a) Original model

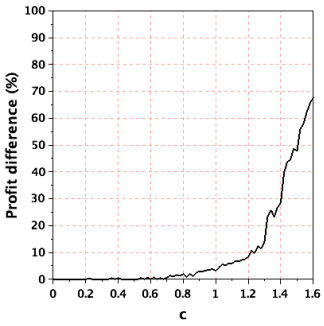

(b) Low-mode θ distribution with parameter $\lambda = 1.5$.

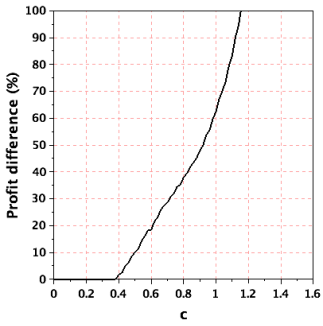

(c) High-mode θ distribution with parameter $\lambda = 1.5$.

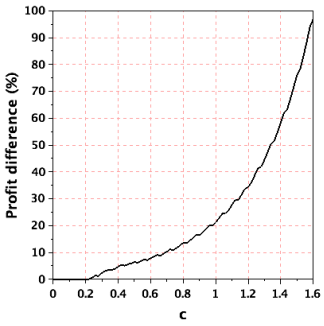

(d) Non-linear utility function

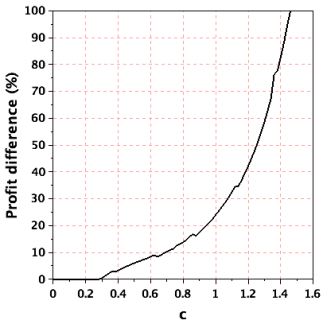

(e) Upper-bounded roaming ($\tau = 0.8$)

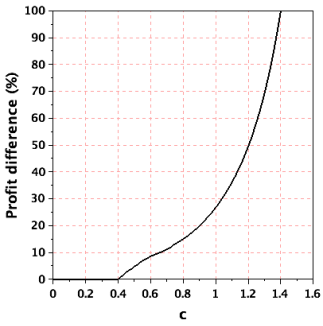

(f) Minimum useful coverage ($\kappa_{\text{th}} = 0.2$)

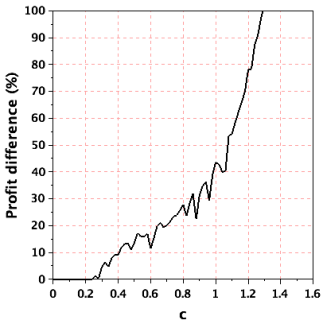

(g) Heterogeneous population

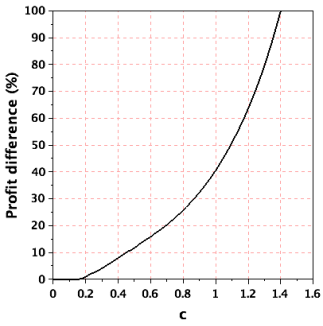

(h) Coverage saturation with adoption

Figure A.16: Relative profit drop from profit maximization to welfare maximization (fixed-price policy $\gamma = 1, r = 2$ and $e = 0.3$).

A.8 Usage-based pricing and utility functions with minimum useful coverage

In this section we analyze user adoption under the usage-based pricing policy and the utility function with *minimum useful coverage* rule.

Putting the usage-based price function of Eq. (3.16) into the utility function of Eq. (A.35), the utility for user θ is found as

$$U(\Theta, \theta) = \begin{cases} a - cm - r\theta x & \text{if } x < \kappa_{\text{th}}, \\ a - cm & \text{if } x \geq \kappa_{\text{th}}. \end{cases} \tag{A.36}$$

In order to analyze the adoption dynamics in this case, we assume that at each "decision time", only the most "eager" of the users adopts (or disadopts) the service. Such a "diffusion-like" adoption mechanism prevents artifacts such as sudden oscillation in the adoption level for the current case.

We first note that by Eq. (A.36), at any adoption level x, the users with smaller roaming frequency θ have higher utility. Therefore, the adoption interval is always of the form $[0, x]$, and consequently $m = x^2/2$. Therefore the utility function of Eq. (A.36) becomes

$$U(\Theta, \theta) = \begin{cases} a - c\frac{x^2}{2} - r\theta x & \text{if } x < \kappa_{\text{th}}, \\ a - c\frac{x^2}{2} & \text{if } x \geq \kappa_{\text{th}}. \end{cases} \tag{A.37}$$

We want to find the conditions under which full adoption $x = 1$ is the *unique* equilibrium and the adoption levels eventually reach this equilibrium. Now assume that adoption levels are initially at $x = 0$. Because of the low adoption level, user utilities are given by the first expression in Eq. (A.37). As adoption levels increase, we want to consistently have the user with $\theta = x^+$ see a positive utility, hence adopt the service. The worst case happens for the

user with $\theta = \kappa_{\text{th}}^{-}$, who at the time of her decision sees a utility of

$$\begin{aligned} U(x \approx \kappa_{\text{th}}, \theta = \kappa_{\text{th}}) &= a - (c/2)\kappa_{\text{th}} - r\kappa_{\text{th}} \\ &= a - \kappa_{\text{th}}(c/2 + r). \end{aligned}$$

Therefore we obtain the extra condition $a > \kappa_{\text{th}}(c/2 + r)$ for $x = 1$ to be a unique equilibrium. Consequently, we get a modified form of proposition 1.

Proposition 12. *Under the usage-based pricing policy of Eq. (3.16), and a utility function with minimum useful coverage rule given in Eq. (A.35), full adoption, $x = 1$, is the **unique** equilibrium if $a > \max\{c/2,\ \kappa_{th}(c/2 + r)\}$, and is not an equilibrium if $a \leq c/2$.*

Note that if the threshold κ_{th} is such that $c/2 \geq \kappa_{\text{th}}(c/2+r)$, then the system's adoption behavior is the same as the original model. On the other hand, If $c/2 < \kappa_{\text{th}}(c/2 + r)$, then for $c/2 < a < \kappa_{\text{th}}(c/2 + r)$, full adoption $x = 1$ is an equilibrium but not unique.

A.9 Contiguity of the optimal adoption set

In this section we provide analytical proof for a more general form of Lemma 1. Namely, in a setting where the users' propensity to roam, θ, has a general arbitrary distribution $f(\theta)$ in $[0, 1]$.

Under a general distribution, the adoption level x, the roaming traffic m and the total welfare $V(\Theta)$ should be computed based on their general expressions, as follows.

$$x(\Theta) = \int_{\theta \in \Theta} f(\theta)\, d\theta, \tag{A.38}$$

$$m(\Theta) = \int_{\theta \in \Theta} \theta\, f(\theta)\, d\theta\,, \tag{A.39}$$

$$V(\Theta) = \int_{\theta \in \Theta} v(\Theta,\, \theta)\, f(\theta)\, d\theta. \tag{A.40}$$

The next Lemma then gives the generalization of Lemma 1.

Generalization of Lemma 1. *Under an arbitrary roaming distribution with density $f(\theta)$*

and for any adoption level x, maximum welfare is always obtained with a set of adopters $\Theta^*(x)$ that exhibit contiguous roaming characteristics. Specifically, $\Theta^*(x)$ is of the form

$$\Theta^*(x) = \begin{cases} \Theta_1^*(x) = [0,\, x) & \text{if } x < \frac{\gamma}{r-c}, \\ \Theta_2^*(x) = [1-x,\, 1] & \text{if } x \geq \frac{\gamma}{r-c}. \end{cases} \tag{A.41}$$

Proof. For any given adoption level x, consider an arbitrary realization Θ^{old} of adopters such that $|\Theta^{\text{old}}| = x$. Now take any two intervals N_1 and N_2 from $[0,\, 1]$ such that

$$N_1 = [\theta_1,\, \theta_1 + \epsilon_1), \quad N_1 \cap \Theta^{\text{old}} = \varnothing,$$
$$N_2 = [\theta_2,\, \theta_2 + \epsilon_2), \quad N_2 \subset \Theta^{\text{old}}$$

where $\theta_2 > \theta_1$, $\epsilon_1 > 0$ and ϵ_2 is selected such that

$$x(N_1) = x(N_2) \triangleq \epsilon, \tag{A.42}$$

$x(\cdot)$ being the coverage generated by a particular set as defined by Eq. (A.38). The above conditions mean that everyone in N_1 is a non-adopter and everyone in N_2 is an adopter, and the population of these two sets is the same, taken to be ϵ. Construct a new set of adopters by having everyone in N_1 adopt and everyone in N_2 disadopt,

$$\Theta^{\text{new}} = (\Theta^{\text{old}} \cup N_1) \backslash N_2,$$

where $\backslash$ indicates the set difference operation. We investigate next the change Δ in welfare when the adopers' set changes from Θ^{old} to Θ^{new}, *i.e.,*

$$\Delta \triangleq V(\Theta^{\text{new}}) - V(\Theta^{\text{old}}). \tag{A.43}$$

Using Eq. (A.40) and splitting the bounds of the integral, we can write

$$\begin{aligned} V(\Theta^{\text{old}}) &= \int_{\Theta^{\text{old}}} v(\Theta^{\text{old}}, \theta)\, f(\theta)\, d\theta \\ &= \int_{\Theta^{\text{old}} \setminus N_2} v(\Theta^{\text{old}}, \theta)\, f(\theta)\, d\theta + \int_{N_2} v(\Theta^{\text{old}}, \theta)\, f(\theta)\, d\theta, \end{aligned} \tag{A.44}$$

and similarly

$$\begin{aligned} V(\Theta^{\text{new}}) &= \int_{\Theta^{\text{new}}} v(\Theta^{\text{new}}, \theta)\, f(\theta)\, d\theta \\ &= \int_{\Theta^{\text{new}} \setminus N_1} v(\Theta^{\text{new}}, \theta)\, f(\theta)\, d\theta + \int_{N_1} v(\Theta^{\text{new}}, \theta)\, f(\theta)\, d\theta, \end{aligned} \tag{A.45}$$

Note that

$$\Theta^{\text{old}} \setminus N_2 = \Theta^{\text{new}} \setminus N_1 = \Theta^{\text{old}} \cap \Theta^{\text{new}},$$

and therefore we can use Eq. (A.44) and Eq. (A.45) in Eq. (A.43) to get

$$\begin{aligned} \Delta = \Delta_1 + \Delta_2, \quad \text{where} \\ \Delta_1 &\triangleq \int_{\Theta^{\text{new}} \cap \Theta^{\text{old}}} \Big(v(\Theta^{\text{new}}, \theta) - v(\Theta^{\text{old}}, \theta) \Big)\, f(\theta)\, d\theta, \qquad \text{and} \\ \Delta_2 &\triangleq \int_{N_1} v(\Theta^{\text{new}}, \theta)\, f(\theta)\, d\theta - \int_{N_2} v(\Theta^{\text{old}}, \theta)\, f(\theta)\, d\theta. \end{aligned}$$

Moreover, from Eq. (3.9) we have

$$v(\Theta^{\text{old}}, \theta) = \gamma + \theta\,(r x^{\text{old}} - \gamma) - c m^{\text{old}} - e,$$

where x^{old} and m^{old} are the adoption level and the volume of roaming traffic corresponding to Θ^{old}. Similarly,

$$v(\Theta^{\text{new}}, \theta) = \gamma + \theta\,(r x^{\text{new}} - \gamma) - c m^{\text{new}} - e,$$

with x^{new} and m^{new} defined respective to Θ^{new}. Note that as a result of the condition in

Eq. (A.42), we have $x^{\text{old}} = x^{\text{new}} = x$. Therefore

$$\begin{aligned}\Delta_1 &= -\int_{\Theta^{\text{new}} \cap \Theta^{\text{old}}} c\left(m^{\text{new}} - m^{\text{old}}\right) f(\theta)\, d\theta \\ &= -c\left(m^{\text{new}} - m^{\text{old}}\right) \int_{\Theta^{\text{new}} \cap \Theta^{\text{old}}} f(\theta)\, d\theta \\ &= -c\left(m(N_1) - m(N_2)\right)(x - \epsilon)\end{aligned}$$

and

$$\begin{aligned}\Delta_2 &= (\gamma - cm^{\text{new}} - e) \int_{N_1} f(\theta)\, d\theta + (rx - \gamma) \int_{N_1} \theta\, f(\theta)\, d\theta \\ &\quad - (\gamma - cm^{\text{old}} - e) \int_{N_2} f(\theta)\, d\theta - (rx - \gamma) \int_{N_2} \theta\, f(\theta)\, d\theta \\ &= (\gamma - cm^{\text{new}} - e)\epsilon + (rx - \gamma)\, m(N_1) - (\gamma - cm^{\text{old}} - e)\epsilon - (rx - \gamma)\, m(N_2) \\ &= -\epsilon c\left(m(N_1) - m(N_2)\right) + (rx - \gamma)\left(m(N_1) - m(N_2)\right),\end{aligned}$$

Where $m(\cdot)$ is as given by Eq. (A.39). Thus, we compute Δ as

$$\begin{aligned}\Delta &= -cx\left(m(N_1) - m(N_2)\right) + (rx - \gamma)(m(N_1) - m(N_2)) \\ &= (m(N_2) - m(N_1))(cx - rx + \gamma).\end{aligned} \tag{A.46}$$

We also have

$$\begin{aligned}m(N_2) &= \int_{\theta_2}^{\theta_2 + \epsilon_2} \theta\, f(\theta)\, d\theta \\ &> \theta_2 \int_{\theta_2}^{\theta_2 + \epsilon_2} f(\theta)\, d\theta = \theta_2 \int_{\theta_1}^{\theta_1 + \epsilon_1} f(\theta)\, d\theta \\ &> (\theta_1 + \epsilon_1) \int_{\theta_1}^{\theta_1 + \epsilon_1} f(\theta)\, d\theta \\ &> \int_{\theta_1}^{\theta_1 + \epsilon_1} \theta\, f(\theta)\, d\theta = m(N_1),\end{aligned}$$

where $\theta_2 > \theta_1 + \epsilon_1$ holds since by construction N_1 and N_2 are mutually exclusive.

Consequently $m(N_2) - m(N_1) > 0$, and Eq. (A.46) indicates that $\Delta > 0$ if and only if $x < \frac{\gamma}{r-c}$. But a $\Delta > 0$ (positivity independent of the specific choices of N_1 and N_2)

means that welfare always increases if an interval of high-θ users leave and a same-size interval of low-θ users join. Repeating this for multiple intervals of suitable sizes will create a contiguous set of adopters in $[0,\, x)$ that generates more welfare than any other set. Similarly, the case of $\Delta \leq 0$ creates[15] a contiguous set of adopters in the other end of $[0,\, 1]$ interval, *i.e.,* $[1 - x,\, 1]$. □

The generalization of Lemma 1 characterizes the structure of optimal adoption set for any given x and establishes that is a contiguous set of adopters.

[15] When $\Delta = 0$, this optimal contiguous Θ is not the only optimum.

Appendix B

Extras for Ising models

B.1 Modified edge-weights in Random Influence Model

Theorems 1 and 2 were stated based on zero self-weight $w_{ii} = 0$ for the nodes and a uniform p value for all edge-weights. Similar results hold even if $w_{ii} = W_i > 0$, and every edge-weight w_{ij} arises from a different Bernoulli process, each with a probability p_{ij} of being $+1$. Denote $W_{\min} = \min_i\{W_i\}$, and $p_{\min} = \min_{i,j}\{p_{ij}\}$. A modified version of Theorem 1 can then be obtained as follows.

Theorem 7. *Fix any $0 < \delta < 1$ and suppose*

$$p_{\min} \geq \frac{1}{2} - \frac{W_{\min}}{2(n-1)} + \sqrt{\frac{\log(n/\delta)}{2(n-1)}}.$$

Then $P_n^+ \geq 1 - \delta$. In particular, if $p_{\min} > 1/2$ is bounded away from $1/2$, then $P_n^+ \to 1$ as $n \to \infty$.

Proof. Similar to the steps in the proof of Theorem 1 we have

$$\begin{aligned}
&\mathbf{P}(x_i^+ S_i^+ \leq 0) \\
&= \mathbf{P}\left(W_i + \sum_{j \neq i} (w_{ij} - (2p_{ij} - 1)) \leq -\sum_{j \neq i} (2p_{ij} - 1) \right)
\end{aligned}$$

$$
\begin{aligned}
&\leq \exp\left(-\frac{\left(W_i + \sum_{j\neq i}(2p_{ij}-1)\right)^2}{2(n-1)}\right) \\
&\leq \exp\left(-\frac{\left(W_i + \sum_{j\neq i}(2p_{i,\min}-1)\right)^2}{2(n-1)}\right) \\
&\leq \exp\left(-\frac{(n-1)^2(\frac{W_i}{n-1} + 2p_{i,\min}-1)^2}{2(n-1)}\right) \\
&= \exp\left(-2(n-1)\left(\frac{W_i}{2(n-1)} + p_{i,\min} - \frac{1}{2}\right)^2\right),
\end{aligned}
$$

where $p_{i,\min} = \min_j\{p_{ij}\}$. Continuing in the steps of the proof of Theorem 1, we get

$$
\begin{aligned}
&\mathbf{P}\left(\bigcup_{i=1}^{n}\left(x_i^+ S_i^+ \leq 0\right)\right) \\
&\leq \sum_{i=1}^{n}\mathbf{P}\left(x_i^+ S_i^+ \leq 0\right) \\
&\leq \sum_{i=1}^{n}\exp\left(-2(n-1)\left(\frac{W_i}{2(n-1)} + p_{i,\min} - \frac{1}{2}\right)^2\right) \\
&\leq \sum_{i=1}^{n}\exp\left(-2(n-1)\left(\frac{W_{\min}}{2(n-1)} + p_{\min} - \frac{1}{2}\right)^2\right) \\
&= n\cdot\exp\left(-2(n-1)\left(\frac{W_{\min}}{2(n-1)} + p_{\min} - \frac{1}{2}\right)^2\right)
\end{aligned}
$$

where $p_{\min} = \min_i\{p_{i,\min}\} = \min_{i,j}\{p_{ij}\}$ and $W_{\min} = \min_i\{W_i\}$. This means that

$$
\mathbf{P}\left(\bigcup_{i=1}^{n}\left(x_i^+ S_i^+ \leq 0\right)\right) \leq \delta,
$$

for the given selection of $p_{\min}$. □

Next we derive a modified version of Lemma 4.

Lemma 13. *Fix any $m < n/2$ and suppose $\mathbf{x} \in B_m$. Then*

$$\mathbf{P}\left(\bigcap_{i=1}^{n}(S_i(\mathbf{x}) > 0)\right)$$
$$\geq 1 - n \cdot \exp\left(-\frac{\left[(n-1-2m)\ (2p_{\min}-1) - W_{\max} - 2m\Delta_{\max}\right]^2}{2(n-1)}\right).$$

In these expressions,

$$p_{i,\min} = \min_j\{p_{ij}\},$$
$$p_{\min} = \min_{i,j}\{p_{ij}\},$$
$$W_{\max} = \max_i\{W_i\},$$
$$\textit{and} \qquad \Delta_{\max} = \max_i\{\Delta_i\}.$$

where $\Delta_i = p_{i,\max,} - p_{i,\min}$. Furthermore, and in order to get a simpler expression, $W > p_{i,\min} - 1/2$ is assumed.

Proof. Following the same steps as in the proof of lemma 4, for $i \in M(\mathbf{x})$ we get

$$\mathbf{P}\left(S_i(\mathbf{x}) \leq 0\right) \leq \exp\left(-\frac{(t_1)^2}{2(n-1)}\right) \text{ for } i \in M(\mathbf{x}),$$

where

$$t_1 \triangleq -\sum_{\substack{j\in M(\mathbf{x}),\\ j\neq i}}(2p_{ij}-1) + \sum_{j\notin M(\mathbf{x})}(2p_{ij}-1) - W_i > 0.$$

We note that

$$\begin{aligned} t_1 &\geq -\sum_{\substack{j\in M(\mathbf{x}),\\ j\neq i}}(2p_{i,\max}-1) + \sum_{j\notin M(\mathbf{x})}(2p_{i,\min}-1) - W_i \\ &= (n+1-2m)(2p_{i,\min}-1) - W_i - 2(m-1)\Delta_i \\ &\geq (n-2m)(2p_{i,\min}-1) - W_i - 2m\Delta_i \\ &\geq (n-1-2m)(2p_{i,\min}-1) - W_i - 2m\Delta_i. \end{aligned}$$

Similarly, for $i \notin M(\mathbf{x})$ we get

$$\mathbf{P}\left(S_i(\mathbf{x}) \leq 0\right) \leq \exp\left(-\frac{(t_2)^2}{2(n-1)}\right) \text{ for } i \notin M(\mathbf{x}),$$

where

$$t_2 \triangleq -\sum_{j \in M(\mathbf{x})} (2p_{ij} - 1) + \sum_{\substack{j \notin M(\mathbf{x}), \\ j \neq i}} (2p_{ij} - 1) - W_i > 0.$$

We note that

$$\begin{aligned} t_2 &\geq -\sum_{j \in M(\mathbf{x})} (2p_{\max,i} - 1) + \sum_{\substack{j \notin M(\mathbf{x}), \\ j \neq i}} (2p_{\min,i} - 1) - W_i \\ &= (n - 1 - 2m)(2p_{i,\min} - 1) + W_i - 2m\Delta_i \\ &\geq (n - 1 - 2m)(2p_{i,\min} - 1) - W_i - 2m\Delta_i. \end{aligned}$$

Hence we have

$$t_1,\, t_2 \geq (n - 1 - 2m)(2p_{i,\min} - 1) - W_i - 2m\Delta_i,$$

and as a result

$$\begin{aligned} &\forall i,\ \mathbf{P}\left(S_i(\mathbf{x}) \leq 0\right) \\ &\leq \exp\left(-\frac{\left[(n - 1 - 2m)\ (2p_{i,\min} - 1) - W_i - 2m\Delta_i\right]^2}{2(n-1)}\right) \\ &\leq \exp\left(-\frac{\left[(n - 1 - 2m)\ (2p_{\min} - 1) - W_{\max} - 2m\Delta_{\max}\right]^2}{2(n-1)}\right), \end{aligned}$$

Where $p_{\min} = \min_i\{p_{i,\min}\} = \min_{i,j}\{p_{ij}\}$, and $\Delta_{\max} = \max_i\{\Delta_i\}$. An application of union bound and conjugation, as done in the proof of lemma 4, will conclude the proof. □

We conclude with the modified version of Theorem 2, which is identical to it except for the value of $\alpha_0(p)$.

Theorem 8. *Select any tiny, positive ϵ. Fix any $1/2 < p < 1$ and any value $0 < \alpha < \alpha_0(p)$. If $\mathbf{x}$ is any state with $d(\mathbf{x}, \mathbf{x}^+) \leq \alpha n$, then $\mathbf{P}(A_x^+) > 1 - \epsilon$ whenever n is sufficiently large.*

The value $\alpha_0(p)$ *is the solution to*

$$f(\alpha, p) = 0,$$

where

$$f(\alpha,p) = 2\left[(1-2\alpha-1/n)\,(p_{\min}-1/2) - \frac{W_{\max}}{2n} - \alpha\Delta_{\max}\right]^2 + \alpha\log(\alpha) + (1-\alpha)\log(1-\alpha).$$

Proof. Using the result of lemma 13 and following the same steps as in the proof of Theorem 2, we see that

$$\begin{aligned}
&\mathbf{P}\left(R_x^c\right)\\
&\leq n\cdot\exp\left(-\frac{4n^2\left[(1-2\alpha-\frac{1}{n})\,(p_{\min}-\frac{1}{2}) - \frac{W_{\max}}{2n} - \alpha\Delta_{\max}\right]^2}{2(n-1)}\right)\\
&\leq n\cdot\exp\left(-2n\left[(1-2\alpha-\frac{1}{n})\left(p_{\min}-\frac{1}{2}\right) - \frac{W_{\max}}{2n} - \alpha\Delta_{\max}\right]^2\right).
\end{aligned}$$

The rest of the proof is the same as that of Theorem 2. □

B.2 Independents in the Random Influence Model

This section analyzes the Random Influence model in the presence of a group of *independents* G_a in addition to the two parties G_1 and G_2 that were described in section 4.2.2. The independents have non-biased affinities towards every node in the network, *i.e.,* the interaction weights $\{w_{ij}^a,\, i \in G_a\}$ between a node $i \in G_a$ and any node j in the network form a system of signed Bernoulli trials with success parameter $\mathbf{P}\{w_{ij}^a = 1\} = 1/2$.

In this case the arguments of section 4.2.3 can still be used to merge the two parties into one party G_b. However, the model may not be further simplified and we are left with one party G_b and the independents. As before, the interaction weights $\{w_{ij}^b,\, i, j \in G_b,\, i \leq j\}$ between two nodes[1] $i, j \in G_b$ form a system of signed Bernoulli trials with success parameter $p = \mathbf{P}\{w_{ij}^b = 1\} > 1/2$.

Let the size of the party be $|G_b| = n_b$ and the size of the independent group be $|G_a| =$

[1] For conciseness of representation, we assume that self-weights w_{ii} are of the same nature as cross-weights. Generalizations to this can be easily obtained.

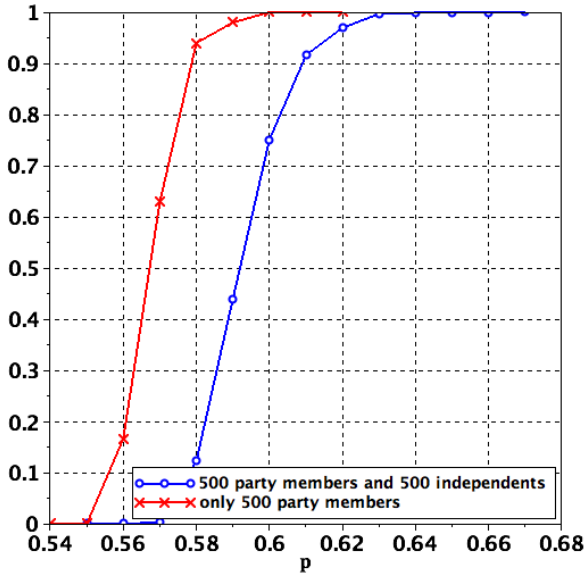

Figure B.1: The fraction of time that the system converges to a meta-partisan fixed point, when 1/2 of the total 1000 nodes are independents, and the fraction of the times that the system converges to a partisan fixed point, when there are 500 party members without any independents. In both cases, the number of party members is 500. Also in both cases we pick random, non-biased starting points.

$n_a = n - n_b$. Define a *meta-partisan* state $\mathbf{x}^{\mu+}$ (with positive polarity) as any state[2] for which $x_i^{\mu+} = +1$, $\forall i \in G_b$ and define $S_i(\mathbf{x}^{\mu+}) = S_i^{\mu+}$. A meta-partisan state $\mathbf{x}^{\mu+}$ is similar to the partisan state $\mathbf{x}^+$ of section 4.3 with regards to the party nodes $i \in G_b$, but allows for any opinion at the independent nodes $i \in G_a$. Therefore there are a total of 2^{n_a} different meta-partisan states (with positive polarity) which we index by $1 \leq \mu \leq 2^{n_a}$. In the remainder of this section we show that starting from any of the meta-partisan states $\mathbf{x}^{\mu+}$, there is a high probability $\widehat{\mathbf{P}^+}$ that the system remains within the set of the meta-partisan states indefinitely.

Let $E^{\mu+}$ be the *exit* event for the meta-partisan state $\mathbf{x}^{\mu+}$, which occurs if $\mathbf{x}^{\mu+}$ updates to a non-meta-partisan state, *i.e.,* there exists at least one party member $i \in G_b$ such that

[2] Similar to the partisan states defined in section 4.3, a meta-partisan state may be defined with positive or negative polarity. Here we concentrate on the states $\mathbf{x}^{\mu+}$ with positive polarity. The negative-polarity states are symmetrical to the positive-polarity ones and can be similarly discussed.

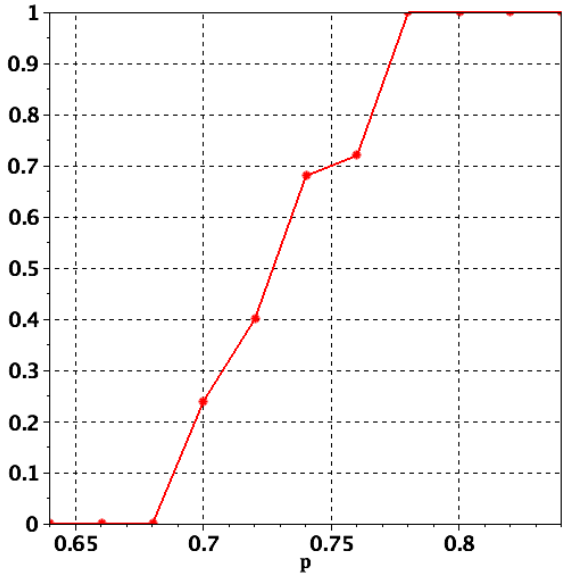

Figure B.2: The fraction of time that the system converges to a meta-partisan fixed point, when a fraction 0.90 of the total 4000 nodes are independents At each p value, 5 different initializations of edge-weights are considered and for each of those, 5 initialization of random opinions.

$x_i^{\mu+} S_i^{\mu+} \leq 0$. Specifically

$$E^{\mu+} = \bigcup_{i \in G_b} x_i^{\mu+} S_i^{\mu+} \leq 0. \tag{B.1}$$

The next Theorem determines the probability of the exit event.

Theorem 9. *Assume p is large enough so that*

$$n_b (2p-1) - n_a \geq 0. \tag{B.2}$$

Then at any meta-partisan state $\mathbf{x}^{\mu+}$, the probability of the exit event defined by Eq. (B.1) satisfies the following inequality.

$$\mathbf{P}\left(E^{\mu+}\right) \leq n_b \cdot \exp\left(-\frac{\left[n_b (2p-1) - n_a\right]^2}{2n_b}\right).$$

Proof. If the system is in the meta-state $\mathbf{x}^{\mu+}$ then the partial sums for any node $i \in G_b$ are

given by

$$\begin{aligned} x_i^{\mu+} S_i^{\mu+} = S_i^{\mu+} &= \sum_{j \in G_b} w_{ij}^b x_j^{\mu+} + \sum_{j \in G_a} w_{ij}^a x_j^{\mu+} \\ &= \sum_{j \in G_b} w_{ij}^b + \sum_{j \in G_a} w_{ij}^a x_j^{\mu+} \\ &\geq \sum_{j \in G_b} w_{ij}^b - n_a. \end{aligned}$$

The sum on the right represents a random walk with a positive drift, and $-n_a$ is a lower-bound (worst case) for the effect from the independents. The signed Bernoulli variables w_{ij}^b have expectation $2p-1$. From the above it results that

$$\begin{aligned} \mathbf{P}(x_i^{\mu+} S_i^{\mu+} \leq 0) &\leq \mathbf{P}\left(\sum_{j \in G_b} w_{ij}^b - n_a \leq 0 \right) \\ &= \mathbf{P}\left(\sum_{j \in G_b} \left(w_{ij}^b - (2p-1) \right) \leq n_a - n_b\,(2p-1) \right). \end{aligned}$$

From Eq. (B.2) we have

$$[n_a - n_b\,(2p-1)] \leq 0,$$

and the Hoeffding's inequality can therefore be used as before. We obtain

$$\mathbf{P}(x_i^{\mu+} S_i^{\mu+} \leq 0) \;\leq\; \exp\left(-\frac{[n_b\,(2p-1) - n_a]^2}{2n_b} \right).$$

By Boole's inequality, it follows that

$$\begin{aligned} \mathbf{P}\left(\bigcup_{i \in G_b} \left(x_i^{\mu+} S_i^{\mu+} \leq 0 \right) \right) &\leq \sum_{i \in G_b} \mathbf{P}\left(x_i^{\mu+} S_i^{\mu+} \leq 0 \right) \\ &\leq n_b \cdot \exp\left(-\frac{[n_b\,(2p-1) - n_a]^2}{2n_b} \right). \end{aligned}$$

□

Corollary. *Separate deterministic calculations easily show that if* $p = 1$ *and* $n_a < n_b$ *then* $\mathbf{P}\left(E^{\mu+}\right) = 0$.

We note that if none of the meta-partisan states yields to the exit event, then the system does remain within the set of the meta-partisan states indefinitely (but the inverse is not true). Therefore the probability of the latter is at least as high as the probability of the former, *i.e.*,

$$\widehat{\mathbf{P}^+} \geq 1 - \mathbf{P}\left(\bigcup_{\mu=1}^{2^{n_a}} E^{\mu+}\right). \tag{B.3}$$

Now assume $n_a = \epsilon n$ (and $n_b = (1-\epsilon)n$). Then the following theorem shows how $\widehat{\mathbf{P}^+}$ can be made arbitrarily large.

Theorem 10. *Fix any* $0 < \delta < 1$ *and suppose*

$$p \geq \frac{1}{2} + \frac{\epsilon}{2(1-\epsilon)} + \sqrt{\frac{\epsilon \log 2 + \frac{\log((1-\epsilon)n/\delta)}{n}}{2(1-\epsilon)}}. \tag{B.4}$$

Then $\widehat{\mathbf{P}^+} \geq 1 - \delta$. *In particular, if* $p > 1/2$ *is bounded away from (and more than)*

$$p_\epsilon = \frac{1}{2} + \frac{\epsilon}{2(1-\epsilon)} + \sqrt{\frac{\epsilon \log 2}{2(1-\epsilon)}}, \tag{B.5}$$

then $\widehat{\mathbf{P}^+} \to 1$ *as* $n \to \infty$.

Proof. From Eq. (B.3) we use Boole's inequality to obtain

$$\widehat{\mathbf{P}^+} \geq 1 - \sum_{\mu=1}^{2^{n_a}} \mathbf{P}\left(E^{\mu+}\right).$$

Since Theorem 9 holds for all values of μ, and since the condition in Eq. (B.4) subsumes the condition in Eq. (B.2), we can apply Theorem 9 to the above equation to get

$$\widehat{\mathbf{P}^+} \geq 1 - 2^{n_a} n_b \cdot \exp\left(-\frac{\left[n_b\left(2p-1\right) - n_a\right]^2}{2n_b}\right).$$

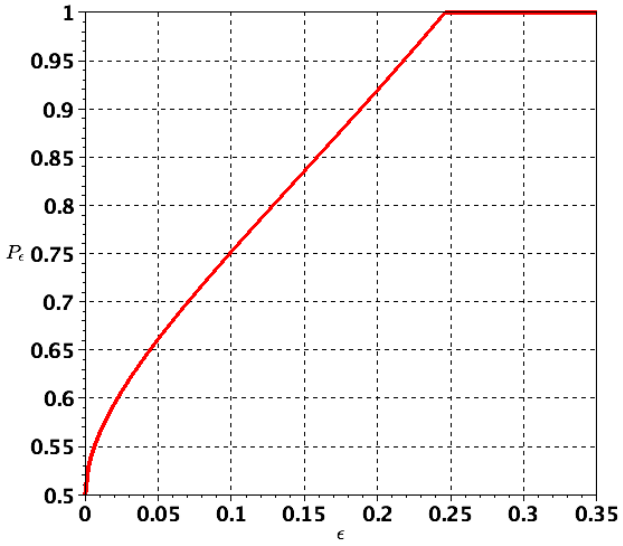

Figure B.3: Lower bound of p required for $\widehat{\mathbf{P}^+}_{n\to\infty} \to 1$ as given by Eq. (B.5). Note that according to the corollary to Theorem 10, even where Eq. (B.5) gives a $p_\epsilon > 1$, a value of $p = 1$ guarantees that $\widehat{\mathbf{P}^+} = 1 \geq 1 - \delta$ provided that $\epsilon < 1/2$.

Replacing $n_a = \epsilon n$ and $n_b = (1-\epsilon)n$ in the above gives

$$\begin{aligned}\widehat{\mathbf{P}^+} &\geq 1 - 2^{\epsilon n}(1-\epsilon)n \cdot \exp\left(-\frac{n\,(2p - 2\epsilon p - 1)^2}{2(1-\epsilon)}\right) \\ &\geq 1 - \delta,\end{aligned}$$

where the last inequality holds for the given selection of p from Eq. (B.4). □

Corollary. *Following the corollary to Theorem 9, it is again straight forward to show that if $p = 1$ and $\epsilon < 1/2$, then $\widehat{\mathbf{P}^+} = 1$.*

Fig. B.3 plots p_ϵ from Eq. (B.5) as a function of ϵ.

B.3 Isolation of centric clusters

When κ is an even number, there are *centric* clusters that have exactly $\kappa/2$ entries of $+1$ in their profiles. The next proposition shows that these centric clusters are not affected by

the dominance effect of Theorem 6.

Proposition 13. *There exists $p^* < 1$ such that $\forall p$, $p^* \leq p < 1$, the overall ifnfluence of the outer world on the clusters of type $C^{(\kappa/2)}$ is zero.*

Proof. We will separately consider the effect of clusters $C^{(\lambda)}$ with different values of $\lambda \neq \kappa/2$ over clusters of type $C^{(\kappa/2)}$. Without loss of generality, consider a $C^{(\kappa/2)}$ cluster with a profile of the form $[+1, +1, \ldots, -1, -1]$, *i.e.,* all the $+1$ entries are in the beginning of the profile. Now for any $C^{(\lambda)}$, let λ_1 be the number of $+1$ entries in the profile of $C^{(\lambda)}$ from position 1 to $\kappa/2$. Furthermore, let λ_2 be the number of $+1$ entries from position $\kappa/2+1$ to κ. Obviously, we have $\lambda_1 + \lambda_2 = \lambda$. We will denote such a cluster by $C^{(\lambda_1, \lambda_2)}$.

Without loss of generality, we assume that $\lambda < \kappa/2$. If that is not the case, one can redefine λ as the number of -1 entries in the profile, and the following steps will still hold. The edge-weight between $C^{(\lambda_1, \lambda_2)}$ and $C^{(\kappa/2)}$ is

$$\lambda_1 - (\kappa/2 - \lambda_1) - \lambda_2 + (\kappa/2 - \lambda_2) = 2(2\lambda_1 - \lambda).$$

Moreover, there are a total of $\binom{\kappa/2}{\lambda_1}\binom{\kappa/2}{\lambda_2}$ clusters of type $C^{(\lambda)}$, and all of them have the same opinion $x^{(\lambda)}$ by Theorem 6. Moreover, they all have the same expected size $p^\lambda q^{(\kappa-\lambda)}$.

Therefore the total influence of clusters $C^{(\lambda)}$ over a cluster $C^{(\kappa/2)}$ can be written as

$$\begin{aligned}\Gamma^{(\lambda)} &= \sum_{\lambda_1=0}^{\lambda} 2(2\lambda_1 - \lambda)\binom{\kappa/2}{\lambda_1}\binom{\kappa/2}{\lambda_2} p^\lambda q^{(\kappa-\lambda)} \\ &= 2p^\lambda q^{(\kappa-\lambda)} \sum_{\lambda_1=0}^{\lambda} (2\lambda_1 - \lambda)\binom{\kappa/2}{\lambda_1}\binom{\kappa/2}{\lambda_2}.\end{aligned}$$

Now it suffices to show that

$$\sum_{\lambda_1=0}^{\lambda} \lambda\binom{\kappa/2}{\lambda_1}\binom{\kappa/2}{\lambda_2} = \sum_{\lambda_1=0}^{\lambda} 2\lambda_1\binom{\kappa/2}{\lambda_1}\binom{\kappa/2}{\lambda_2}. \tag{B.6}$$

We start from the right hand side of Eq. (B.6),

$$\begin{aligned}\text{RHS} &= \sum_{\lambda_1=0}^{\lambda} 2\lambda_1 \binom{\kappa/2}{\lambda_1}\binom{\kappa/2}{\lambda_2} \\ &= \sum_{\lambda_1=0}^{\lambda} 2\lambda_1 \binom{\kappa/2}{\lambda_1}\binom{\kappa/2}{\lambda-\lambda_1},\end{aligned}$$

and apply the change of variable $t = \lambda - \lambda_1$ to get

$$\begin{aligned}\text{RHS} &= \sum_{t=\lambda}^{0} 2(\lambda - t) \binom{\kappa/2}{\lambda-t}\binom{\kappa/2}{t} \\ &= \sum_{t=0}^{\lambda} 2(\lambda - t) \binom{\kappa/2}{t}\binom{\kappa/2}{\lambda-t} \\ &= \sum_{\lambda_1=0}^{\lambda} 2(\lambda - \lambda_1) \binom{\kappa/2}{\lambda_1}\binom{\kappa/2}{\lambda-\lambda_1}.\end{aligned}$$

Adding up the two equivalent expressions above, gives

$$\begin{aligned}2 \times \text{RHS} &= \sum_{\lambda_1=0}^{\lambda} 2\lambda \binom{\kappa/2}{\lambda_1}\binom{\kappa/2}{\lambda-\lambda_1} \\ &= \sum_{\lambda_1=0}^{\lambda} 2\lambda \binom{\kappa/2}{\lambda_1}\binom{\kappa/2}{\lambda_2}.\end{aligned}$$

Therefore

$$\text{RHS} = \sum_{\lambda_1=0}^{\lambda} \lambda \binom{\kappa/2}{\lambda_1}\binom{\kappa/2}{\lambda_2} = \text{LHS}.$$

This concludes the proof. □

B.4 Proof for special cases of profile-based model

Profile of size 1

The following theorem says that for $\kappa = 1$, the system has only two fixed points. After that, we consider a profile of length 2 and a profile that is very large. Note that when $\kappa = 1$, the

profile vector π_i is just a scalar and $\pi_i = \pi_{i1}$.

Proposition 7. For any network size n, the profile-based model with profile size $\kappa = 1$ has exactly two fixed point that are *stochastic*, *i.e.,* they are determined by the specific realization of profile values, as given in Eq. (B.7).

$$x^a : x_i^a = \begin{cases} +1 & \text{if } \pi_i = +1 \\ -1 & \text{if } \pi_i = -1 \end{cases} \tag{B.7a}$$

$$x^b : x_i^b = \begin{cases} -1 & \text{if } \pi_i = +1 \\ +1 & \text{if } \pi_i = -1 \end{cases} \tag{B.7b}$$

Proof. Profile vectors of size 1 are simply scalars $\pi_i = \pm 1$. Consider a state x at a Hamming distance m to x^a. Note that such a state has $n-m$ *a-conforming* nodes that are in accordance with x^a, and m *b-conforming* nodes that are in accordance with x^b.

Now take i to be any of the m *b-conforming* nodes with $x_i = x_i^b = -\pi_i$. The update sum for this node is

$$\begin{aligned} S_i &= \sum_{j \neq i} \pi_i \pi_j x_j = \pi_i \sum_{j \neq i} \pi_j x_j \\ &= \pi_i \left(\sum_{j : x_j = x_j^a} \pi_j x_j + \sum_{\substack{j : x_j = x_j^b, \\ j \neq i}} \pi_j x_j \right) \\ &= \pi_i \left(\sum_{j : x_j = x_j^a} (+1) + \sum_{\substack{j : x_j = x_j^b, \\ j \neq i}} (-1) \right) \\ &= \pi_i \left((n-m) - (m-1) \right) \\ &= \pi_i (n - 2m + 1). \end{aligned}$$

If

$$m < \frac{n+1}{2}, \tag{B.8}$$

then $\text{Sign}\,(\pi_i(n-2m+1)) = \text{Sign}\,(\pi_i) = \pi_i$ and therefore node i will update its opinion x_i to match $x_i^a = \pi_i$ and become a-conforming, *i.e.,*

$$x_i^{\text{new}} = x_i^a = \pi_i.$$

So the number of b-conforming nodes is reduced to $m-1$. Furthermore, If $m > \frac{n+1}{2}$, then $\text{Sign}\,(\pi_i(n-2m+1)) = -\text{Sign}\,(\pi_i) = -\pi_i$ and therefore node i will remain b-conforming, *i.e.,*

$$x_i^{\text{new}} = x_i = x_i^b = -\pi_i.$$

So the number of b-conforming nodes remains m.

On the other hand, if i is an a-conforming node with $x_i = x_i^a = \pi_i$, then the update sum for this node is

$$\begin{aligned}
S_i &= \sum_{j\neq i} \pi_i\pi_j x_j = \pi_i \sum_{j\neq i} \pi_j x_j \\
&= \pi_i \left(\sum_{\substack{j:x_j=x_j^a,\\ j\neq i}} \pi_j x_j + \sum_{j:x_j=x_j^b} \pi_j x_j \right) \\
&= \pi_i \left(\sum_{\substack{j:x_j=x_j^a,\\ j\neq i}} (+1) + \sum_{j:x_j=x_j^b} (-1) \right) \\
&= \pi_i \left((n-m-1) - (m) \right) \\
&= \pi_i (n-2m-1).
\end{aligned}$$

If

$$m < \frac{n-1}{2}, \tag{B.9}$$

then $\text{Sign}\,(\pi_i(n-2m-1)) = \text{Sign}\,(\pi_i) = \pi_i$ and therefore node i will remain a-conforming, *i.e.,*

$$x_i^{\text{new}} = x_i = x_i^a = \pi_i.$$

So the number of b-conforming nodes stays at m. Furthermore, If $m > \frac{n-1}{2}$, then

$$\text{Sign}\left(\pi_i(n-2m+1)\right) = -\text{Sign}\left(\pi_i\right) = -\pi_i$$

and therefore node i will become b-conforming, *i.e.,*

$$x_i^{\text{new}} = x_i^b = -\pi_i.$$

So the number of b-conforming nodes in increased to $m+1$.

Combining the above results, we see that if the system starts from a state with $m < \min\left\{\frac{n+1}{2}, \frac{n-1}{2}\right\} = \frac{n-1}{2}$ b-conforming nodes, under an arbitrary sequence of node updates that ensures every node is visited in finite time, all of the b-conforming nodes will eventually be met and transformed into an a-conforming node. At each such incident the number of b-conforming nodes decreases by 1 unit, until it becomes zero and the system converges to x^a.

On the other hand, if the system starts from a node with $m > \max\left\{\frac{n+1}{2}, \frac{n-1}{2}\right\} = \frac{n+1}{2}$ b-conforming nodes, under an arbitrary sequence of node updates that ensures every node is visited in finite time, all of the a-conforming nodes will eventually be met and transformed into a b-conforming node. At each such incident the number of b-conforming nodes increases by 1 unit, until it becomes n and the system converges to x^b.

$$x \text{ will converge to } \begin{cases} x^a & \text{if } \ m < \frac{n-1}{2}, \\ x^b & \text{if } \ m > \frac{n+1}{2}. \end{cases} \tag{B.10}$$

If m is any integer $\frac{n-1}{2} \leq m \leq \frac{n+1}{2}$, the convergence outcome depends on the first node to update, and the value assumed for Sign(0). For example, if n is even, then the only integer in $\left[\frac{n-1}{2}, \frac{n+1}{2}\right]$ is $n/2$. With $m = n/2$ b-conforming nodes, if the first node to update is a b-conforming one, then $m < \frac{n+1}{2}$ is satisfied and it will become a-conforming, changing m to $n/2 - 1$. The system will hence converge to x^a by Eq. (B.10). If, on the

other hand, the first node to update is an a-conforming one, then $m > \frac{n-1}{2}$ is satisfied and it will become b-conforming, changing m to $n/2+1$. The system will hence converge to x^b by Eq. (B.10). □

Proposition 7 showed that with profiles being of the extreme size $\kappa = 1$, the outcome of the system is either of the two fixed points that are determined wholly by the particular realization of profile values. Next we study another extreme profile size, $\kappa = \infty$.

Profile of size ∞

Proposition 8. or any network size n, and with arbitrarily large probability, the profile-based model with profile size κ sufficiently larger than $\frac{2n^2}{(4p^2-4p+1)^2}(\log(n)+\log(n+1))$, has exactly two fixed points that are determined by the party affiliation of the nodes, as given in Eq. (B.11).

$$x^a : x_i^a = \begin{cases} +1 & \text{if } i \in G_1 \\ -1 & \text{if } i \in G_2 \end{cases} \tag{B.11a}$$

$$x^b : x_i^b = \begin{cases} -1 & \text{if } i \in G_1 \\ +1 & \text{if } i \in G_2 \end{cases} \tag{B.11b}$$

Proof. We first show that the relative sizes of G_1 and G_2 do not affect the result, and in particular, we can assume that all nodes belong to G_1 without loss of generality, *i.e.,* $n_1 = n$ and $n_2 = 0$. In order to show this, we will use the result of Section 4.2.3 iteratively. In what follows, we show that the discussion of Section 4.2.3 is indeed applicable.

Consider any two nodes i and j both from party G_1. The k^{th} entry of their profiles, π_{ik}

and π_{jk}, each have a probability p of being positive. Therefore

$$\begin{aligned}\mathbf{P}\left(\pi_{ik}\pi_{jk}=1\right) &= p^2+(1-p)^2\\ &= 2p^2-2p+1\\ &\triangleq \widetilde{p},\end{aligned}$$

and

$$\begin{aligned}\mathbf{P}\left(\pi_{ik}\pi_{jk}=-1\right) &= 2p(1-p)\\ &= -2p^2+2p\\ &= 1-\widetilde{p}.\end{aligned}$$

Now consider a node j' from party G_2. Since $\pi_{j'k}$ has a probability $(1-p)$ of being positive, we have

$$\begin{aligned}\mathbf{P}\left(\pi_{ik}\pi_{j'k}=1\right) &= 2p(1-p)\\ &= 1-\widetilde{p},\end{aligned}$$

and

$$\begin{aligned}\mathbf{P}\left(\pi_{ik}\pi_{j'k}=-1\right) &= p^2+(1-p)^2\\ &= \widetilde{p}.\end{aligned}$$

Consequently, $(-\pi_{ik}\pi_{j'k})$ has the same probability distribution as $(\pi_{ik}\pi_{jk})$. As a result,

$$\begin{aligned}-\widehat{w}_{ij'} &= -\frac{1}{\kappa}\sum_{k=1}^{\kappa}\pi_{ik}\pi_{j'k}\\ &= \frac{1}{\kappa}\sum_{k=1}^{\kappa}-\pi_{ik}\pi_{j'k}\end{aligned}$$

has also the same probability distribution as

$$\check{w}_{ij} = \frac{1}{\kappa} \sum_{k=1}^{\kappa} \pi_{ik}\pi_{jk}.$$

Therefore the result of Section 4.2.3 is applicable, and by iteratively applying it, we can assume that all the nodes belong to party G_1.

Since profile entries with different k indices are independent of each other, the product $\pi_{ik}\pi_{jk}$, $\forall k$, makes a set of k independent Bernoulli random variables that take values $+1$ and -1 with probabilities $\widetilde{p}$ and $1-\widetilde{p}$. Therefore we can use Hoeffding's inequality to bound the probability that $\sum_{k=1}^{\kappa} \pi_{ik}\pi_{jk}$ deviates from its mean. Before we proceed, we find its expected value, $E(\cdot)$, as

$$\begin{aligned}
&E\left(\sum_{k=1}^{\kappa} \pi_{ik}\pi_{jk}\right) \\
&= \sum_{k=1}^{\kappa} E\left(\pi_{ik}\pi_{jk}\right) \\
&= \sum_{k=1}^{\kappa} \left(\mathbf{P}\left(\pi_{ik}\pi_{jk} = 1\right) - \mathbf{P}\left(\pi_{ik}\pi_{jk} = -1\right)\right) \\
&= \sum_{k=1}^{\kappa} \left(4p^2 - 4p + 1\right) \\
&= \kappa \left(4p^2 - 4p + 1\right) \\
&\triangleq \kappa\, \mu,
\end{aligned}$$

Where $\mu \triangleq 4p^2 - 4p + 1$ is the expected value of $\pi_{ik}\pi_{jk}$, and $\mu > 0$ for $p > 1/2$. For any

$\epsilon > 0$ we have by Hoeffding's inequality,

$$\begin{aligned}
&\mathbf{P}\left(\sum_{k=1}^{\kappa} \pi_{ik}\pi_{jk} \geq (\mu+\epsilon)\kappa\right) \\
&= \mathbf{P}\left(\sum_{k=1}^{\kappa} \pi_{ik}\pi_{jk} \leq (\mu-\epsilon)\kappa\right) \\
&= \mathbf{P}\left(\sum_{k=1}^{\kappa} (\pi_{ik}\pi_{jk} - \mu) \leq -\epsilon\kappa\right) \\
&\leq \exp\left(-\frac{\epsilon^2\kappa^2}{2\kappa}\right) \\
&= \exp\left(-\frac{\epsilon^2\kappa}{2}\right),
\end{aligned}$$

which bounds the value of $w_{ij} = \frac{1}{\kappa}\sum_{k=1}^{\kappa} \pi_{ik}\pi_{jk}$ to the interval $(\mu-\epsilon,\, \mu+\epsilon)$ with high probability. More accurately, let $D_{ij}(\epsilon)$ be the event that w_{ij} deviates from this interval. We have

$$\begin{aligned}
\forall i, j,\ \mathbf{P}\left(D_{ij}(\epsilon)\right) &\triangleq \mathbf{P}\left((w_{ij} \leq \mu-\epsilon) \cup (w_{ij} \geq \mu+\epsilon)\right) \\
&\leq \mathbf{P}\left(w_{ij} \leq \mu-\epsilon\right) + \mathbf{P}\left(w_{ij} \geq \mu+\epsilon\right) \\
&\leq 2\exp\left(-\frac{\epsilon^2\kappa}{2}\right).
\end{aligned}$$

The above relation is for a specific i and j. Now the probability that of all the different $\{i,\, j\}$ pairs, at least one of the edge-weights w_{ij} deviates from the interval $(\mu-\epsilon,\, \mu+\epsilon)$, is

$$\begin{aligned}
\mathbf{P}\left(\bigcup_{i>j} D_{ij}(\epsilon)\right) &\leq \sum_{i>j} \mathbf{P}\left(D_{ij}(\epsilon)\right) \\
&\leq n(n+1)\exp\left(-\frac{\epsilon^2\kappa}{2}\right). \qquad \text{(B.12)}
\end{aligned}$$

For κ large enough, this probability goes to 0 and therefore with a high probability, *all* of w_{ij} values are inside $(\mu-\epsilon,\, \mu+\epsilon)$, *i.e.,* the probability

$$\mathbf{P}\left(\bigcap_{i>j} [D_{ij}(\epsilon)]^c\right) \geq 1 - n(n+1)\exp\left(-\frac{\epsilon^2\kappa}{2}\right)$$

will go to 1. Note that this is the measure of the set of different profile realizations for which, *all* w_{ij} values are bounded in $(\mu-\epsilon,\,\mu+\epsilon)$. Now assume that one of these profile realizations has indeed happened, and consider any state x with a Hamming distance m from x^a. Under this state, the update sum of a node i with $x_i = x_i^a$ can be written as

$$\begin{aligned} S_i &= \sum_{\substack{j:x_j=x_j^a,\\ j\neq i}} w_{ij}x_j + \sum_{j:x_j\neq x_j^a} w_{ij}x_j \\ &= \sum_{\substack{j:x_j=x_j^a,\\ j\neq i}} w_{ij} - \sum_{j:x_j\neq x_j^a} w_{ij} \\ &\geq (n-m-1)(\mu-\epsilon) - (m)(\mu+\epsilon) \\ &= \mu(n-2m-1-n\epsilon/\mu+\epsilon/\mu), \end{aligned}$$

which is positive for

$$m < \frac{n-1-\epsilon/\mu(n-1)}{2}. \tag{B.13}$$

On the other hand, for a node i with $x_i \neq x_i^a$, the update sum is

$$\begin{aligned} S_i &= \sum_{j:x_j=x_j^a} w_{ij}x_j + \sum_{\substack{j:x_j\neq x_j^a,\\ j\neq i}} w_{ij}x_j \\ &= \sum_{j:x_j=x_j^a} w_{ij} - \sum_{\substack{j:x_j\neq x_j^a,\\ j\neq i}} w_{ij} \\ &\geq (n-m)(\mu-\epsilon) - (m-1)(\mu+\epsilon) \\ &= \mu(n-2m+1-n\epsilon/\mu+\epsilon/\mu). \end{aligned}$$

which is positive for

$$m < \frac{n+1-\epsilon/\mu(n-1)}{2}. \tag{B.14}$$

If $\epsilon/\mu(n-1) < 1$, then Eq. (B.13) and Eq. (B.14) are equivalent to Eq. (B.9) and Eq. (B.8). Moreover, since *all* the w_{ij} values are bounded, the computations that lead to Eq. (B.13) and Eq. (B.14) stay valid as the system evolves. Therefore by the same

arguments as in the proof of Proposition 7, convergence to the proposed fixed points is obtained.

It only remains to show that even for such small ϵ values, the expression in Eq. (B.12) still goes to 0 as κ increases. In particular, $\epsilon = \mu/n$ satisfies $\epsilon/\mu(n-1) < 1$. For this ϵ we have

$$n(n+1)\exp\left(-\frac{\epsilon^2\kappa}{2}\right) = n(n+1)\exp\left(-\frac{\kappa\mu^2}{2n^2}\right).$$

We can take $\kappa \gg \frac{2n^2}{\mu^2}(\log(n) + \log(n+1))$ sufficiently large to make the above expression arbitrarily small. This concludes the proof.

□

Appendix C

Lists

List of Tables

List of Figures

Bibliography

[1] M. H. Afrasiabi and R. Guérin. Exploring user-provided connectivity - A simple model. In *Economics of Converged, Internet-Based Networks - 7th International Workshop on Internet Charging and QoS Technologies, ICQT 2011, Paris, France, October 24, 2011. Proceedings*, pages 38–49, 2011.

[2] M. H. Afrasiabi and R. Guérin. Pricing strategies for user-provided connectivity services. In *Proceedings of the IEEE INFOCOM 2012, Orlando, FL, USA, March 25-30, 2012*, pages 2766–2770, 2012.

[3] M. H. Afrasiabi and R. Guerin. Exploring user-provided connectivity. *IEEE/ACM Transactions on Networking*, PP(99), 2014. To appear.

[4] M. H. Afrasiabi and R. Guérin. Choice-based pricing for user-provided connectivity. In *Proceedings of the 10th Workshop on the Economics of Networks, Systems and Computation, NetEcon 2015, Portland, OR, June 2015*, 2015. To appear.

[5] M. H. Afrasiabi, R. Guérin, and S. S. Venkatesh. Opinion formation in Ising networks. In *2013 Information Theory and Applications Workshop, ITA 2013, San Diego, CA, USA, February 10-15, 2013*, pages 1–10. IEEE, 2013.

[6] M. H. Afrasiabi, R. Guérin, and S. S. Venkatesh. Spin glasses with attitude: Opinion formation in a partisan Erdős-Rényi world. In *2014 Information Theory and Applications Workshop, ITA 2014, San Diego, CA, USA, February 9-14, 2014*, pages 1–5. IEEE, 2014.

[7] H. Akhlaghpour, M. Ghodsi, N. Haghpanah, H. Mahini, V. Mirrokni, and A. Nikzad. Optimal iterative pricing over social networks. In *Proc. WINE'10*, Stanford U., CA, December 2010.

[8] T. Ali-Vehmas and S. Luukkainen. Service adoption strategies of push over cellular. *Personal Ubiquitous Comput.*, 12(1):35–44, Jan. 2008.

[9] E. Altman, J. Rojas, S. Wong, M. Hanawal, and Y. Xu. Net neutrality and quality of service. In R. Jain and R. Kannan, editors, *Game Theory for Networks*, volume 75 of *Lecture Notes of the Institute for Computer Sciences, Social Informatics and Telecommunications Engineering*, pages 137–152. Springer Berlin Heidelberg, 2012.

[10] G. M. Anderson, W. F. Shughart II, and E. D. Tollison. The economic theory of clubs. In C. K. Rowley and F. Schneider, editors, *The Encyclopedia of Public Choice*. Springer, 2003.

[11] M. Armstrong. Price discrimination. In P. Buccirossi, editor, *Handbook of Antitrust Economics*. MIT Press, 2008.

[12] D. K. Arrowsmith and C. M. Place. *An Introduction to Dynamical Systems*. Cambridge University Press, 1990.

[13] C. Augsburg and J. Hedman. Value added services and adoption of mobile payments. In *Proceedings of the Sixteenth International Conference on Electronic Commerce*, ICEC '14, pages 27:27–27:32, New York, NY, USA, 2014. ACM.

[14] B. Awerbuch, Y. Azar, A. Epstein, V. S. Mirrokni, and A. Skopalik. Fast convergence to nearly optimal solutions in potential games. In *Proceedings of the 9th ACM Conference on Electronic Commerce*, EC '08, pages 264–273, New York, NY, USA, 2008. ACM.

[15] P. Baldi and S. S. Venkatesh. Number of stable points for spin-glasses and neural networks of higher orders. *Physical Review Letters*, 58:913–916, 1987.

[16] M. Beckmann, C. B. McGuire, and C. B. Winsten. *Studies in the Economics of Transportation. Cowles Commission Monograph*. Yale University Press, 1956.

[17] E. Ben-naim, P. L. Krapivsky, F. Vazquez, and S. Redner. Unity and discord in opinion dynamics. *Physica A*, 2003.

[18] G. Bianconi, R. K. Darst, J. Iacovacci, and S. Fortunato. Triadic closure as a basic generating mechanism of communities in complex networks. *Phys. Rev. E*, 90:042806, Oct 2014.

[19] S. Biswas, A. Chatterjee, and P. Sen. Disorder induced phase transition in kinetic models of opinion dynamics. *Physica A: Statistical Mechanics and its Applications*, 391(11):3257 – 3265, 2012.

[20] J.-P. Bouchaud. The (unfortunate) complexity of the economy. *ArXiv e-prints*, Apr. 2009.

[21] J. K. Brueckner. Tastes, skills, and local public goods. *Journal of Urban Economics*, 35(2):201 – 220, 1994.

[22] J. M. Buchanan. An economic theory of clubs. *Economica*, 32(125), February 1965.

[23] K. J. Button and E. T. Verhoef, editors. *Road Pricing, Traffic Congestion and the Environment: Issues of Efficiency and Social Feasibility*. Edward Elgar Pub., 1999.

[24] L. M. B. Cabral. On the adoption of innovation with network externalities. *Mathematical Social Sciences*, 19, 1990.

[25] O. Candogan, K. Bimpikis, and A. Ozdaglar. Optimal pricing in the presence of local network effects. In A. Saberi, editor, *Internet and Network Economics*, volume 6484 of *Lecture Notes in Computer Science*, pages 118–132. Springer Berlin Heidelberg, 2010.

[26] C. Castellano, M. A. Muñoz, and R. Pastor-Satorras. Nonlinear q-voter model. *Phys. Rev. E*, 80:041129, Oct 2009.

[27] M. Castells. *The Rise of the Network Society: The Information Age: Economy, Society, and Culture*, volume I. Wiley-Blackwell, 2nd edition, 2010.

[28] M. Castells and G. Cardoso, editors. *The Network Society – From Knowledge to Policy*. Johns Hopkins Center for Transatlantic Relations, Washington, D.C., 2005.

[29] S. Chao. *Positive and Negative Externality Effects on Product Pricing and Capacity Planning*. PhD thesis, Stanford University, 1996.

[30] J. P. Choi. The provision of (two-way) converters in the transition process to a new incompatible technology. *The Journal of Industrial Economics*, 45(2), 1997.

[31] B. Cohen. Incentives build robustness in BitTorrent. In *Proc. 1st Workshop Econ. Peer-to-Peer Sys.*, Berkeley, CA, June 2003.

[32] C. Courcoubetis and R. Weber. Incentives for large peer-to-peer systems. *J. Select. Areas. Commun.*, 24(5), May 2006.

[33] D. Easley and J. Kleinberg. *Networks, Crowds, and Markets: Reasoning About a Highly Connected World*. Cambridge University Press, 2010.

[34] N. Economides. The economics of networks. *International Journal of Industrial Organization*, 14(2):673–699, March 1996.

[35] Ericsson. *Networked Society Essentials*, March 2014. White Paper Uen 284 23-3242.

[36] Ericsson. *Understanding the Networked Society new logics for an age of empowerment*, February 2015. White Paper Uen 284 23-3242.

[37] D. L. M. et al. Diversity in the social, behavioral and economic sciences. SBE 2020 of National Science Foundation.

[38] J. Farrell and P. Klemperer. Coordination and lock-in: Competition with switching costs and network effects. In M. Armstrong and R. Porter, editors, *Handbook of Industrial Organization, Vol. 3*. Elsevier, 2007.

[39] J. Farrell and G. Saloner. Installed base and compatibility: Innovation, product preannouncements, and predation. *American Economic Review*, 76, 1986.

[40] D. Fudenberg and D. K. Levine. *The Theory of Learning in Games (Economic Learning and Social Evolution)*. The MIT Press, 5 1998.

[41] D. Fudenberg and J. Tirole. *Game Theory*. The MIT Press, 11th printing edition, 8 1991.

[42] B. Fung. Don't use all your mobile data in a month? this company will give you a refund. The Washington Post. April 21, 2015.

[43] R. J. Gibbens and F. P. Kelly. Resource pricing and the evolution of congestion control. *Automatica*, 35, 1999.

[44] M. Girvan and M. E. J. Newman. Community structure in social and biological networks. *Proceedings of the National Academy of Sciences*, 99(12):7821–7826, 2002.

[45] P. E. Green, A. Krieger, and Y.Wind. Thirty years of conjoint analysis: Reflections and prospects. *Interfaces*, 31(3):S56–S73, 2001.

[46] R. Guérin, J. C. de Oliveira, and S. Weber. Adoption of bundled services with network externalities and correlated affinities. *ACM Trans. Internet Technol.*, 14(2-3):13:1–13:32, Oct. 2014.

[47] E. J. Hackett and S. v. d. Leeuw. A synthesis center for the social, behavioral, and economic sciences. SBE 2020 of National Science Foundation. September, 2010.

[48] W. Hoeffding. Probability inequalities for sums of bounded random variables. *Journal of the American Statistical Association*, 58(301):13–30, 1963.

[49] J. J. Hopfield. Neural networks and physical systems with emergent collective computational abilities. *Proceedings of the National Academy of Sciences of the USA*, 79:2554–2558, 1982.

[50] M. O. Jackson. Research opportunities in the study of social and economic networks. SBE 2020 of National Science Foundation. September, 2010.

[51] M. O. Jackson. *Social and Economic Networks*. Princeton University Press, 2010.

[52] R. Johari and S. Kumar. Congestible services and network effects. In *Proc. ACM EC 2010*, Cambridge, MA, June 2010. (Extended abstract – Full version available at http://www.stanford.edu/rjohari/uploads/posex.pdf).

[53] D. Joseph, N. Shetty, J. Chuang, and I. Stoica. Modeling the adoption of new network architectures. In *CoNEXT'07 Conference*. CM, 2007.

[54] C. Kadushin. *Understanding Social Networks: Theories, Concepts, and Findings*. Oxford University Press, 2011.

[55] M. Katz and C. Shapiro. Network externalities, competition and compatibility. *American Economic Review*, 75(3):420–440, June 1985.

[56] M. Katz and C. Shapiro. Technology adoption in the presence of network externalities. *Journal of Political Economy*, 94(4):822–841, June 1986.

[57] F. P. Kelly. Charging and rate control for elastic traffic. *European Transactions on Telecommunications*, 8, 1997.

[58] F. P. Kelly. Road pricing. *Ingenia*, 29:34–40, 2006.

[59] E. Koutsoupias and C. Papadimitriou. Worst-case equilibria. In *Proceedings of the 16th annual conference on Theoretical aspects of computer science*, pages 404–413. Springer-Verlag, 1999.

[60] R. Lambiotte and M. Ausloos. Coexistence of opposite opinions in a network with communities. *Journal of Statistical Mechanics: Theory and Experiment*, 2007(08):P08026, 2007.

[61] A. Lambrecht and B. Skiera. Paying too much and being happy about it: Existence, causes and consequences of tariff-choice biases. *Journal of Marketing Research*, XLIII:212–223, 2006.

[62] S. J. Liebowitz and S. E. Margolis. Network effects and externalities. In P. Newman, editor, *The New Palgrave Dictionary of Economics and the Law*. Stockton Press, 1998.

[63] S. J. Liebowitz and S. E. Margolis. Network effects. In M. Cave, S. Majumdar, and I. Vogelsang, editors, *Handbook of Telecommunications Economics*, volume 1. Elsevier, 2002.

[64] J. Linshi. Comcast turns 50,000 homes into wi-fi hotspots. TIME. June 12, 2014, Available at http://ti.me/1lewL87.

[65] J. Lorenz. Continuous opinion dynamics under bounded confidence:: A survey. *International Journal of Modern Physics C: Computational Physics & Physical Computation*, 18(12):1819 – 1838, 2007.

[66] J. K. MacKie-Mason and H. R. Varian. Pricing the Internet. Computational Economics 9401002, EconWPA, January 1994.

[67] A. C. R. Martins. Continuous opinions and discrete actions in opinion dynamics problems. *International Journal of Modern Physics C: Computational Physics & Physical Computation*, 19(4):617 – 624, 2008.

[68] W. G. Mitchener. The evolution of natural computation, behavior, and instinct, and the need for mathematical modeling and mathematical literacy in the social, behavioral, cognitive, and economic sciences. SBE 2020 of National Science Foundation. 2010.

[69] D. Monderer and L. S. Shapley. Potential games. *Games and economic behavior*, 14(1):124–143, 1996.

[70] J. Musacchio and J. C. Walrand. Wifi access point pricing as a dynamic game. *IEEE/ACM Trans. Netw.*, 14(2):289–301, 2006.

[71] J. Nadal, D. Phan, M. Gordon, and J. Vannimenus. Multiple equilibria in a monopoly market with heterogeneous agents and externalities. *Quantitative Finance*, 5(6):557–568, 2005.

[72] M. Newman. *Networks: An Introduction*. Oxford University Press, 2010.

[73] A. Odlyzko. The evolution of price discrimination in transportation and its implications for the Internet. *Review of Network Economics*, 3, 2004.

[74] M. Ostilli, E. Yoneki, I. Leung, J. Mendes, P. Lio, and J. Crowcroft. Ising model of rumour spreading in interacting communities. Technical Report UCAM-CL-TR-767, University of Cambridge, 2010.

[75] I. C. Paschalidis and J. N. Tsitsiklis. Congestion-dependent pricing of network services. *IEEE/ACM Transactions on Networking*, 8(2), April 2000.

[76] B. A. Pescosolido. The role and potential impact of social, behavioral and economic science approaches to networks in the first half of the 21st century: Grand challenges of substance and methods. SBE 2020 of National Science Foundation. 2010.

[77] M. Potoski and A. Prakash, editors. *Voluntary Programs: A Club Theory Perspective*. The MIT Press, 2009.

[78] T. Roughgarden. Algorithmic game theory. Lecture 16 notes, Stanford University, 2013.

[79] C. I. N. Sampaio-Filho and F. G. B. Moreira. Block voter model: Phase diagram and critical behavior. *Phys. Rev. E*, 84:051133, Nov 2011.

[80] T. Sandler and J. T. Tschirhart. The economic theory of clubs: An evaluative survey. *Journal of Economic Literature*, 18(4), December 1980.

[81] S. Scotchemer. Externality pricing in club economies. *Ricerche Economiche*, 50(4):347 – 366, 1996.

[82] S. Sen, Y. Jin, R. Guérin, and K. Hosanagar. Modeling the dynamics of network technology adoption and the role of converters. *IEEE/ACM Trans. Netw.*, 18(6):1793–1805, December 2010.

[83] S. Sen, C. Joe-Wong, S. Ha, and M. Chiang. A survey of smart data pricing: Past proposals, current plans, and future trends. *ACM Comput. Surv.*, 46(2):15:1–15:37, Nov. 2013.

[84] J. Simmermon. Launching an optional usage-based broadband pricing plan. http://www.twcableuntangled.com/2012/02/launching-an-optional-usage-based-pricing-plan-in-southern-texas-2/. February 27, 2012.

[85] R. Srikant. *The Mathematics of Internet Congestion Control*. Birkhauser, 2004.

[86] K. Sznajd-Weron and J. Sznajd. Opinion evolution in closed community. *International Journal of Modern Physics C: Computational Physics & Physical Computation*, 11(6):1157, 2000.

[87] E. van Damme. *Stability and Perfection of Nash Equilibria*. Springer, 2nd edition, 10 2002.

[88] S. S. Venkatesh. *The Theory of Probability, Explorations and Applications*. Cambridge University Press, 2013.

[89] K. Wallace. It's a new day for unlimited data. http://newsroom.sprint.com/news-releases/its-a-new-day-for-unlimited-data.htm. August 21, 2014.

[90] D. J. Watts. *Six Degrees: The Science of a Connected Age*. W. W. Norton & Company, 2004.

[91] J. Wortham. Customers angered as iPhones overload AT&T. The New York Times. September 2, 2009.